NEACRP-L-331

NEACRP COMPARISON OF CODES FOR THE RADIATION PROTECTION ASSESSMENT OF TRANSPORTATION PACKAGES. SOLUTIONS TO PROBLEMS 1 - 4

by

A F AVERY

and

MRS H F LOCKE

Safety Engineering Systems Division
RPSC Department
AEA Technology
Winfrith

March 1992

	NAME	SIGNATURE	POSITION	DATE
Lead Author	A.F. AVERY	A.F. Avery	Section Leader	17/11/92
Checked	H F Locke	H.F. Locke.	Analyst.	7/12/92
Approved	G J Lloyd	G J Lloyd	DIVISION MANAGER SESA	17.12.92

NEACRP-L-331

NEACRP COMPARISON OF CODES FOR THE RADIATION PROTECTION ASSESSMENT OF TRANSPORTATION PACKAGES SOLUTIONS TO PROBLEMS 1-4

BY

A F AVERY

AND

MRS H F LOCKE

Safety Engineering Systems Division
RPSC Department
AEA Technology
Winfrith

March 1992

Contents

Tables

Figures

ABSTRACT

In 1985 the Reactor Physics Committee of the Nuclear Energy Agency initiated an intercomparison of codes for the calculation of the performance of shielding for the transportation of spent reactor fuel. The results of the application of a range of codes to the prediction of the dose-rates in the four theoretical benchmarks set to examine the attenuation of radiation through a variety of cask geometries are presented in this report. The contributions from neutrons, fission product gamma-rays and secondary gamma-rays are tabulated separately, and grouped according to the type of method of calculation employed. A brief discussion is included for each set of results, and overall comparisons of the methods, codes, and nuclear data are made. A number of conclusions are drawn on the advantages and disadvantages of the various methods of calculation, based upon the results of their application to these four benchmark problems.

1 Introduction

The Reactor Physics Committee of the Nuclear Energy Agency set up a project in 1985 to exchange information and experience on shielding calculations for the transportation of spent reactor fuel. This took the form of an intercomparison of codes for carrying out such calculations, and it followed the pattern of similar exercises which had been set up for criticality and heat transfer assessments of fuel transport. The proposal (1) contained six theoretical benchmark problems for which participants were invited to submit results together with details of the methods of calculation employed. The problems could be divided into two groups; the first four had sources which were defined in terms of their strengths and spectra while problems 5 and 6 involved the calculation of the sources from data provided on the fuel assemblies and their radiation histories. Modifications were subsequently made to the specification at meetings of participants and issued in an addendum (1). The purpose of the present paper is to summarise the results obtained for the first four problems, and to draw conclusions from a comparison of the performance of the various codes.

The first meeting to discuss the results was held at the OECD Headquarters in Paris in June 1986 and it was attended by participants from ten countries. At this meeting the comparison concentrated on the results for problem 1 and revealed wide discrepancies between solutions. Differences of factors of 10 were present between calculated dose-rates. Subsequently as inconsistencies in the interpretation of the problem definitions were resolved and errors removed from the data, the agreement improved, although factors of 2 between solutions are still present in some cases.

The second meeting was held at the OECD Headquarters in May 1987 and this was attended by 14 participants from 10 countries. Solutions to problems 1-4 were discussed at this meeting and in particular the possible reasons for the improved agreement and for the remaining differences were considered. Again most attention was devoted to problem 1, with fewer solutions being available for the remainder. A summary of this meeting and the results was issued in NEACRP-A-864. (2)

The third meeting was held at the NEA Databank at Saclay in May 1988 with ten participants from seven countries. Additional results for problems 2-4 were submitted, and some participants had re-calculated for problems 1 using improved data libraries. Later in 1988 many of the participants attended the 7th International Conference on Radiation Shielding at Bournemouth, and the opportunity was taken to hold an ad-hoc meeting. The collected results and a summary of the discussions were issued as NEACRP-A-895. (3) A further status report was issued in October 1989. (4)

The fourth meeting was held at the OECD Headquaters in March 1990. Discussions at this meeting concentrated on the results for problems 5 and 6, and on the experimental benchmark based on the TN-12 flask. It was agreed that work on problems 1-4 was mostly complete at this stage. A report summarising the status of the comparison was presented to the NEACRP in October 1990. (5)

A list of the participants who have contributed to the intercomparison is given at the end of this report. Details of the problems and a summary of the methods and data employed are given in sections 2,3 and 4 below.

2. Description of Problems 1-4

2.1 General Description

The flasks for the theoretical benchmarks are cylindrical with an internal cavity of diameter 800mm and height 4500mm as shown in Figure 1. The sources are identical for problems 1-3 being specified as having uniform strength within an homogenous region, with problem 4 including a detailed representation of the fuel elements. The cavity is either dry or flooded with water in the volume not occupied by the fuel and its basket. The flask wall is always 380mm thick, being mainly composed of either cast iron or steel, although in some problems some of this material is replaced by neutron shielding in the form of polyethylene or epoxy resin. For problem 3 the flask wall has fins added. The base is always 380mm thick, being composed of either cast iron or steel to match the flask wall. The lid is always 420mm thick and composed of stainless steel, this material differing from that used for the flask wall. The compositions of the materials are given in Table 1. The problems are subdivided so that in total there are 9 different combinations of flask and source. Three separate contributions to the total dose-rates are considered in most cases, namely those from primary neutrons, fisson-product gamma-rays and secondary gamma-rays. The multiplication of neutrons is specifically excluded in problems 1-4.

In problem 1 the flask designs are straightforward and uniform axially. In problem 2 discrete regions of neutron shielding are introduced in two different ways. In problem 3 fins are added to the flask in company with neutron shielding in 3b, whilst problem 4 has the simple flask of problem 1a with the detailed fuel elements as sources in a five-element basket.

The required outputs are the neutron and gamma-ray dose-rates on the outer surface of flasks. Flux-to-dose conversion factors are provided for neutrons and gamma-rays in the form of coefficients for polynomial expansions taken from ANSI/ANS 6.1.1-1977. These are given in Tables 2 and 3. The dose-rates are requested in the form of surface-average values and also values at distances of 1m, 2m and 10m from the surface, or from the fin tips. The dose-rates were requested outside the radial surface and also above and below the lid and base of the flask. It was subsequently agreed that the surface value should be averaged over the height of the cavity for the radial surface, and over the area of the cavity for the lid and base. In the event some contributors gave the dose-rates at the mid-height of the cavity and on the centre point of the end faces, and both types of result are presented in this report.

2.2 Sources

For problems 1-4 the primary sources of neutrons and gamma-rays are defined. The total neutron source is 1×10^9 neutrons/sec with a fission spectrum given by

$$S(E) = A \exp(-B.E).\sinh(C.E)^{1/2}$$

Where $A = 0.451$
$B = 1.035$
$C = 2.29$

and E is the energy in MeV.

Multiplication of the neutron source by secondary fissions is to be omitted in the calculations.

The total gamma-ray source is 5.0×10^{16} photons/sec with a spectrum defined by emission at 8 discrete energies. These are given in Table 4. The contributions of secondary gamma-rays arising from neutron reactions are to be calculated as part of the solution where relevant, and the results provided separately.

For problems 1-3 the source is assumed to be uniformly distributed throughout the volume of the cavity. The material within this region is a homogeneous mixture of fuel assemblies and stainless steel basket with water also being present in some problems.

For problem 4 the fuel elements and their basket are specified explicitly, and the sources in this case are uniformly distributed throughout the active fuel. The total source strengths and their spectra remain the same as for problems 1-3.

2.3 Problem 1

The flask body for problems 1a and 1c is composed of cast iron, with both the wall and the base having thicknesses of 380mm. The lid is stainless steel of thickness 420mm. For problem 1a the flask is dry, while for problem 1c the cavity also contains water. The appropriate compositions for the source region are given in Table 1, together with those for the flask and fuel materials.

For problem 1b the flask cavity is dry but the radial wall is composed of 320mm of cast iron with 60mm of polyethylene surrounding it over the full length of the flask. The base and the lid are identical to those in problems 1a and 1c.

2.4 Problem 2a

Problem 2a has a cylindrical wall of stainless steel with circular holes containing 60 cylindrical polyethylene rods which extend axially over the height of the cavity, the latter having been decided at the 1986 meeting. The rods are 70mm in diameter and are arranged in two rings as shown in Figure 2, the angular interval between rods in the same ring being 12° with the centres of the rods being on circles of diameter 1200mm and 1370mm.

The base of the flask in this case is stainless steel and the source region is dry.

2.5 Problem 2b

Problem 2b has a cast iron wall with bands of epoxy resin set in the outer surface as shown in Figure 3. These are 80mm in height and 50mm in depth, the bands being separated by 50mm of cast iron. The base of the flask is cast iron and the lid is stainless steel. The flask is dry.

2.6 Problem 3a

Problem 3a has a steel flask wall of thickness 380mm with steel fins added outside. The latter extend circumferentially around the flask being 120mm long with a width of 50mm at the base and 20mm at the tip. The separation is 80mm at the base of the fins as shown in Figure 4 . The midplane of the top fin is located at the level of the top of the cavity. The base of the flask is steel and the cavity is dry.

Problem 3b has a similar configuration of fins but the flask and fins are composed of cast iron. In addition bands of epoxy resin similar to those in Problem 2b are set into the outer 50mm of the flask wall between fins as show in Figure 5. They are thus 80mm in length and 50mm in depth. The cavity is again dry.

2.7 Problem 4

The flask for Problem 4 is similar to that for Problem 1a, ie cast iron with no neutron shielding, and a steel lid.

The source is not the uniform cylinder but is instead a detailed representation of five fuel assemblies contained in a steel basket as shown in Figure 6. The basket is made of steel plate of thickness 10mm, the composition of the steel being similar to that of the flask in Problems 2a and 3a. The plates form five square compartments of internal dimension 239mm with a height of 4400mm, the basket resting on the base of the 4500mm high cavity. Each compartment contains a fuel assembly with a square array of 15 x 15 pin positions, 210 of which are occupied by fuel rods with the remaining 15 being control rod tubes. The overall length of an assembly is 4450mm and the width across the flats is 230mm. Each fuel pin is 3930mm long, having zircalloy cladding of inner diameter 10mm and outer diameter 11.5mm. The rods are on a square 15.3mm pitch. Each rod has a steel plug of length 18mm at both top and bottom, with void expansion spaces within the cladding of length 314mm at the bottom and 160mm at the top. Between the expansion spaces is the active fuel region of length 3420mm containing UO_2 pellets of 9.69mm outer diameter. The control rod positions contain zircalloy guide tubes of 12.5mm inside diameter and 14.0mm outside diameter. Above and below the rods there are gaps of length 10mm which are treated as being voids. The bottom end fitting is 230mm in length while the top fitting is 270mm long. These end fittings are represented by smeared material so that they are assumed to be square of outer dimensions 230mm and to be composed of steel of uniform density 1.01 gm/cm^3. The fuel assembly is shown in Figure 7 , while the dimensions and materials are summarised in Table 5.

3. Methods of Calculation

The methods of calculation which were applied by participants in the comparison are briefly summarised below.

3.1 Line-of-Sight Kernels

The kernel method was used by several participants for predicting gamma-ray dose-rates. It is based on the calculation of the uncollided flux which can always be achieved by determining the thicknesses of materials penetrated along the direct path from the source point to the dose-point. The contributions of scattered gamma-rays are then derived by applying build-up factors which give the ratio of the total dose-rate to that from the uncollided component. The latter are available for a range of situations, libraries of parameters having been set up from the results of transport calculations. The dose build-up factors are usually given for point isotropic sources in infinite regions of a single material and they are functions of the source energy, the thickness of material penetrated, and the atomic number of the material. Some data and recipes have been derived for build-up in multi-layered shields, but the common practice is to adopt a single equivalent material. For distributed sources it is necessary to integrate the kernels over the energy spectrum and spatial variation of the gamma-ray emitters in order to obtain the total dose-rate.

3.2 Discrete Ordinates

The discrete ordinates method solves the transport equation rigorously by expressing it in terms of the flux per unit solid angle in a number of directions at spatial mesh points for each energy group. In this way a set of simultaneous equations is developed which is then solved iteratively for the angular fluxes at each energy and mesh point. The accuracy of the method depends upon the validity of the transformation of the differential transport equation into the set of difference equations.

The number of directions which need to be considered is determined by the angular variation in the flux. Typically in plane geometry 8 or 16 angles are sufficient to describe this distribution and to enable integration over all directions for the flux and for the source of scattered particles to be performed accurately. For cylindrical or two-dimensional cases the equivalent numbers of directions increase as azimuthal variation must be taken into account.

The differential terms of the transport equation involving the spatial variable are replaced by difference equations in which a linear variation of angular flux is assumed between mesh points. In most shielding problems the attenuation is close to exponential so that the linear approximation is only valid if the mesh points are sufficiently close together to enable higher order terms to be neglected. It is important in the application of the discrete ordinates method to ensure that there are sufficient mesh points to achieve this.

The energy variable is usually treated by integrating the transport equation over energy intervals so that the angular flux is expressed as the sum over all energies within an interval or group. The terms of the transport equation which involve reaction rates then become products of the group fluxes and the group-averaged cross-sections. In order to derive the latter it is necessary to assume a shape for the flux spectrum within the group, and also for the variation of the angular distribution with energy in the treatment of the scatter source. Multigroup cross-section libraries are produced with a range of assumptions for the weighting spectrum, and it

is necessary to choose a library which is appropriate to the problem which is being solved. The dependence on the assumed spectrum becomes less important as the width of the energy group is reduced, and calculators have to compromise between the accuracy of using a large number of groups and the speed of calculation achieved with fewer. The multigroup libraries also introduce another variable in the accuracy with which they treat the angular distribution of the transfer between energy groups. This is usually expressed as an expansion in Legendre polynomials with terms extending to P_3 or P_5 in most cases. Again the order which is needed for accurate results depends upon the angular distribution of the flux in a particular problem as well as the fundamental distribution of the angular deflections produced in a scatter process. The order which is appropriate in a given situation is usually determined from trial cases or previous experience.

The discrete ordinates method requires orthogonal spatial mesh arrays in order to develop the difference equations, so that its application is limited to regular geometries. Because of the iterative nature of the solution there is a practical limitation on the number of mesh points which may be specified if convergence is to be achieved, and this effectively restricts its application to two-dimensional problems for most shielding calculations. In these cases it will provide accurate solutions to the transport equation provided that the mesh intervals, angular quadrature and multigroup data are chosen appropriately.

3.3 Monte Carlo

In Monte Carlo calculations the required response is estimated by generating a number of typical particle tracks. At each stage the position of the next collision, the type of interaction which then occurs and the energy and direction of the resulting particles are all sampled from the known physical laws by choosing random numbers. In this way a particle in the calculation follows the same procedure as it would experience in reality. By recording properties of the tracks which reach the regions of interest for a given number of samples started it is possible to estimate a response such as dose-rate and normalise it to the actual source strength for the problem. The generation of tracks requires the boundary surfaces of each region to be specified, and the nuclear data for the material within the region to be provided. The former can be achieved in a general way by giving the equation for each of a large number of surfaces so that Monte Carlo calculations are not restricted to regular orthogonal geometries. The cross-sections may be taken from a multigroup library similar to that used for discrete ordinate calculations or alternatively they may refer directly to the basic nuclear data files with very little pre-processing being required. The latter approach is feasible because the cross-sections, energy loss-laws, and angular distribution can be read for the energy corresponding to that of the particle at a particular stage in its track. This contrasts with the discrete ordinates method where the transport equation is solved throughout the problem for each of the selected energy groups.

The disadvantages of the Monte Carlo method arise from the stochastic nature of the result where the accuracy depends upon the number of particles which reach the region of interest. The same stochastic considerations apply to the particle fluxes in the practical situation, but it would not be possible in a Monte Carlo calculation to generate the same number of tracks as there are source particles. (In the theoretical

benchmarks, for example, there are 5 x 10^{16} gamma-rays and 10^{9} neutrons emitted every second). Because far fewer tracks are generated in a calculation it is necessary to concentrate the tracking on those particles which are most likely to reach the region of interest if sufficient tracks are to contribute to the score to give satisfactory statistical accuracies.

The most common approach for accelerating a calculation is to use splitting and Russian roulette. In this process a particle is split so that it has more chance of continuing if it appears to be promising, or alternatively it is killed with a probability determined by the reduction in its likelihood of reaching the region of interest. The weights of the particles which are used in the scoring process are adjusted at each stage so that there is no bias in the result. The application of Russian roulette and splitting thus requires a method of assessing the probability of a particle reaching the scoring region as a function of its position and energy. There are various ways of obtaining these probabilities or importances, but they usually require the application of some skill by the calculator, a fact which has been a hindrance to the wide use of the method. Other techniques for acceleration are also applied in which the tracks are distorted by increasing the path lengths or biasing the angle of scatter, but these require the user to have considerable experience and understanding of the problem if bias is not to be introduced. It is essential that the distortions produce tracks which are similar to those which dominate the response in the physical situation, and it is not always possible to ensure that this is achieved. Even with the sound use of acceleration techniques it is difficult to obtain good statistical accuracy in many applications.

The most common method of recording the response in Monte Carlo calculations is to score the lengths of the tracks passing through a specified region. This gives the mean flux within the region. For good spatial resolution the region should be small while for high statistical accuracy it should be large so that many tracks pass through it. The same consideration applies to boundary crossing estimators and the area of the scoring surface. In many applications it is necessary to achieve a compromise between spatial resolution and statistical accuracy. Other methods of scoring can give the response at a point, but these are not suitable for all situations and they imply some distortion of the track which could introduce bias if not used with understanding.

The need to accelerate Monte Carlo calculations by concentrating tracking towards a particular response leads to the other disadvantage of the method. The result is only valid for that particular region, and the general distribution of fluxes throughout the problem which is provided by deterministic methods such as discrete ordinates is not available from Monte Carlo. The number of scoring regions can be increased but only at the expense of longer computing times.

Thus Monte Carlo has the advantage of being applicable to general geometries and to be able to use nuclear data which is effectively specified at point energies. It suffers from the statistical uncertainties on its results, and the need to apply methods of accelerating the calculation which require skill. It does not give the general distribution of fluxes nor the spatial resolution which are available from deterministic methods.

4 Nuclear Data

4.1 Introduction

Calculations which were carried out by the various participants for problems 1-4 involved the use of many data libraries. Details of these are briefly summarised in sections 4.2 and 4.3 below, covering multigroup and point-energy data separately.

4.2. Multigroup Data

4.2.1 SCALE

The special SCALE library is a 22 neutron group - 18 gamma-ray group set of cross-sections which has been derived by condensing the CSRL-V library with its 227 neutron groups and 44 gamma-ray groups. The latter is based on ENDF/B-V Mod 1 data and the condensed set was obtained by using a weighting spectrum appropriate to the cast iron cask. The selection of this library was based on an extensive study of various libraries and comparisons between the results obtained with a range of fine-group and broad-group data (6). This library was used in the US calculations and differs from the standard SCALE library which has the same group structure but is based on ENDF/B-IV data. The latter was used by ENEA participants (7).

4.2.2 BUGLE

The BUGLE library has 47 neutron groups and 20 gamma-ray groups, being a condensation of the VITAMIN C library with its 171 neutron groups and 36 gamma-ray groups. The fine-group library is derived from ENDF/B-IV data with a weighting spectrum for concrete being used to collapse it to the broad group data. Resonance self-shielding for iron is not included. BUGLE was used in the calculations of Wasastjerna (7)

4.2.3 RADHEAT

The RADHEAT-V3 library is prepared from infinitely dilute cross-sections (JSD-100) with self-shielding factors for neutrons being taken from a table. There are 100 neutron groups and 20 gamma-ray groups in the library with scatter cross-sections being expressed in Legendre expansions to order P_5. This library was used in the contributions from the Japanese participants.

4.2.4 EURLIB

The EURLIB library was used in several versions in the calculations. The full library has 100 neutron groups and 20 gamma-ray groups, and is derived from ENDF/B-IV data. Version III was restricted to P_3 expansions of the transfer cross-sections while version IV was extended to P_5. A condensed version of EURLIB III having 15 neutron groups and 5 gamma-ray groups was also used in some calculations. This library was used in the ANISN and TWODANT calculations carried out by the participants from Germany, Switzerland, and Belgium.

4.2.5 GAM50

GAM50 is a gamma-ray library which was derived from ENDF/B-IV data using the AMPX-II code package to produce data in 50 energy groups. This library was used in the contributions from Germany.

4.2.6 NGCP9-70

This library is based on ENDF/B-IV data and has 50 neutron groups with 20 gamma-ray groups. Its treatment of the angular distribution extends to a P_9 expansion. The library was used in Monte Carlo calculations with the MORSE code.

4.3 "Point" Energy Data

4.3.1 THEMIS

The code system THEMIS (9) was used to process JEFI data into formats for use with the MCNP code. In this scheme the data are essentially read at energies corresponding to those of the particles being tracked, with the explicit energy-loss laws and angular distribution of scatter being retained. The modules of THEMIS which were used to prepare this point-wise cross-section library were C MODE, RECONS, DOPPLER, UNRESE, KERMA, GROUPN and ACER. Some compromise was necessary in ACER to reduce the number of energy points whilst not losing accuracy in the cross-sections. The largest number of points for an element was 10,636 for iron which required 216 Kbyte of store.

4.3.2 TRIPOLI

The library of data used in TRIPOLI is a 315 group set for neutrons based on ENDF/B-IV, while for gamma-rays there are 21 groups with the cross-sections being taken from the UKNDL. In both cases the cross-sections are averaged over the groups, but the energy-loss laws and the angular distributions of scatter are retained in their explicit forms as functions of energy. Because of the large number of neutron groups and the absence of inter-group transfer cross-sections these data are considered to be equivalent to a 'point-energy' representation when the results are discussed.

4.3.3 DICE/GAMBLE

The DICE library expresses the neutron cross-sections in 8200 energy groups so that there is very little averaging, the angular distributions of scatter and the energy loss laws being sampled directly as they are in the THEMIS and TRIPOLI libraries. For gamma-rays the GAMBLE routines interpolate the cross-sections to give values corresponding to the actual energy of the particle being tracked, the angular distribution of the Compton scatter being sampled also at the appropriate energy with the energy loss being derived analytically from the scatter angle.

4.3.4 MCNP Library

The data used in the US calculations with the MCNP code were taken from the standard library issued with the code. The basic data were those in ENDF/B-V, and the code interpolates cross-sections and interaction laws to give point-energy values corresponding to the energy of the particle being tracked.

5 Codes

5.1 Kernel Codes

The codes QAD, and RANKERN were used in calculations of the gamma-ray dose-rates outside the flask. In these codes the geometry can be specified in a very general way so that it is possible to represent the flask and the source regions precisely, even when the latter are fuel assemblies in a basket. QAD performs the integration over the source volume by sub-dividing it into a specified number of regions each of which is replaced by a point source at its centre. In RANKERN (10) the integration is achieved by the Monte Carlo approach in which the position of the source point is randomly sampled over the volume. Two versions of QAD were used in the comparison, QAD-CGGP (11) and QAD-CG (12) with participants employing different cross-section data and build-up factors. In some cases cross-sections corresponding to the disecrete-energies of the sources were fed into the code whilst in others standard group libraries were applied with the discrete lines being converted into sources within the appropriate groups.

5.2 Discrete Ordinates

ANISN(13) was the code most widely applied in the comparisons. This code obtains discrete ordinates solutions in one dimension and has the advantage of being quick and convenient to use with convergence being readily achieved in most problems. It was used with the following data libraries:-RADHEAT (Japan), EURLIB III (Switzerland), EURLIB IV (FRG), Reduced EURLIB III (Belgium), BUGLE (Finland) and SCALE (Italy). For gamma-rays alone the GAM50 (FRG) library was also used.

The order of quadrature and order of expansion of the angular dependence of the transfer cross-sections varied with user although these were not specified in all cases. In summary they were S_{16} P_5 (Japan), S_{16} P_3 (Italy) S_{12} P_3 (Switzerland), S_8 P_5 (FRG), and S_8 P_3 (Finland)

SAS1 is the one-dimensional component for calculations in the SCALE Modular Code System (14). The transport solution is obtained with the XSDRNPM-S code which is a highly developed version of ANISN. It is used with the Special SCALE library in the calculations performed for the comparisons, with S_{16} P_3 quadrature and expansion. For dose-points external to the shield SAS1 uses the XSDOSE code to integrate over the angular distribution of the currents leaving the shield surface.

ONEDANT is also a development of ANISN which was used with the EURLIB III (Switzerland) library in several calculations, with an S_{12} P_3 angular description. (15)

FALSTF (16) is a code that estimates the detector responses at points external to the shield. It is run in conjunction with the DORT code in two dimensional geometries, and calculates a scattered flux using a last collision estimator for each of the mesh cells of the problem, and adding this to an analytically calculated uncollided flux.

DOT 3.5 (17) is a two-dimensional discrete ordinates which was used by one participant (Japan) in R-Z calculations performed with the RADHEAT library. It was mostly used with S_8 P_3 approximations but the effect of increasing this to S_{16} P_5 was also studied in some cases.

DORT(18) is an updated version of DOT which was used with the Special SCALE library. In the comparisons it was used for R-Z and R-θ calculations with an S_8 P_3 representation of the angular parameters.

TWODANT(15) is a two-dimensional discrete ordinates code which was used in R,θ calculations for problem 2a with the EURLIB III data library. The quadrature and angular expansion in these cases was $S_{12}P_3$.

5.3 Monte Carlo

MCNP(19) was applied by two participants using point-energy nuclear data in all cases. The code enables the geometries of all the problems to be described without approximations. For acceleration the technique of splitting/Russian roulette was mostly used. Each cell in the problem is assigned an importance by the user, the value being proportional to the estimated probability that particles in the cell will contribute to the quantity being scored. The splitting/Russian roulette process is controlled by changes in the importance as the particle moves from cell to cell. In the calculations carried out by ENEA the importances were derived by using the DSA procedure (20) (21) in which the probabilities of particles progressing from one boundary to the next are assessed in preliminary calculations. The scoring methods used boundary crossing estimation and the once-more collided flux estimator for the dose-rates at a surface with point-estimation for the dose-points remote from the flask.

MCBEND(22) also allows the geometry to be represented explicitly in all cases, and uses nuclear data from the DICE-GAMBLE libraries which are effectively point-energy cross-sections. It is accelerated by superimposing a separate orthogonal mesh over the geometry of the material regions and specifying importances as a function of energy for each of the mesh intervals. The latter are derived by performing an adjoint diffusion calculation an operation which is carried out automatically by the code. Russian roulette and splitting are then controlled by this importance map. Scoring in the problems was performed by track length estimation for thin regions located at the flask surface and at the 1m, 2m and 10m positions.

TRIPOLI (23) is another code which enables the geometry to be treated without approximation, and which uses cross-section data in 315 groups for neutrons which is close to a point energy representation (The energy loss laws and scatter distributions are explicitly sampled). The code has a wide range of acceleration techniques which include splitting and Russian roulette, exponential transform and angular biasing. It has been applied to the benchmark problems for primary neutron and gamma-ray sources, but not for secondary gamma-ray dose-rates.

MORSE (24) is a multigroup code which has been applied by one participant using the NGCP9-70 library. It is also the central transport analysis code of the SAS4 sequence (14) which was applied to the problems with the same SCALE library as was used in SAS1 and DORT calculations. Again the geometry can be described explicitly in the code, and acceleration is achieved by splitting and Russian roulette. In the SAS4 approach the importances which control this process are obtained from adjoint solutions of the discrete ordinates equations in one dimension.

6. Results

6.1 Tabulation of the Results

The results of the calculations as submitted by participants are presented in Tables 7 to 53. In many cases these results have been published in reports issued by the participants. (References 25 to 34). As dose-rates were calculated for points opposite the centre of the cavity, and for values averaged over the cavity area each Table usually shows two separate sets of results. In many cases participants have given dose-rates in both forms obtained with the same method and data, so that it is possible to derive a factor which enables the results in the two sets to be compared. Mean values for the ratio of maximum to cavity-averaged dose-rates, have been obtained from the results for problems 1-4 thus providing factors which can then be used to relate the two sets of results. These ratios are summarised below.

	Neutron	Fission product gamma-rays	Secondary gamma-rays
Radial Surface	1.07	1.03	1.09
Top/Bottom Surface	1.33	1.37	1.28

The results are presented graphically showing the distribution of each set of results, ie cavity centre or cavity-averaged values about the mean. In some cases where results appear to be grossly anomolous they have been omitted from the mean and this is indicated in the table by asterisks. In the discussions on the sets of results for each problem the standard deviation of the distribution of the individual dose-rates about the mean is quoted as an indication of the consistency of the methods. The dose-rates predicted at distances from the flask surface are presented as ratios to the corresponding dose-rate given at the surface. This enables the geometric factors to be compared independently of any differences in the predicted surface dose-rates.

Comments on the results are given for each of the tables. In general these consider the spread on the predictions and mention factors which might explain the observed pattern. In the best cases the standard deviation on the distribution of the predicted dose-rates is less than 10%. In other problems the results of the "exact" methods are found to have a distribution with standard deviations approaching 30%, with the approximate methods showing larger discrepancies. The factors which are possible contributors to the spread in the results are discussed in the sections below.

6.2 Nuclear Data

The results of the comparisons clearly show the importance of the nuclear data. If for example one examines the results for the neutron dose-rate outside the radial shield for problem 1b in Table 16 there is almost a factor of 2 between the maximum and minimum dose-rates calculated by six participants using the ANISN code with different data libraries.

Similarly for primary gamma-rays the FRG calculations with ANISN have in most cases been carried out with two data libraries, EURLIB IV and GAM50, and the ratio of 1.7 between the two results which is observed in problem 1a is typical of the disagreement found in all cases. Many of the libraries are derived from the same basic data file, ENDF/B-IV, so that the differences demonstrate the effect of the choice of group schemes and the weighting spectrum used in group averaging.

This problem was examined in detail by Parks et al (6) who compared calculations for Problem 1a which were performed with seventeen different multigroup libraries. Their results show ratios of factors of 4.08, 1.96, and 1.24 between the maximum and minimum values of the neutron, primary gamma-ray, and secondary gamma-ray dose-rates respectively at the flask surface. For neutrons the conclusion was that the treatment of resonance self-shielding in iron was an important feature of the processing of cross-sections. The introduction of resonance self-shielding in the derivation of a 47 group neutron library increased the dose-rate by a factor of 1.5. The data without self-shielding formed the BUGLE library, which explains why calculations carried out by one participant with this library consistently under-estimated the neutron dose-rate. The other important factors were the energy boundaries of the group scheme, and in particular their relation to the dominant threshold for inelastic scatter in iron at 0.86 MeV. The neutron spectrum in a thick region of iron shows a rapid change in the vicinity of this threshold where the flux per unit lethargy rises with decreasing energy as elastic scatter becomes the only moderating process. As a result of this spectrum and the energy dependence of the conversion factor, the dose-rate outside a steel shield is dominated by neutrons in the range 0.2 MeV to 1 MeV. If a broad group spans this threshold, then the inelastic scatter process is in effect extended down to the lower energy boundary of the group, and it will underestimate the fluxes unless the weighting spectrum used in the preparation of the data was that appropriate to iron. Thus the third key factor in the adequacy of a multigroup library is the choice of the weighting spectrum.

An example quoted by Parks et al (6) was in the use of a spectrum having a 1/E variation matched to a fission spectrum at a chosen energy. When this energy was 0.75 MeV the results were good, but they were poor when the break-point was at 0.1 MeV.

In summary the conclusions of the study of Parks et al for preparing multigroup cross-sections for neutrons were that:-

(a) it is essential to include a proper allowance for self-shielding,

(b) proper weighting spectra must be used when condensing fine-group libraries, and

(c) energy group boundaries must be carefully selected for the particular problem being analysed.

In the calculations the specially selected SCALE library gave results which were in general in excellent agreement with those from the point energy codes for gamma-rays, with a tendancy to underestimate by about 15% for neutrons penetrating cast iron, and by slightly larger amounts for steel.

A further study of the effect of group averaging for neutron cross-sections was carried out by Avery and Locke (35), who calculated the neutron spectrum as a function of the distance penetrated through the wall of the flask in Problem 1a. These results were then used to derive group-averaged total cross-sections for iron at radii of 400mm, 520mm, 650mm, 780mm corresponding to penetrations through the flask wall of 0mm, 120mm, 250mm and 380mm. The energy boundaries were those of the EURLIB scheme with its 100 neutron groups, and for comparison the values were also calculated using $1/E$ and $1/E\Sigma_T$ weighting spectra. The results are shown in Table 54 for those groups in the important energy range 50 KeV to 1 MeV. The Table also includes maximum and minimum values of the cross-section in each energy group to indicate the range of variation. The results show that where this range is large, then the mean cross-section varies significantly with penetration. For example in group 47 where the cross-section has a maximum value of 15.41 barns and a minimum value of 0.27 barns, it is found that the group averaged value decreases from 3.05 barns to 1.28 barns with penetration through the flask wall. The corresponding $1/E$ and $1/E\Sigma_T$ values are 5.91 barns and 1.21 barns so that neither is suitable for calculations for this group. This behaviour is due to the increasing build-up of neutron flux with penetration at those energies where the cross-section is low, and it illustrates the difficulty in deriving a suitable average value for multigroup libraries. For energy groups where the variation is less there is no such problem. In group 53 for example with its maximum and minimum cross-sections of 6.07 barns and 3.81 barns the effective cross-section shows no variation at 4.3 barns compared with $1/E$ and $1/E\Sigma_T$ averaged values of 4.39 and 4.32 barns. In general however, for a material such as iron with its many resonances the appropriate mean-value will be spatially dependent.

For gamma-rays the study by Parks et al (6) showed that the important feature of the libraries was the group width in the key energy range. This can be illustrated by considering the variation of the cross-sections with energy. For Problem 1-4 the gamma-ray sources are given at eight discrete energies, but supplementary calculations (Reference 30 for example) have shown that the external dose-rate is dominated by the source at 2.1 MeV. The accuracy of the multigroup data is largely dependent on how closely the cross-section for the group containing this energy matches the value at the energy itself.

The flask wall is nearly 13 mean-free-paths thick at this energy so that a 1% increase in cross-section is approximately equivalent to a 14% decrease in the external dose-rate. The cross-section of iron at 2.1 MeV is 3.87 barns/atom whereas the cross-sections averaged over typical groups of 2.0 - 2.5 MeV and 2.0 - 3.0 MeV with a flat weighting are 3.74 barns/atom and 3.65 barns/atom respectively. On the assumption of the simple exponential attenuation law this would lead to overestimates by 55% and 109% in the two cases. The effect would be less important if the sources were distributed in energy instead of being discrete lines, so that the difficulty might not arise in general applications. The results do however indicate that care is needed in the choice of group-averaged data for particular cases.

The problems of group averaging for both neutrons and gamma-rays are avoided in Monte Carlo calculations when point-energy data are used. In the comparisons results were obtained with the MCNP, TRIPOLI, and MCBEND codes using four different data libraries. The results are usually in excellent agreement for gamma-rays, as for example on the lid for Problem

1a, 1b where the dose-rates are 29.0, 29.8, 28.8 and 28.8 μSv/hr. For neutrons the methods show much wider differences as for example in the ratio of 1.32 between the maximum and minimum neutron dose-rates for the lid of Problem 1a. There is no consistent trend that is discernable for the results from the three codes, so that other factors are present in addition to the treatment of the neutron cross-sections.

Because the uncertainties due to the group averaging of nuclear data are not present, the results from the point-energy codes have usually been given more weight when discrepancies are apparent in the analysis of each set of dose-rates predictions.

6.3 Mesh Interval

The sizes of the mesh intervals are required to be specified as input data for the discrete ordinates codes. The choice is made by balancing the need for the spacing to be sufficiently small to ensure that the approximations inherent in the difference equations are valid, against the longer computing times and larger storage requirements resulting from the use of more mesh points. This is not usually a problem in one-dimensional calculations, but it may be necessary to compromise to some extent in two-dimensional cases.

When the initial results were submitted for Problem 1 it was found that some of the large spread in dose-rates was due to insufficient mesh points being used. Several participants (25) (26) (29) carried out studies in order to investigate the variation in predictions with mesh size and to determine the minimum values necessary for treating these problems. The conclusion was that a mesh interval of 0.5cm was needed for predicting gamma-ray attenuation in steel, with larger values being acceptable in the source regions where the flux distributions are flatter, and for neutrons where the rate of attenuation is less. However for neutrons in polyethylene an interval of 0.25cm was recommended by Jaeger and Lanfranchi (29). The need was to keep the ratio of the fluxes predicted at adjacent mesh points within an acceptable range, and while there was no agreement on the precise requirement, a value below 0.7 was considered to be one which could lead to errors.

The angular representation of the flux was also examined in several cases. Wasastjerna (8) found that changes of less than 1% in the neutron and gamma-ray dose-rates outside flask 1a resulted from increasing the angular quadrature from S_8 to S_{16}. Jaeger and Lanfranchi (28) observed changes of only 2% in the neutron flux at high energy when moving from S_{12} to S_{16}, while the DOT results of Tanaka in Table 28 show only a 4% increase in the gamma-ray dose-rate outside flask 2a when raising the angular parameters from S_8 P_3 to S_{16} P_5. This is consistent with the conclusion of other participants that S_8 P_3 calculations are satisfactory for these problems.

6.4 Monte Carlo Statistics

A feature of the results obtained with the Monte Carlo Codes is the presence of associated statistical uncertainties. The codes give the standard deviations on the mean of the scores of individual samples. The question which then arises is the significance which can be attached to results in the form of confidence limits based on these uncertainties. Because the distribution is not normal the conventional values are not

applicable, and calculators observe changes in the results as more samples are taken which exceed, on the basis of size and frequency, those which would be expected from assuming such a distribution. In the results presented by participants there are examples of this. For Problem 3b MCBEND has been used to calculate the secondary gamma-ray dose-rate at the surface of the epoxy band at the mid-plane of the flask using one model of an infinitely high flask and another of the actual dimensions of the problem. The difference at the mid-plane is expected to be small and this is confirmed by the MCBEND results for the neutron dose-rates. The MCBEND ratio of the secondary gamma-ray dose-rates with the two models is however, 1.34, and it would be necessary to move both calculations by almost three standard deviations in order to make them consistent. This would be very unlikely if the distributions were normal.

A further example of difficulties experienced in Monte Carlo was shown in the early results obtained by one participant for Problem 1 which were subsequently withdrawn and are not included in the tables. These were calculated with MCNP and gave values which were lower than those of other participants, particularly for the lid of the flask. For problem 1a two other MCNP calculations give neutron dose-rates of 524 μSv/hr which are higher by a factor of 4.0 than the withdrawn value. Similarly for problem 1c the neutron dose-rate at the lid was predicted to be 23 μSv/hr compared with a mean of 61.2 μSv/hr from the other two point-energy codes. The reasons for this discrepancy were never positively identified, but the introduction of bias in the acceleration of the calculation is the likely explanation.

The variation due to statistics and perhaps to the acceleration and scoring techniques is also evident in the absence of any consistent trends in the predictions of the codes. Thus while the MCNP predictions of the fission-product gamma-ray dose-rate outside the radial shield for flask 1a exceed those of MCBEND by 15%, they are in excellent agreement for the corresponding results for Problem 1b.

This suggests that the acceleration techniques must be used with care and that some skill is needed in their application.

6.5 Geometric Modelling

The primary purpose of Problems 2,3 and 4 was to assess the geometric capabilities of the codes and to indicate the accuracies achieved by various simplifications in the representation of the flask and source. There were also geometric approximations involved in Problem 1 when one-dimensional codes were applied. As might be expected with a long flask, the peak dose-rates at the radial surface are predicted satisfactorily by such codes as demonstrated by the results for Problem 1a. For the lid and base of the flask, however, there are difficulties in using one-dimensional methods because there is such a severe radial variation in the dose. (The ratio of the peak value to the mean over the area of the cavity is about 1.35 for neutrons and gamma-rays at the top and bottom surfaces of the flask). It is therefore necessary to apply recipes such as the inclusion of buckling terms, or the reduction to a spherical model equivalent. These procedures are not very reliable, and most of the one-dimensional results submitted for the lid or the base were subsequently withdrawn. The problem is particularly difficult for neutrons as can be seen from the results in the tables, and it is not an approach that can be recommended other than in initial survey calculations.

Problem 2a included two rings of polyethylene rods extending axially within the radial wall of the flask. Explicit representation of this geometry required a three-dimensional capability, although a two-dimensional R-Θ treatment was also able to model the polyethylene discretely, albeit with slightly distorted shapes and for an infinitely high flask. In one-dimensional cases the rods were smeared into annular rings, and four simplified models were employed by various participants. In some the polyethylene was retained as a single material in either one or two rings, the total area of the rings being equal to the sum of the area of the rods in both cases. Alternatively the rods were smeared with steel in annuli enclosed by cylinders of radii equal to those bounding the rings of rods. Calculations performed with MCBEND for an explicit model and for one with two smeared annuli of steel and polyethylene showed that the simplified model underestimated the mean surface dose-rates by factors of 0.62 and 0.70 for neutrons and gamma-rays respectively with the secondary gamma-ray dose-rate being overestimated by 80%. MORSE results for a model with a single ring of polyethylene gave underestimates of the neutron dose-rate by a factor of 0.75 when compared with similar calculations for the full model. This tendency to underestimate is confirmed by the comparison of the one-dimensional results with those obtained with the explicit models.

Problem 2a also showed considerable azimuthal variations in the dose-rate. This was most clearly illustrated in the results obtained with the two-dimensional discrete ordinates codes DORT and TWODANT in R-8 models, as shown in Figures 8, 9 and 10. The azimuthal mesh points over the sector of the flask represented in the model enabled the fine structure to be determined giving a value of approximately 1.2 for the ratio of the maximum to minimum neutron dose-rate. For gamma-rays the two codes give corresponding ratios of 3.3 and 2.0 so that they are not consistent, but this could be due to differences in the nuclear data or mesh specification. The Monte Carlo code MCNP was also used to calculate the azimuthal fine structure, but the need to score in finite volumes meant that the resolution was not as good with each one spanning a 2° sector.

Problem 2b had circumferential bands of epoxy resin set into the outer region of the wall of the flask. Again for one-dimensional models it was necessary to smear the cast iron and polyethylene into a single radial region for the outer 50mm of the wall. MORSE calculations for the neutrons with a smeared model and with the bands retained explicitly showed that the simplification led to an underestimate of the dose-rate at the surface by a a factor of 0.74.

Problem 3b had fins added to the outside of the flask specified for problem 2b so that these had to be smeared with void in a one-dimensional model in addition to the smeared epoxy bands. MCBEND calculations for the model with two smeared bands gave dose-rates which were lower than those for the explicit model by factors of 0.79 and 0.53 for neutrons and gamma-rays respectively, while the secondary gamma-ray dose-rate was higher by a factor of 1.1. This is qualitatively similar to the effect of smearing in problem 2a. An alternative approach for one-dimensional calculations for neutrons was to derive answers with two models, one with a cast iron wall including fins, and one without fins but having the epoxy layer included. A weighted combination of the two results was used to provide the dose-rate, and this was found to agree more closely with the multi-dimensional predictions than that from a single smeared model.

In Problem 4a the source region was specified explicitly as five fuel assemblies contained in a steel basket, the cavity being dry for 4a and flooded for 4b. Again a detailed model would require a three-dimensional capability so that the one and two-dimensional codes have been applied with simplifications. For DOT the central sub-assembly is represented by a cylinder of diameter 269.7mm surrounded by a steel basket wall of thickness 10mm. The remaining four elements are smeared into an annular ring of equal area having an inner diameter 289.7mm and an outer diameter of 613mm. The outer basket wall is again represented by an annulus of steel of thickness 10mm, with the remaining 83.5mm between it and the outer wall of the cavity being a void in Problem 4a, and water-filled in Problem 4b. For SAS1 the model was similar to that for DOT except that the outer wall of the basket was in contact with the inner surface of the flask so that the annular region of thickness 83.5mm was now included with the outer four sub-assemblies. The results show that both smeared models tend to over-estimate the dose-rates slightly for problem 4a, particularly for the SAS1 model where sources have been moved to the outer regions of the cavity. This approach in which sources are moved towards the wall of the cavity is expected to give conservative results. For problem 4b the gamma-ray results are again high with both models, but the ANISN results with the DOT model are low for the neutron dose-rate, presumably because of the shielding effect of the 83.5mm annulus of water surrounding the fuel.

For Problem 4b a series of approximations was applied by Wasastjerna using the ANISN code. The cavity was divided into a number of annular regions and in each case the materials were homogenised within the region. The results for the neutron dose-rate show an increase by a factor of 1.9 as the number of regions is progressively reduced. It is difficult to comment on the absolute accuracy because the data library employed was BUGLE 80 which was shown to underestimate the neutron dose-rates in Problem 1.

The study of the effect of smearing the fuel pins within the compartment of the basket is shown to produce insignificant changes. It is concluded that pins can be smeared without loss of accuracy, provided of course that multiplication within the fuel is not to be included in the shielding calculation.

The comparisons show that simplification of the geometry by smearing shield materials can produce errors, with the primary radiations being underestimated by as much as a factor of 2 in the theoretical exercise. The calculator who employs such methods must be aware that he is sacrificing accuracy for the benefit of computational speed.

6.6 Geometric Attenuation

The attenuation of the dose-rate with distance from the flask wall is determined by the spatial and angular distribution of the particles leaking from its outer surface. The results show that this varies significantly in the problems. For neutrons in problem 1a for example, the attenuation factor for the cavity-averaged dose-rate at 10 metres from the radial surface as predicted by the Monte Carlo Codes is 0.014 while that for gamma-rays is 0.025, which is consistent with the physical picture that gamma-rays penetrating through the steel are more forward peaked than the neutrons which are undergoing more elastic scatter collisions during this

process. For problem 1b with its outer layer of polyethylene the corresponding attenuation factors as calculated for neutrons, fission-product gamma-rays, and secondary gamma-rays are respectively 0.0178, 0.0232, and 0.009. This suggests that the secondary gamma-rays which are born in the outer region of the shield show a smaller degree of collimation than the neutrons or fission product-gammas because they have not suffered much attenuation.

For the lid and the base of the flask where the area of the leakage source is smaller there will be much more attenuation. The calculated factors for the cavity-averaged attenuation at 10 metres for neutrons and gamma-rays are about 0.0025 and 0.006 respectively, with the lid values tending to be slightly higher than for the base.

The variation in the values shows that it is important that the method of calculation is able to accurately predict the angular distribution of the particles leaking from the flask surface. In the Monte Carlo calculations the distribution is automatically included in the tracking of the particles when track length estimation is used to score in volumes centred about the dose-point. The latter have to be made sufficiently large to achieve a satisfactory statistical accuracy without prejudicing the spatial resolution. Alternatively for these remote points a point-estimator can be used where the probabilities of particles reaching the dose-point from each of the collision sites created during tracking enables the dose-rate to be scored, and this approach was used in some of the MCNP calculations. Many of the Monte Carlo results obtained with the SAS4 code appear to give too much attenuation, as is evident from the results at 1 metre from the lid of flask 1a for both neutrons and gamma-rays where its values of 0.08 and 0.11 for the respective attenuation factors are lower than those of 0.147 and 0.289 obtained with the other Monte Carlo codes. Broadhead et al (25) have determinated that this error is due to scoring over an area greater than that of the cavity thus leading to values which are too low. This is consistent with the improvement of the SAS4 results for the 2m point where the effect would be less.

For the two-dimensional discrete ordinates codes it is possible to extend the calculation to mesh points outside the flask and this approach was followed in the application of DOT 3.5. This has produced some results which appear to be anomolous. For example the gamma-rays outside the radial shield of problem 1a show an attenuation factor predicted by DOT of 0.0188 compared with 0.025 from the Monte Carlo results, with corresponding values of 0.0023 and 0.0055 for the base of the flask in the same problem. In other problems the method gives agreement with the Monte Carlo results. Tanaka has postulated that these calculations are distorted by ray-effects which can arise in the discrete-ordinates method when there is penetration with very little scatter. These lead to spatial distributions which are physically unrealistic, and Tanaka has pointed out that this is occuring for gamma-rays at the flask lid of problem 1a where the dose-rates at the mid-point are less than those averaged over the area of the cavity.

In the two-dimensional discrete ordinates code DORT, the possibility of ray-effects distorting the geometric attenuation is avoided by the use of an auxiliary code FALSTF (16) which evaluates the dose-rates at the remote points by integrating last-flight contributions over the density of collisions in the shield as predicted by DORT.

For one-dimensional discrete-ordinates codes the angular distribution as calculated at the flask surface, is combined with an assumed axial distribution in order to derive the dose-rates at the remote points. In general this procedure gives predictions of the attenuation of the dose with distance from the radial shield which are in good agreement with those from other methods, thus confirming that the angular distributions are being calculated accurately.

The kernel method for gamma-rays is based on the calculation of the uncollided flux with the subsequent application of a build-up factor. Thus the attenuation with distance from the flask is effectively that of the uncollided gamma-rays, and these will be much more forward peaked than the scattered component. The attenuation factors are therefore expected to give overestimates of the dose-rates at the 1m, 2m and 10m points, and this behaviour is evident in the results. For problem 1a for example, the attenuation factor at 10m given by the kernel method is 0.039, whereas that from Monte Carlo is 0.025. For the lid the corresponding values are 0.01 and 0.05, the latter being based on the Monte Carlo value of 0.063 for the cavity averaged factor scaled by a peak-to-mean ratio of 1.37.

The results of the comparisons show that the methods which have been applied to predict the geometric attenuation give results which are mostly in agreement and this suggests that they will all give satisfactory accuracy. The exceptions are the use of two dimensional discrete ordinates to predict attenuation through large void regions, which can suffer from ray effects in some cases, and the use of kernel techniques which will always tend to give conservative answers. The flask in the problems 1-4 was assumed to be in vacuum so that the external attenuation was due to geometry and no account was taken of scatter by the air. This is not significant over short distances, but Gualdrini et al (7) have pointed out that the sky-shine effect can significantly increase the dose-rates at large distances from the end of the flask.

7. Conclusions

The contributions of the many participants in the intercomparison of codes have enabled the performances of a wide range of codes and data libraries to be assessed for Problems 1-4. However the exercise suffers from the usual drawback of such theoretical benchmarks because there are no definitive answers against which results can be checked. In some instances the agreement of a number of contributions gives confidence in the predictions, but in other cases where differences exist it is not possible to say which answer is correct. This highlights the second difficulty of the intercomparison; participants were able to apply the methods and data which were in current use at their own establishments to a number of the problems but usually they did not have the time or resources available to enable them to carry out further investigations to try to pin-point the reasons for differences. However the study did stimulate a number of papers on the nuclear data (6) (35) and the problems of carrying out shielding calculations for transport flasks (36) (37) (38) as well as providing a body of results for the four benchmark problems. It is therefore possible to draw useful conclusions from the results of this work based on the points discussed in section 6 above, even though all of the discrepancies have not been resolved.

The first conclusion is that wherever possible it is preferable to use point-energy data in order to avoid the difficulties associated with the averaging of cross-sections in multigroup libraries. It is possible to choose a particular library and validate it for a given application, but unless this process has been undertaken, the results obtained from multigroup calculations cannot be used with confidence. The usual approaches for averaging neutron cross-sections which are based on slowing-down spectra in infinite regions, can produce anomolies in typical flask shields where there is very little moderating material and the spectrum changes with penetration. However, multigroup data such as the special SCALE library which was validated for this type of problem have been shown to perform reasonably well. It is also advisable to validate the point-energy data by comparison with the results from experimental benchmarks, but such validations may be expected to have a wider range of application because they do not include the need for the assumptions inherent in the multigroup approach.

For gamma-rays the comparison illustrated a further difficulty in the use of group data when the sources are specified at discrete energies. If such an energy is close to the boundary of the appropriate group, then errors can arise over the large attenuations involved in the shields of spent fuel flasks unless the group widths are kept small. These errors can be estimated from the variation of the cross-section within a group and the number of mean-free-paths involved in the attenuation.

The second conclusion is that it is beneficial to be able to model the flask and its contents in three dimensions if accurate answers are required. Whilst it was possible in most cases to treat the theoretical Problems 1-3 with two-dimensional models, the results for Problem 4 in which the fuel and basket are specified explicitly show that a three-dimensional representation has advantages. This is similar to the practical problem in which fuel assemblies of rectangular shape are carried in flasks having cylindrical cavities. The smearing of the assemblies into simplified geometries was shown to introduce errors into the calculations, the size and nature of which depended upon the type of radiation and the choice of the approximate model. Again it would be possible to validate a simplified representation of a particular geometry but this would require comparisons either with calculations using an exact model or with measurements on a practical flask.

The results given in this report should be helpful in choosing such approximations. It should be noted however, that the simplified models of the fuel assemblies were in R or R-Z geometry. It would be possible to achieve a closer representation for the mid-plane of the flask by using an R-θ mesh and neglecting the axial variation, but this approach was not examined in this study.

The first two conclusions point to the advantage of using Monte Carlo methods with point-energy data. This is counterbalanced by the experience of some participants who obtained erroneous answers when using such codes. This was evident in the MCNP predictions which were withdrawn from the final tables of results, and it may still be present to a lesser extent in one or two of the remaining dose-rates obtained with Monte Carlo methods. It is therefore concluded that there is a need to make such codes robust so that they are less susceptible to bias and do not require special skills in

their application. The principal danger lies in the use of techniques and scoring methods which distort the generation of the tracks, in particular by stretching path lengths when such distorted tracks are not similar to those which dominate the penetration in the physical situation. It may be that these facilities should be retained only in special versions for use by skilled calculators, whilst a more robust code is made available for the general shield designer. Alternatively it might be possible to automate the choice of methods of acceleration and scoring so that the code itself would be able to avoid such errors.

The third conclusion is that the deterministic methods using the discrete ordinate approach show advantages in calculating fine structures in the dose-rates at the flask surface where these arise from discontinuities in the configuration of shield materials. The Monte Carlo codes cannot match the spatial resolution obtained with such methods.

The fourth conclusion is that the mesh intervals in discrete ordinates calculations are of vital importance and checks must be carried out to ensure that they are sufficiently fine to avoid the introduction of errors.

The fifth conclusion is that the kernel methods are very useful tools for gamma-ray calculations. In general they perform satisfactorily, and in Problem 4 it was clear that the use of an approximate method with a detailed representation of the geometry was preferable to some of the transport solutions with simplified models.

In looking to the future, the increases in the speed and capacity of the computing facilities which are becoming generally available suggest that the intensive computing requirements for the Monte Carlo method may become less of a barrier to its wider application. In the intercomparison study it has been seen to have advantages in its direct use of nuclear data and its ability to model flask geometries, so that the need for reliable Monte Carlo codes which can be readily applied without the danger of introducing bias is likely to become more pressing.

Acknowledgements

The authors would like to thank the many participants in the inter-comparisions for their contributions to the work and for their helpful comments in the preparation of this report. A list of the participants for problems 1-4 is given below. In additional we would particularly thank P Nagel and E Sartori and their staff at the NEA for their contributions in organising the exercise and arranging the meetings.

Participants

The many participants who have carried out calculations for the intercomparison for Problems 1-4 and contributed to the study through discussions at the meetings are listed below

Belgium

A Renard, Belgonucleaire, Brussels

Canada

G B Wilkin, AECL, Whiteshell

Finland

F Wasastjerna, Nuclear Engineering Laboratory, Helsinki

France

L Bourdet, CEN, Saclay
I Bresard, CEN, Saclay
C Diop, CEN, Saclay
J C Nimal, CEN, Saclay

Germany

W Denk, GRS, Garching
K Gewehr, GRS, Garching
J Weber, GRS, Garching

Italy

K W Burn, ENEA, Bologna
L Casalini, ENEA, Bologna
G F Gualdrini, ENEA, Bologna
S Mancioppi, ENEA, Rome
S Monti, ENEA, Bologna
P Peerani, ENEA, Bologna

Japan

Y Sakamoto, JAERI, Tokai-Mora
S Tanaka, JAERI, Tokai-Mora
K Ueki, Ship Reasearch Institute, Tokyo

NEA

P Nagel, NEA, Paris
E Satori, NEA, Paris

Netherlands

J E Hoogenboom, Delft Technology University
J Kloosterman, Delft Technology University

Sweden

D Mennerdahl, P1 457, 5-186 00 Vallentuna

Switzerland

J F Jaeger, Paul Scherrer Institute
M Lanfranchi, Paul Scherrer Institute

United Kingdom

A F Avery, AEA Technology, Winfrith
J Hobson, BNFL, Risley
Mrs H F Locke, AEA Technology, Winfrith

United States

M C Brady	Oak Ridge National Laboratory
B L Broadhead	"
S N Cramer	"
B L Kirk	"
C B Parks	"
J S Tang	"
R M Westfall	"

References

1 Denk W "An FRG Proposal for an International Intercomparison of Codes for Radiation Protection Assessment of Transportation Packages". NEACRP-L-290 plus Addendum (Avery A F, AEA Winfrith, UK, November 1987).

2 Avery A F. "Summary of the Second Meeting of the NEACRP Intercomparison of Codes for the Shielding Assessment of Transportation Packages" NEACRP-A-864, AEE Winfrith, UK. September 1987.

3 Avery A F. "Progress with the NEACRP Intercomparison of Codes for the Shielding Assessment of Transportation Packages" NEACRP-A-895, AEE Winfrith, UK, October 1988.

4. Avery A F. "Status Report on the Intercomparison of Shielding Codes for Transport Flasks - October 1989" NEACRP-A-1004, Winfrith Technology Centre, Dorchester, Dorset, UK.

5. Avery A F. "Status Report on the Intercomparison of Shielding Codes for Transport Flasks - October 1990" NEACRP-A-1107, Winfrith Technology Centre, Dorchester, Dorset, UK.

6 Parks C V. Broadhead B L, Roussin R W, Gautley J C, Cramer S N, and Kirk B L. "Intercomparison of Cross-Section Libraries used for Spent Fuel Cask Shielding Analysis". Paper presented at ANS Topical Conference on Theory and Practices in Radiation Protection and Shielding, Knoxville, Tennessee. April 1987.

7 Gualdrini G F, Burn KW, Casalini L, Peerani P, "The ENEA contribution to the NEA-CRP International Intercomparison of Codes for Radiation Protection Assessment of Spent Fuel Transport Flasks" ENEA/RT(AMB)(1991) ENEA, Bologna, Italy.

8 Wasastjerna F. "Finnish Results for the Intercomparison of Codes for Radiation Protection Assessment of Transportation Packages: Case 1" RFTT-3/86. Technical Research Centre of Finland, Nuclear Engineering Laboratory, Helsinki (1986).

9 Burn K W, Panini G C. "THEMIS Modules used at ENEA to produce an ACE Format Neutron Cross-Section Library for the Monte Carlo code MCNP" Paper presented at AGT-3 meeting, March 1987.

10 "RANKERN-A Point Kernel Integration Code for Complicated Geometry Probems". User Guide for RANKERN 12 available from the ANSWERS Service, AEA Technology, Winfrith UK (November 1986).

11 "QAD-CGGP. A combinatorial Geometry Version of QAD-P5A. A Point Kernel Code System for Neutron and Gamma-ray Shielding Calculations using the GP Build-up Factor". Available from Radiation Shielding Information Center at Oak Ridge National Laboratory as CCC/493/QAD-CGGP

12 QAD CG "A Combinatorial Geometry Version of QAD P5A -A Point Kernel Code for Neutron and Gamma-ray Shielding Calculations", available from Radiation Shielding Information Center at Oak Ridge National Laboratory as CCC-307

13 ENGLE W W. "A User's Manual for ANISN - A One-Dimensional Discrete Ordinate Code with Anisotropic Scattering". K-1693, Union Carbide Corp. Nuclear Div, Oak Ridge Gaseous Diffusion Plant (March 1967). Available from Radiation Shielding Information Center at Oak Ridge National Laboratory as CCC-254.

14 "SCALE": A Modular Code System for Performing Standardised Computer Analyses for Licensing Evaluation" Vol 1-3 "NUREG/CR-0200, Rev 4, US Nuclear Regulatory Commission final draft issued February 1990. Available from Radiation Shielding Information Centre at Oak Ridge National Laboratory.

15 Jaeger J F. "Intercomparison of Codes for Shielding Assessment of Transportation Packages-Detailed Analysis of Case 2a" TM-41-89-14. Paul Scherrer Institute (1988).

16 Baker V and Childs RL. "FALSTF: Calculator of Response of Detectors External to Shielding Configuration", available from the Radiation Shielding Information Centre at Oak Ridge National Laboratory as CCC-351.

17 Rhoades W A and Mynatt F R. "The DOT 3.5 Two-Dimensional Discrete Ordinates Code", available from the Radiation Sheilding Information Centre at Oak Ridge National Laboratory as CCC-276.

18 Rhoades W A and Childs R L. "The DORT Two-Dimensional Discrete Ordinates Code" Nuc. Sci and Eng Vol 99 pp 88-89. May 1988.

19 "MCNP-A Generalised Monte Carlo Code For Neutron and Photon Transport Version 3A" LA-7396-M, Rev.2. Los Alomos Monte Carlo Group Los Alamos National Laboratory, September 1986. Available from Radiation Shielding Information Centre at Oak Ridge National Laboratory as CCC-200.

20 Dubi A, Goldfield A, Burn K W. "An Automatic Package for Optimisation of Splitting in the MCNP Code" Proc. of Int. Topical Meeting on Advances in Reactor Physics, Mathematics and Computation.. OECD/NEA Paris (1987).

21 Burn K W, Dubi A, Goldfield A, and Tinti R. "Developments in the Direct Statistical Approach to Monte Carlo Optimisation" Proceedings of the 7th International Conference in Radiation Shielding Bournemouth 1988.

22 "MCBEND-A General Geometry Monte Carlo Program for Deep Penetration Studies". User Guide for MCBEND 7 available from the ANSWERS Service, AEA Technology, Winfrith UK. (January 1989).

23 Nimal J C. "TRIPOLI-2. A Three-Dimensional Monte Carlo Code System" ORNL-OLS-80.110.

24 Emmett M B. "The MORSE Monte Carlo Radiation Transport Code System" ORNL-4972, February 1983; ORNL - 4972/Rs, July 1984, Union Carbide Corp, Nuclear Div, Oak Ridge National Laboratory.

25 Broadhead B L, Brady M C, and Parkes C V. "Benchmark Shielding Calculations for the NEACRP Working Group on Shielding Assessment of Transportation Packages". ORNL/CSD/TM-272, Martin Marietta Energy Systems, Inc, Oak Ridge National Laboratory, (November 1990).

26 Renard A. "Intercomparison of Codes for Shielding Assessment of Transportation Packages OECD/NEA Problems 1a, 1b, and 1c". Belgonucleaire Report 098.31/22/n/6015, (September 1986).

27 Renard A. "Intercomparison of Codes for Shielding Assessment of Transportation Packages Problems 2a, 3b,and 4a". Belgonucleaire Report 098.31/22/n/7002, (March 1981).

28 Jaeger J F and Lanfranchi M. "Intercomparison of Codes for Shielding Assessment of Transportation Packages - Detailed Analysis of Case 1a Side Wall" TM-22-87-03, EIR, Wurenlingen, Switzerland (February 1987).

29 Jaeger J F and Lanfranchi M. "Intercomparison of Codes for Shielding Assessment of Transportation Packages. Detailed Analysis of Case 1b Side Wall" TM-22-87-13, EIR, Wurenlingen, Switzerland (April 1987).

30 Locke Mrs H F. "NEACRP Intercomparison of Codes for the Shielding Assessment of Transport Packages - Solution to Problem 1a" RP&SG/HL/P(87)26. AEE, Winfrith, UK (1987).

31 Locke Mrs H F. "NEACRP Intercomparison of Codes for the Shielding Assessment of Transport Packages - Solution to Problem 1(b)" RP&SG/AL/P(87)86, AEE, Winfrith, UK (1987).

32 Locke Mrs H F. "NEACRP Intercomparison of Codes for the Shielding Assessment of Transport Packages - Solution to Problem 2(a)" RP&SG/AL/P(87)87, AEE, Winfrith UK (1987).

33 Locke Mrs H F. "NEACRP Intercomparisons of Codes for the Shielding Assessment of Transport Packages - Solution to Problem 3(b)"RP&SG/AL/P(87)88, AEE, Winfrith UK (1987)

34 Locke Mrs H F. "NEACRP Intercomparison of Codes of the Shielding Assessment of Transport packages - Solutions to Problems 4(b) and 1(c)" RP&SG/HL/P(88)20, AEE, Winfrith, UK (1988).

35 Avery A F and Locke Mrs H F. "The use of Multigroup Cross-Sections in Neutron Calculations for NEACRP Flask Problem 1(a)" RP&SG HFL/P87(94), AEE Winfith UK (1987).

36 Parks C V, Broadhead B L and Tang J S. "Comparison of Calculational Methods for Analysis of Spent Fuel Cask Shielding" Proceedings of the 7th International Conference on Radiation Shielding, Bournemouth 1988.

37 Avery A F. and Locke Mrs H F. "Shielding Calculations for Fuel Transport Flasks" Proceedings of the 7th International Conference on Radiation Shielding, Bournemouth 1988"

38 Gualdrini G F, Burn K W, Casalini L, and Peerani P. "The ENEA Contribution to the NEA-CRP Internationsl Intercomparison of Codes for Radiation Protection Assessment of Spent Fuel Transport Flask" Proceedings of the 7th International Conference on Radiation Shielding, Bournemouth 1988"

TABLE 1

MATERIAL COMPOSITIONS

Material	Density (g/cm^3)	Content	(% by weight)
Stainless Steel A (Cask, Fuel and Basket)	7.8	Mn Cr Ni Fe	2.0 18.0 10.0 70.0
Stainless Steel B (Lid only)	7.7	Mn Cr Ni Fe	1.5 12.5 4.0 82.0
Cast Iron	7.0	C Si Ni Fe	3.25 1.40 1.10 94.25
Polyethylene	0.91	C H	85.6 14.4
Epoxy Resin	1.25	C H O	76.3 6.7 17.0
Zircalloy -4	6.5	Zr Sn Fe	97.9 1.6 0.5
Source (Dry)	1.97	U-235 U-238 O Zr-4 Steel (A)	1.6 49.1 6.1 16.6 26.6
Source (Wet)	2.81	U-235 U-238 O Zr 4 Steel (A) Water	1.1 34.4 4.3 11.6 18.6 30.0

TABLE 2

NEUTRON FLUX-TO-DOSE CONVERSION FACTORS

$$\ln (F_n(E)) = A + BX + CX^2 + DX^3$$

where $F_n(E)$ is the conversion factor (rem/hr per $n/cm^2.s$)

E is the neutron energy (MeV), and

$X = \ln E$

Values of A, B, C and D are specified for the energy ranges in the table below.

Neutron Energy (MeV)	A	B	C	D
2.5, -8 to 1.0, -7	-1.2514, 1	-	-	-
1.0, -7 to 1.0, -2	-1.2210, 1	1.7165, -1	2.6034, -2	1.0273, -3
0.01 to 0.1	-8.9302	7.8440, -1	-	-
0.1 to 0.5	-8.6632	9.0037, -1	-	-
0.5 to 0.1	-8.9359	5.0696, -1	-	-
1.0 to 2.5	-8.9359	-5.5979, -2	-	-
2.5 to 5.0	-9.2822	3.2193, -1	-	-
5.0 to 7.0	-8.4741	-1.8018, -1	-	-
7.0 to 10.0	-8.8247	-	-	-
10.0 to 14.0	-1.1208, 1	1.0352	-	-
14.0 to 20.0	-9.1202	2.4395, -1	-	-

Note: 2.5, -8 = 2.5×10^{-8}

The factors are taken from ANSI/ANS 6.1.1 - 1977

TABLE 3

GAMMA-RAY FLUX-TO-DOSE CONVERSION FACTORS

$$\ln (F_g(E)) = A + BX + CX^2 + DX^3$$

where $F_g(E)$ is the conversion factor (rem/hr per $\gamma/cm^2.s$)

E is the gamma-ray energy (MeV), and

$X = \ln E$

Values of A, B, C and D are specified for the energy ranges in the table below.

Photon Energy (MeV)	A	B	C	D
0.01 to 0.03	-2.0477, 1	-1.7454	-	-
0.03 to 0.5	-1.3626, 1	-5.7117, -1	-1.0954	-2.4897, -1
0.5 to 5.0	-1.3133, 1	7.2008, -1	-3.3603, -2	-
5.0 to 15.0	-1.2791, 1	2.8309, -1	1.0873, -1	-

Note -2.0477, 1 = -2.0477×10^1

The factors are taken from ANSI/ANS 6.1.1 - 1977

Table 4

Gamma-ray Source Strengths

Energy (MeV)	Source Strength (γ/s)
0.6	2.53×10^{16}
0.7	2.32×10^{16}
1.0	6.95×10^{14}
1.3	5.50×10^{14}
1.7	6.15×10^{12}
2.1	2.70×10^{14}
2.4	2.54×10^{12}
2.8	1.32×10^{12}

The above are the total sources from fission products within the flask.

DIMENSIONS AND MATERIALS

Component	Size		Materials and Problems
Cavity (See Fig 1)	Diameter Height	800 mm 4500 mm	Smeared Source (Dry) 1a, 1b, 2a, 2b, 3a, 3b Smeared Source (Wet) 1c Assemblies and Basket (Dry) 4a Assemblies and Basket (Wet) 4b
Flask Wall	Inner Diameter Outer Diameter	800 mm 1560 mm	Cast Iron 1a, 1c Steel (A) 3a Cast Iron and Polythene Layer 1b Steel (A) with Polythene Rods 2a Cast Iron and Epoxy Bands 2b, 3b
Lid (See Fig 1)	Thickness	420 mm	Steel (B) All problems
Base (See Fig 1)	Thickness	380 mm	Cast Iron 1a, 1b, 1c, 2b, 3b, 4a, 4b Steel (A) 2a, 3a
Polythene Rods (See Fig 2)	Diameter Length	70 mm 5300 mm	2a
Epoxy Bands (See Figs 3 and 5)	Height Inner Diameter Outer Diameter Vertical Separation	80 mm 1460 mm 1560 mm 80 mm	2b and 3b
Fins (See Figs 4 and 5)	Length Height at Base Height at Tip Vertical Separation Number (Mid-plane of first fin is level with the top of the cavity)	120 mm 50 mm 20 mm 80 mm 35	Steel (A) 3a Cast Iron 3b
Basket (See Fig 6)	Height Plate Thickness Weight Compartment Size	4400 mm 10 mm 1043 Kgm 239 x 239 mm	Steel (A) 4a, 4b

TABLE 6

FUEL ASSEMBLY

Component	Dimension	Material	Weight per Assembly (Kgm)
Total Length	4450 mm		
Width over Flats	230 mm		
Total Length of Rods	3930 mm		
Length of Active Fuel	3420 mm	UO_2	513.7
Length of Lower Rod Plug	18 mm	Steel A	0.74
Length of Bottom Expansion Space	314 mm		
Length of Top Expansion Space	160 mm		
Length of Upper Rod Plug	18 mm	Steel A	0.74
Height of Bottom End Fitting	230 mm	Steel A (density 1.01gm/cc)	12.3
Height of Top End Fitting	270 mm	Steel A (density 1.01gm/cc)	14.4
Void between Rods and Bottom End Fitting	10 mm		
Void between Rods and Top End Fitting	10 mm		
Number of Rod Positions	15 x 15		
Number of Fuel Rods	210		
Number of Control Tubes	15		
Rod Pitch (Square)	15.3 mm		
Pellet Outer Diameter	9.69 mm	UO_2	
Cladding Inner Diameter	10 mm	Zr-4	135.9
Outer Diameter	11.5 mm		
Guide Tube Inner Diameter	12.5 mm	Zr-4	11.9
Outer Diameter	14.0 mm		

Note Fuel Assemblies rest on the flask base positioned centrally within each compartment

Problem 1a Radial Neutron

Cylindrical Source, Dry, Cast Iron Wall, No Neutron Shielding

For the dose-rates averaged over the height of the cavity the mean value is 532 μSv/hr with a standard deviation on the distribution of 44μSv/hr (8%). Three of the four point energy Monte Carlo calculations are above this mean, while four of the five multigroup results lie below it.

The four calculations which give results for both the cavity-averaged and the mid-height dose-rate show a consistent ratio of 1.07 between the two. The mean dose-rate of 532 μSv/hr thus translates to 569 μSv/hr at the mid-height.

The mean value of the one-dimensional results for the mid-height value is 568 μSv/hr with a standard deviation on the distribution of 51 μSv/hr (9%).

The agreement is very good, especially when it is remembered that the attenuation though the flask wall is a factor of 80. The geometric attenuations are in general agreement apart from the SAS4 values for the cavity-average dose-rate which appears to give too much attenuation. This is attributed by Broadhead et al (25) to the use of a large scoring region in SAS4 which extends beyond the height of the cavity thus giving a lower dose-rate.

Table 7. 1a radial neutron

METHOD	CODE	CONTRIBUTOR	DOSE RATE AT SURFACE (microSv/h)	DOSE ATTENUATION 1 m	2 m	10m
Values at the axial mid-point						
1D Sn	ANISN	Italy	618	0.303	0.162	0.0131
	ANISN	Belgium	647	0.346	0.190	0.0144
	ANISN	Japan	553			
	ANISN	Switzerland	580	0.328	0.155	
	SAS1	USA	517	0.311	0.173	0.0155
	ANISN	FRG	580	0.310	0.172	0.0155
	ANISN	Finland	350**	0.314	0.166	0.0131
2D	DOT 3.5	Japan	544	0.281	0.161	0.0132
	DORT	USA	518	0.305	0.162	0.0131
Monte Carlo (Gp)	SAS4	USA	508*	0.299	0.159	0.0129
Monte Carlo (Pt)	MCBEND	UK	552 (11%)			
	MCNP	Italy	625 (1.8%)	0.307	0.165	0.0133
Axially averaged values over the cavity area						
2D	DOT 3.5	Japan	510	0.264	0.150	0.0137
	DORT	USA	485			
Monte Carlo (Gp)	SAS4	USA	476 (4%)	0.223	0.124	
	MORSE	Japan	524 (3%)	0.300	0.155	0.0125
Monte Carlo (Pt)	MCNP	USA	589 (2%)	0.336	0.177	0.0144
	MCNP	Italy	581 (1%)	0.286	0.151	0.0143
	MCBEND	UK	513 (5%)	0.314	0.170	
	TRIPOLI	France	574 (6%)	0.286	0.151	0.0140

Monte Carlo uncertainties=1 standard deviation

*surface value not directly calculated, inferred from SAS4(ave.) x DORT(midpoint)/DORT(ave.)
**not included in mean

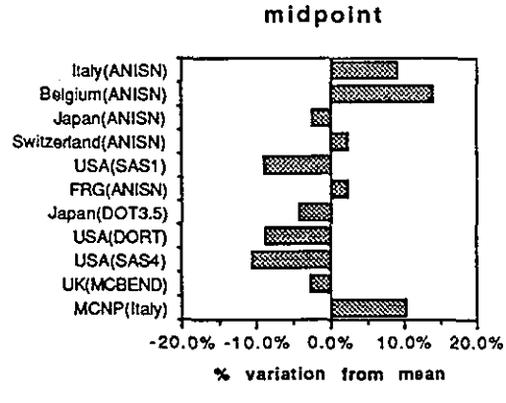

Mean = 567.5μSv/h

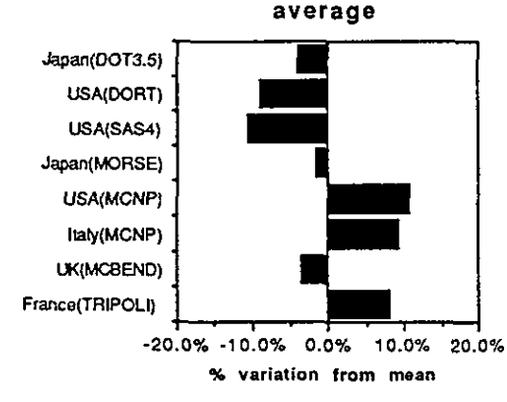

Mean = 531.5μSv/h

Problem 1a Radial-Fission Product Gamma-rays

Cylindrical Source, Dry, Cast Iron Wall, No Neutron Shielding

The mean value of the dose-rate averaged over the height of the cavity as calculated by the four point-energy methods is 284 μSv/hr with a standard deviation on the distribution of 16.4 μSv/hr (6%). This is in good agreement with the multigroup results from SAS4 and DORT.

The multigroup results at the axial mid-point show a wider spread ranging from 250 μSv/hr to 417 μSv/hr (omitting the value of 610 μSv/hr) and the ANISN results with the GAM5O and EURLIB libraries show a ratio of 1.67 in the predicted dose-rates. The attenuation is large, a factor of 4.5×10^6 between that at the inner and outer surfaces of the radial wall, which explains the sensitivity to changes in cross-section. For exponential attenuation a 1% uncertainty in cross-section would lead to a 17% uncertainty in dose-rate. Because gamma-rays migrate less readily in iron than neutrons, the ratio of the mid-height dose-rate to that averaged over the cavity height should be less than that for neutrons. Using the mean ratio of 1.03 (see section 6.1) gives a mid-height dose-rate of 292 μSv/hr equivalent to the cavity-averaged value of 284 μSv/hr.

This is in excellent agreement with the results of the kernel codes, apart from the QAD-CGGP value obtained with group-averaged cross-section. This clearly shows the superior accuracy of the use of point energy cross-sections when the sources are specified at discrete energies. The spread of the mid-height dose-rates obtained with the one-dimensional discrete-ordinates codes is indicative of the variety of libraries employed.

The geometric attenuation factors are higher than those for neutrons indicating a more forward peaked angular distribution of the dose-rate at the flask surface. The kernel methods give too little attenuation because the scattered gamma-rays are assumed to have the same angular distribution as those which are uncollided. The SAS4 values for the cavity-averaged factors again appear to be too small, due to the larger scoring volumes employed as discussed for the radial neutron results for Problem 1a.

Table 8. 1a radial FP gamma

METHOD	CODE	CONTRIBUTOR	DOSE RATE AT SURFACE (microSv/h)	DOSE ATTENUATION 1 m	2 m	10 m
Values at the axial mid-point						
Kernel	QAD-CGGP	Japan(a)	364	0.434	0.274	0.0393
		Japan(b)	293	0.433	0.276	0.0396
	QAD-CG	Belgium	282	0.429	0.273	0.0355
	RANKERN	UK	293	0.461	0.289	
	QAD	US	296	0.432	0.275	0.0395
1D Sn	ANISN	Belgium	358	0.405	0.260	0.0316
	ANISN	Japan	404			
	ANISN	Switzerland	410	0.414	0.244	
	SAS1	USA	268	0.381	0.231	0.0278
	ANISN	FRG (c)	250	0.360	0.216	0.0280
	ANISN	FRG (d)	417	0.353	-	0.0230
	ANISN	Finland	610**	0.361	0.197	0.0180
2D	DOT 3.5	Japan	372	0.382	0.221	0.0190
	DORT	USA	268	0.391	0.233	0.0250
Monte Carlo (Gp)	SAS4	USA	264*	0.423	0.215	0.0257
Monte Carlo (Pt)	MCBEND	UK	303 (12%)			
	MCNP	Italy	323 (2.8%)	0.387	0.224	0.0248
Axially averaged values over the cavity area						
2D	DOT 3.5	Japan	361	0.355	0.198	0.0188
	DORT	USA	264			
Monte Carlo (Gp)	SAS4	USA	260 (3%)	0.267	0.161	
Monte Carlo (Pt)	MCNP	USA	279 (6%)	0.398	0.240	0.0269
	MCNP	Italy	304 (1%)	0.348	0.200	0.0247
	MCBEND	UK	265 (4%)	0.362	0.207	
	TRIPOLI	France	289 (4%)	0.349	0.201	0.0249

(a) Group averaged cross section
(b) Discrete energy cross section
(c) GAM50 library
(d) EURLIB library
*surface value not directly calculated, inferred from SAS4(ave.) x DORT(midpoint)/DORT(ave.)
** not included in mean

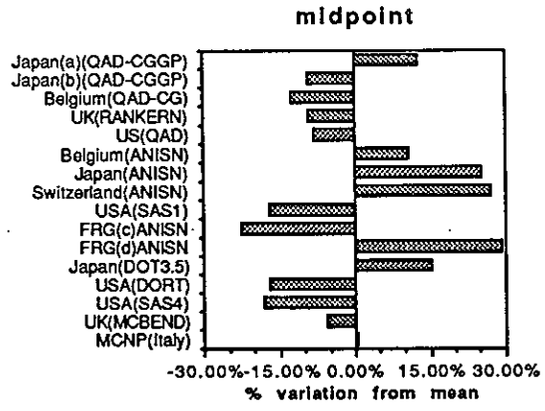

mean = 322.8 μSv/h

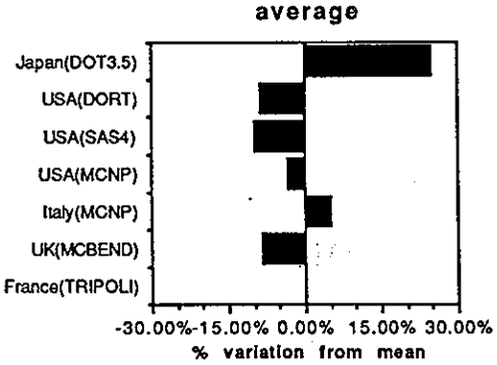

mean = 288.9 μSv/h

Problem 1a Radial Secondary Gamma-rays

Cylindrical Source, Dry, Cast Iron Wall, No Neutron Shielding

Fewer results were submitted for this contribution to the dose-rates outside the radial shield of Flask 1a, presumably because the levels are low compared with those arising from the other sources.

The agreement is good, the value of 4.1 μSv/hr at the mid-height being equivalent to 3.8 μSv/hr averaged over the cavity height. The sensitivity to group data as shown by the GAM50 and EURLIB results is directly opposite to that found for the fission product sources. In that case the EURLIB results were higher by a factor of 1.67 whereas for the secondary gamma-rays they are lower by 0.67. This suggests that the cross-section differences change sign with energy.

The geometric attenuations are closer to those for neutrons than for fission-product gamma-rays which suggests that the important sources are those near to the outer surface of the flask.

Table 9. 1a radial secondary gamma

METHOD	CODE	CONTRIBUTOR	DOSE RATE AT SURFACE (microSv/h)	DOSE ATTENUATION 1 m	2 m	10 m
Values at the axial mid-point						
1D Sn	SAS1	US	4.10	0.322	0.183	0.0163
	ANISN	Italy	4.10	0.317	0.171	0.0146
	ANISN	FRG (a)	4.50	0.311	0.178	0.0156
	ANISN	FRG (b)	3.00	0.300	-	0.0133
2D	DORT	USA	4.10	0.312	0.166	0.0134
Monte Carlo (Gp)	SAS4	USA	3.80*	0.342	0.163	0.0129
Monte Carlo (Pt)						
Axially averaged values over the cavity area						
2D	DORT	USA	3.81			
Monte Carlo (Gp)	SAS4	USA	3.53 (4%)	0.235	0.133	
Monte Carlo (Pt)						

(a) GAM50 library
(b) EURLIB library

*surface value not directly calculated, inferred from SAS4(ave.) x DORT(midpoint)/DORT(ave.)

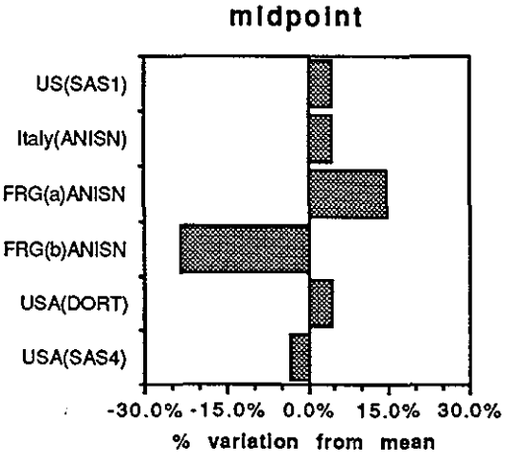

mean = 3.93 μSv/h

Problem 1a/1b Lid Neutron

Cylindrical Source, Dry, Steel Lid, 1a No Neutron Shielding
1b 6cm Polyethylene on outer Radial Surface

The point-energy calculations give a mean dose-rate averaged over the cavity area of 497 μSv/hr with a distribution having a standard deviation of 53 μSv/hr (11%). Without the TRIPOLI result the corresponding values are 520 $\pm$ 3% μSv/hr. This is in good agreement with the DOT 3.5 results but significantly higher than those from DORT which is also a discrete ordinates code. SAS4 which uses the same multigroup data as DORT but with Monte Carlo tracking gives results which are also lower than those of the point energy Monte Carlo but consistent with the DORT value.

The one dimensional results have to use recipes to allow for the severe geometric attenuation and radial leakage in the lid and are therefore subject to large uncertainties.

The overall mean value for the ratio of mid-point cavity-averaged values is 1.33 (see Section 6.1) which is indicative of the severe radial variation in the dose-rates and underlines the difficulty of using a one-dimensional approach.

As might be expected there is much more geometric attenuation than in the radial case. Using the 1.33 factor to scale the values for the mid-point and assuming that there is little variation over the area of the cavity at the 1m, 2m and 10m dose-points gives factors for DORT which agree with those of the point-energy Monte Carlo methods. The DOT 3.5 values seem to be significantly larger. The SAS4 factors for the cavity averaged dose-rates are again smaller than the others,because of the larger scoring areas.

Table 10. 1a/b lid neutron

METHOD	CODE	CONTRIBUTOR	DOSE RATE AT SURFACE (microSv/h)	DOSE ATTENUATION 1m	2m	10m
Values at the mid-point						
1D Sn	ANISN	Belgium	626	0.131	0.046	0.00187
	ANISN	FRG (1a)	330	0.303	0.103	0.00455
	ANISN	FRG (1b)	320	0.300	0.103	0.00468
2D	DOT 3.5	Japan (1a)	687	0.160	0.074	0.00294
	DOT 3.5	Japan (1b)	685	0.159	0.072	0.00206
	DORT	USA (1a)	413	0.115	0.036	0.00160
	DORT	USA (1b)	412	0.114	0.035	0.00160
Monte Carlo (Gp)	SAS4	USA (1a)	401*	0.122	0.038	0.00174
		USA (1b)	375*	0.119	0.037	0.00168
Monte Carlo (Pt)						
Radially averaged values over the cavity area						
2D	DOT 3.5	Japan (1a)	513	0.172	0.078	0.00366
	DOT 3.5	Japan (1b)	512	0.170	0.075	0.00252
	DORT	USA (1a)	313			
	DORT	USA (1b)	312			
Monte Carlo (Gp)	SAS4	USA (1a)	304 (6%)	0.080	0.037	
	SAS4	USA (1b)	284 (5%)	0.077	0.037	
Monte Carlo (Pt)	MCNP	USA	524 (6%)	0.155	0.049	0.00229
	MCBEND	UK(AEA)	536 (7%)	0.146	0.054	
	MCNP	Italy	523 (6%)	0.154	0.053	0.00254
	TRIPOLI	France	406 (5%)	0.144	0.048	0.00217
	MCBEND	UK(BNFL)(1b)	495	0.138	0.049	0.00355

*surface value not directly calculated, inferred from SAS4(ave.) x DORT(midpoint)/DORT(ave.)

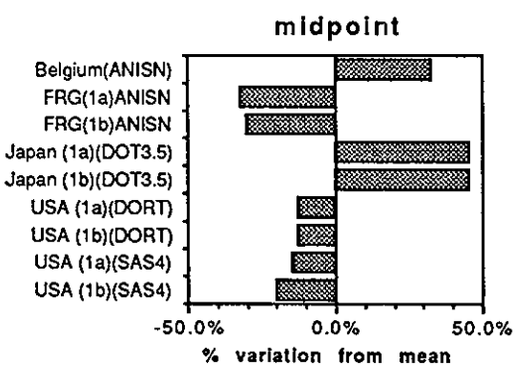

mean = 472.1 μSv/h

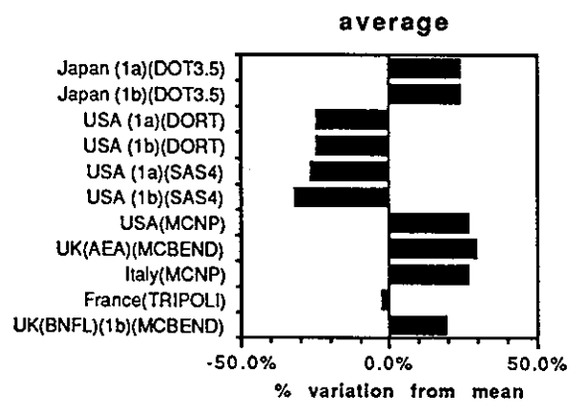

mean = 429.3 μSv/h

Problem 1a/1b Lid Fission Product Gamma-rays.

Cylindrical Source, Dry, Steel Lid, 1a No Neutron Shielding
1b 6cm Polyethylene on outer Radial Surface

The results for the cavity-averaged dose-rates are in better agreement than those for the neutron dose-rate even though the attenuation is much greater. The mean value is 29.1 μSv/hr with a standard deviation on the distribution of 2.4 μSv/hr (8%)

The DOT 3.5 results for the ratio between mid-point and cavity-averaged values give 0.88 which is physically unrealistic. This may be due to ray-effects in the discrete ordinate calculations which would also account for the anomalous values for the geometric attenuation factors in this case and for neutrons.

The overall mean value of 1.37 for the ratio of the mid-point to cavity-averaged dose-rates (see Section 6.1) leads to a mid-point dose-rate of 40.0 μSv/hr when applied to the mean cavity averaged result above. The dose-rates predicted by the kernel methods are close to this having a mean value of 40.3 μSv/hr with a standard deviation on the distribution of 5.3 μSv/hr (13%).

From the point-energy Monte Carlo results the mean values of the geometric factors are 0.289, 0.113 and 0.0063 with corresponding values of 0.247, 0.097, and 0.0054 for those at the mid-points when the value of 1.17 is adopted for the ratio at the surface and dose-rates are assumed to be uniform over the cavity area at distances of 1m and beyond. The kernel codes are again seen to give too little geometric attenuation and the SAS4 result of 0.11 for the cavity-averaged value at 1 metre is again low due to the larger scoring area employed.

Table 11. 1a/b lid FP gamma

METHOD	CODE	CONTRIBUTOR	DOSE RATE AT SURFACE (microSv/h)	DOSE ATTENUATION 1 m	2 m	10 m
Values at the mid-point						
Kernel	QAD-CGGP	Japan(a)	50.1	0.393	0.167	0.0105
		Japan(b)	38.1	0.399	0.170	0.0108
	QAD-CG	Belgium	36.0	0.389	0.158	0.0105
	RANKERN	UK(AEA)	40.6			
	QAD	US	35.6	0.396	0.170	0.0110
	RANKERN	UK(BNFL)	41.4	0.396	0.169	0.0032
1D Sn	ANISN	Belgium	38.0	0.395	0.144	0.0082
	ANISN	FRG	33.0	0.303	0.091	0.0039
2D	DOT 3.5	Japan (1a)	27.8	0.424	0.244	0.0074
	DOT 3.5	Japan (1b)	28.0	0.446	0.270	0.0215
	DORT	USA	38.9	0.191	0.068	0.0035
Monte Carlo (Gp)	SAS4	USA	37.5*	0.295	0.108	0.0061
Monte Carlo (Pt)						
Radially averaged values over the cavity area						
2D	DOT 3.5	Japan (1a)	31.5	0.303	0.153	0.0059
	DOT 3.5	Japan (1b)	31.5	0.327	0.178	0.0182
	DORT	USA	27.6			
Monte Carlo (Gp)	SAS4	USA (1a)	26.6 (7%)	0.111	0.070	
	SAS4	USA (1b)	24.5 (8%)	0.105	0.070	0.0072
Monte Carlo (Pt)	MCNP	USA	29.0 (8%)	0.314	0.114	0.0061
	MCBEND	UK	29.8 (6%)	0.268	0.107	
	MCNP	Italy	28.8 (7%)	0.285	0.115	0.0065
	TRIPOLI	France	28.8 (4%)	0.288	0.115	0.0063

(a) Monoenergetic sources
(b) Group sources

*surface value not directly calculated, inferred from SAS4(ave.) x DORT(midpoint)/DORT(ave.)

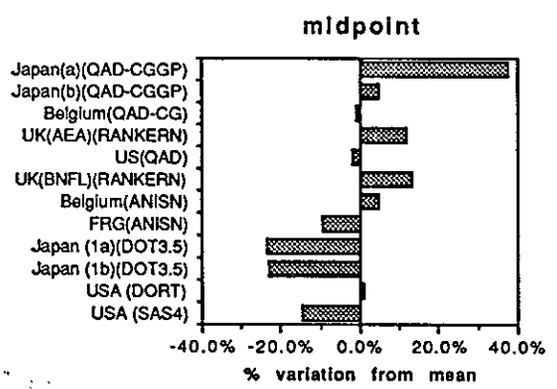

mean = 36.3 μSv/h

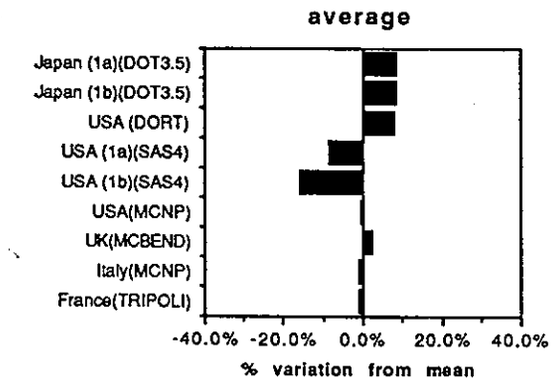

mean = 29.1 μSv/h

Problem 1a/1b Lid Secondary Gamma-rays

Cylindrical Sources, Dry, Steel Lid, 1a No Neutron Shielding
1b 6cm Polyethylene on outer Radial Surface.

No results were submitted for the secondary gamma-rays in this problem.

Table 13. 1 a/b bottom neutron

METHOD	CODE	CONTRIBUTOR	DOSE RATE AT SURFACE (microSv/h)	DOSE ATTENUATION 1m	2m	10m
Values at the mid-point						
1D Sn	ANISN	Belgium	694	0.122	0.042	0.00166
	ANISN	FRG (1a)	310	0.306	0.106	0.00484
	ANISN	FRG (1b)	300	0.307	0.107	0.00500
2D	DOT 3.5	Japan (1a)	629	0.164	0.076	0.00332
	DOT 3.5	Japan (1b)	627	0.161	0.074	0.00234
	DORT	USA(1a&b)	541	0.114	0.036	0.00161
Monte Carlo (Gp)	SAS4	USA(1a)	464*	0.121	0.038	0.00179
	SAS4	USA(1b)	508*	0.112	0.035	0.00157
Monte Carlo (Pt)						
Radially averaged values over the cavity area						
2D	DOT 3.5	Japan (1a)	467	0.175	0.080	0.00420
	DOT 3.5	Japan (1b)	466	0.172	0.077	0.00292
	DORT	USA(1a&b)	410			
Monte Carlo (Gp)	SAS4	USA (1a)	352 (7%)	0.082	0.035	
	SAS4	USA (1b)	385 (10%)	0.071	0.034	
Monte Carlo (Pt)	MCNP	USA (1a)	422 (7%)	0.173	0.057	0.00261
	MCNP	Italy	494 (9%)	0.147	0.050	0.00245
	TRIPOLI	France	543 (11%)	0.145	0.048	0.00230
	MCBEND	UK(BNFL)	457	0.146	0.072	0.00233

*surface value not directly calculated, inferred from SAS4(ave.) x DORT(midpoint)/DORT(ave.)

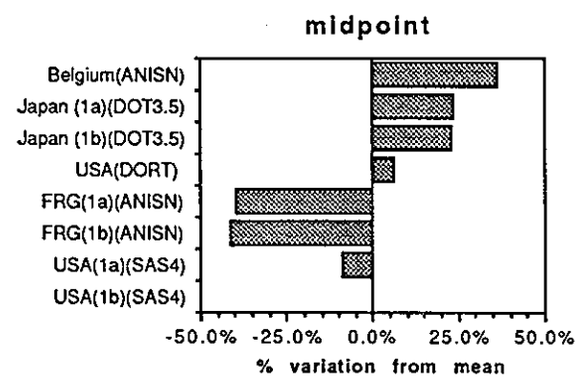

mean = 509.1 μSv/h

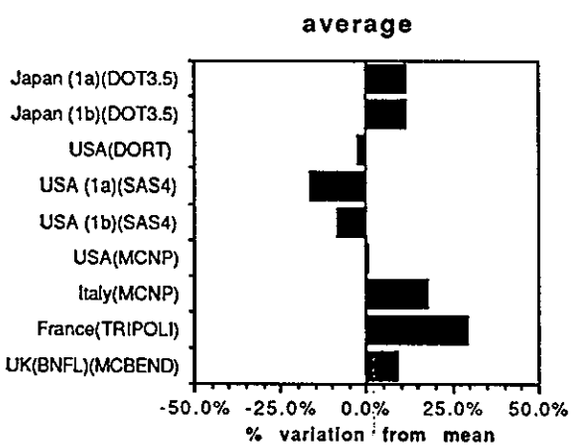

mean = 444.0 μSv/h

Problem 1a/1b Bottom - Fission Product Gamma-rays

Cylindrical Source, Dry, Cast Iron Base, 1(a) No Neutron Shielding
1(b) 6cm Polyethylene on outer Radial Surface.

The results for the dose-rate averaged over the area of the cavity have a mean value of 319 μSv/hr with a standard deviation on the distribution of 33 μSv/hr (10%). The SAS4 value for Problem 1b seem to be low - it is difficult to understand how replacing cast iron by polyethylene for the outermost 6cm of the radial surface could lead to a decrease in dose-rate compared with 1a. This difference is therefore attributed to statistical uncertainty and the weighted mean of 276 μSv/hr $\pm$ 6% illustrates the variation on results which can be obtained with Monte Carlo methods.

Using the overall value of 1.37 for the ratio of the mid-point to cavity-averaged values (see Section 6.1) give a peak dose-rate of 437 μSv/hr when the value of 319 μSv/hr is scaled. The kernel results show a similar spread about this value as was observed for the lid, the range being - 13% to + 16%.

Table 14. 1a/b bottom gamma

METHOD	CODE	CONTRIBUTOR	DOSE RATE AT SURFACE (microSv/h)	DOSE ATTENUATION 1 m	2 m	10 m
Values at the mid-point						
Kernel	QAD-CGGP	Japan(a)	507	0.357	0.148	0.0092
		Japan(b)	410	0.363	0.151	0.0093
	QAD-CG	Belgium	390	0.359	0.146	0.0087
	QAD	US	382	0.366	0.152	0.0094
	RANKERN	UK(BNFL)	432	0.373	0.105	0.0094
1D Sn	ANISN	FRG	350	0.286	0.091	0.0037
2D	DORT	USA	424	0.193	0.068	0.0035
	DOT 3.5	Japan (1a)	362	0.345	0.177	0.0024
	DOT 3.5	Japan (1b)	363	0.347	0.179	0.0038
Monte Carlo (Gp)	SAS4	USA (1a)	437*	0.209	0.080	0.0042
Monte Carlo (Pt)						
Radially averaged values over the cavity area						
2D	DOT 3.5	Japan (1a)	347	0.274	0.128	0.0023
	DOT 3.5	Japan (1b)	347	0.274	0.130	0.0037
	DORT	USA	315			
Monte Carlo (Gp)	SAS4	USA (1a)	325 (10%)	0.080	0.053	
	SAS4	USA (1b)	252 (7%)	0.087	0.058	
Monte Carlo (Pt)	MCNP	USA	316 (10%)	0.311	0.112	0.0059
	MCNP	Italy	351 (13%)	0.238	0.095	0.0052
	TRIPOLI	France	296 (3%)	0.259	0.097	0.0053

(a) Monoenergetic sources
(b) Group sources

*surface value not directly calculated, inferred from SAS4(ave.) x DORT(midpoint)/DORT(ave.)

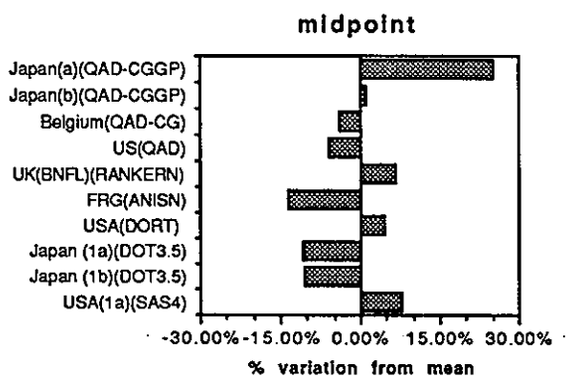

mean = 405.7 μSv/h

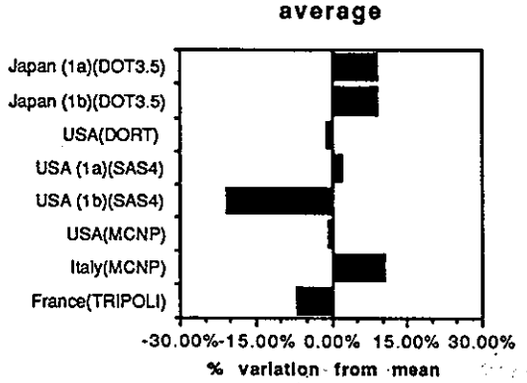

mean = 318.6 μSv/h

Problem 1a/1b Bottom - Secondary Gamma-rays

Cylindrical Source, Dry, Cast Iron Base, 1a No Neutron Shielding
1b 6cm Polyethylene on outer
Radial Surface

The results are consistent and show a geometric attenuation similar to that for neutrons rather than fission product gamma-rays.

Table 15. 1 a/b bottom secondary gamma

METHOD	CODE	CONTRIBUTOR	DOSE RATE AT SURFACE (microSv/h)	DOSE ATTENUATION 1m	2m	10m
Values at the mid-point						
1D Sn						
2D	DORT	USA	3.90	0.136	0.044	0.0021
Monte Carlo (Gp)	SAS4	USA	3.49*	0.146	0.046	0.0020
Monte Carlo (Pt)						
Radially averaged values over the cavity area						
2D	DORT	USA	3.11			
Monte Carlo (Gp)	SAS4	USA	2.78 (8%)	0.094	0.047	
Monte Carlo (Pt)						

(a) Monoenergetic sources
(b) Group sources

*surface value not directly calculated, inferred from SASIV(ave.) x DORT(midpoint)/DORT(ave.)

Problem 1b Radial-Neutrons

Cylindrical Source, Dry, Wall is 32cm Cast Iron Plus 6cm Polyethylene

The mean dose-rate averaged over the cavity height is 56.0 μSv/hr with a standard deviation on the distribution of 9.0 μSv/hr (16%) so that the spread is much greater than that found for the cast iron alone in Problem 1a where the standard deviation was 8%.

Using the ratio of 1.07 from Section 6.1 gives a scaled dose-rate of 59.9 μSv/hr for the centre point.

The one-dimensional results from the discrete ordinate methods have a mean value of 57.8 μSv/hr with a standard deviation of 14.5 μSv/hr (25%). While the mean is in agreement with the value of 59.9 μSv/hr, the wide spread in the dose-rate achieved with the same method emphasises the important role of the multigroup data libraries. The change in performance between 1a and 1b may be due to the rapid change of neutron spectrum with penetration into the polyethylene. The thickness of 6cm produces an attenuation of almost a factor of 10 in the neutron dose-rates.

The geometric factors show no new features with the DOT 3.5 values appearing to be too high. There appears to be slightly less attenuation than was found in problem 1a with no neutron shielding.

Table 16. 1b radial neutron

METHOD	CODE	CONTRIBUTOR	DOSE RATE AT SURFACE (microSv/h)	DOSE ATTENUATION 1m	2m	10m
Values at the axial mid-point						
1D Sn	SAS1	USA	53.7	0.331	0.190	0.0184
	ANISN	Belgium	41.0	0.341	0.192	0.0151
	ANISN	Japan	56.6			
	ANISN	Switzerland	78.0**	0.359	0.218	
	ANISN	Finland	42.0	0.364	0.202	0.0171
	ANISN	Italy	58.6	0.330	0.184	0.0160
	ANISN	FRG	75.0**	0.320	0.187	0.0187
2D	DOT 3.5	Japan	63.2	0.326	0.201	0.0320
	DORT	USA	45.8	0.310	0.162	0.0186
Monte Carlo (Gp)	SAS4	USA	58.6*	0.307	0.179	0.0174
Monte Carlo (Pt)	MCBEND	UK(BNFL)	50.0	0.326	0.199	0.0218
	MCNP	Italy	64.2 (3.5%)			
Axially averaged values over the cavity area						
2D	DOT 3.5	Japan	60.4	0.346	0.212	0.0334
	DORT	USA	40.1			
Monte Carlo (Gp)	SAS4	USA	51.3 (2%)	0.298	0.165	
	MORSE	Japan	60.8 (5%)	0.339	0.191	0.0156
Monte Carlo (Pt)	MCBEND	UK(AEA)	52.3 (5%)	0.331	0.178	0.0172
	MCNP	Italy	59.0 (1%)	0.315	0.169	0.0168
	TRIPOLI	France	68.0	0.341	0.190	0.0194

*surface value not directly calculated, inferred from SAS4(ave.) x DORT(midpoint)/DORT(ave.)
**not included in mean

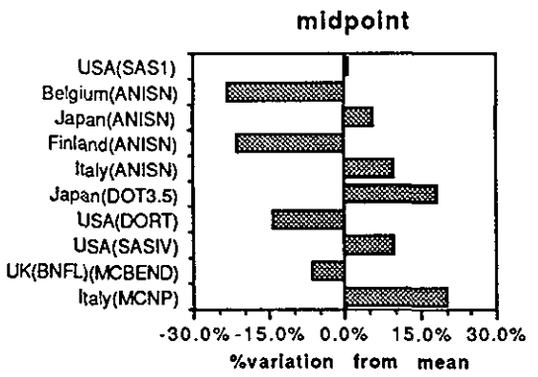

mean = 53.4 μSv/h

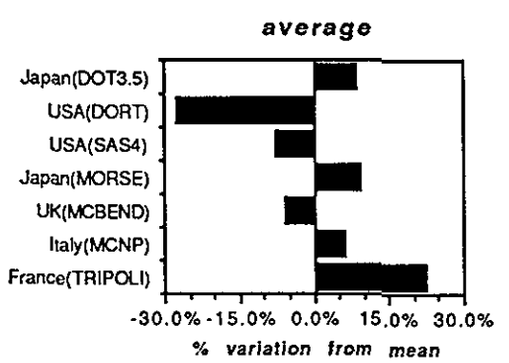

mean = 56.0 μSv/h

Problem 1b Radial-Fission Product Gamma-rays

Cylindrical Source, Dry, Wall is 32cm Cast Iron Plus 6cm Polyethylene

The three point-energy calculations are in excellent agreement with a mean value of 1280 μSv/hr and a standard deviation of 6 μSv/hr (0.5%). The SAS4, DORT, and ANISN (GAM50 Library) results agree with this, while the DOT 3.5 value of 1620 μSv/hr is much higher. This is consistent with the results for Problem 1a.

The ratio of mid-height value to the cavity-averaged dose-rate is given as 1.04 by DOT 3.5 and 1.02 by DORT. These bracket the overall mean ratio of 1.03 which is again applied here to give the peak level of 1318 μSv/hr corresponding to the mean of 1280 μSv/hr.

The kernel methods are mostly in good agreement with this, again illustrating the value of this simple approach. The SAS1 result is also very close, but the other one-dimensional discrete ordinates methods give widely discrepant answers, probably because of the different data libraries employed.

The geometric attenuations show no new features.

Table 17. 1b radial FP gamma

METHOD	CODE	CONTRIBUTOR	DOSE RATE AT SURFACE (microSv/h)	DOSE ATTENUATION 1 m	2 m	10 m
Values at the axial mid-point						
Kernel	QAD	US	1336	0.432	0.274	0.0379
	QAD-CGGP	Japan(a)	1592	0.432	0.229	
		Japan(b)	1325	0.432	0.275	
	QAD-CG	Belgium	1266	0.429	0.271	0.0355
	RANKERN	UK(BNFL)	1380	0.448	0.286	0.0388
1D Sn	SAS1	USA	1300	0.379	0.229	0.0270
	ANISN	Japan	1780			
	ANISN	Switzerland	1900**	0.389	0.242	
	ANISN	Finland	2500**	0.372	0.204	0.0184
	ANISN	FRG (c)	1200	0.350	0.208	0.0267
	ANISN	FRG (d)	1817	0.354	0.211	0.0231
2D	DORT	USA	1297	0.341	0.228	0.0180
	DOT 3.5	Japan	1680	0.376	0.217	0.0183
Monte Carlo (Gp)	SAS4	USA	1268*	0.374	0.250	0.0201
Monte Carlo (Pt)						
Axially averaged values over the cavity area						
2D	DOT 3.5	Japan	1620**	0.351	0.194	0.0183
	DORT	USA	1272			
Monte Carlo (Gp)	SAS4	USA	1244 (5%)	0.267	0.162	
Monte Carlo (Pt)	MCBEND	UK(AEA)	1286 (2%)	0.351	0.200	0.0239
	MCNP	Italy	1274 (4%)	0.338	0.192	0.0220
	TRIPOLI	France	1280	0.346	0.195	0.0238

(a) Monoenergetic sources
(b) Group sources
(c) GAM50 library
(d) EURLIB library

*surface value not directly calculated, inferred from SAS4(ave.) x DORT(midpoint)/DORT(ave.)
**not included in mean

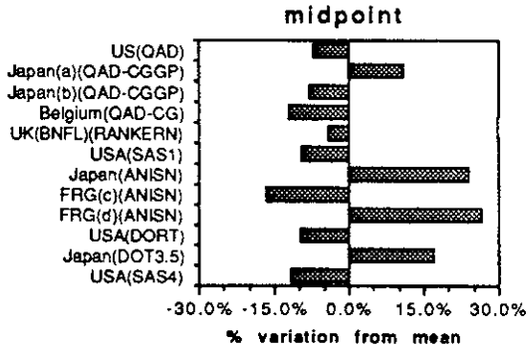

mean = 1436.8 μSv/h

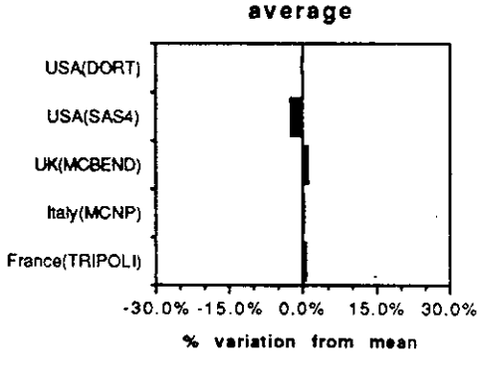

mean = 1271.2 μSv/h

Problem 1b Radial Secondary Gamma-rays

Cylindrical Source, Dry, Wall is 32cm Cast Iron Plus 6cm Polyethylene

The two point-energy calculations agree with a mean value for the dose-rate averaged over the cavity height of 47.7 μSv/hr. This is in good agreement with the discrete ordinates results, with the SAS4 dose-rate being lower by 19%.

The three values for the ratio of the mid-height dose-rate to that averaged over the cavity are identical at 1.09. This is close to the 1.07 value adopted for the neutron dose-rate. When scaled the peak dose-rate corresponding to the above mean is 52.0 μSv/hr. The one-dimensional codes give results below this, although the maximum departure is only 25%.

There is more attenuation due to geometry than was the case for the primary sources, the factors at 10 metres being lower than those for neutrons and primary gamma-rays by 2.0 and 2.5 respectively.

Table 18. 1b radial secondary gamma

METHOD	CODE	CONTRIBUTOR	DOSE RATE AT SURFACE (microSv/h)	DOSE ATTENUATION 1 m	2 m	10 m
Values at the axial mid-point						
1D Sn	SAS1	USA	40.6	0.283	0.147	0.0116
	ANISN	Japan	49.1			
	ANISN	Switzerland	39.0	0.359	0.205	
	ANISN	Italy	46.4	0.269	0.134	0.0097
	ANISN	FRG	48.0	0.292	0.146	0.0125
2D	DOT 3.5	Japan	45.9	0.222	0.123	0.0081
	DORT	USA	49.9	0.236	0.114	0.0082
Monte Carlo (Gp)	SAS4	USA	41.9*	0.258	0.135	0.0091
Monte Carlo (Pt)	MCBEND	UK(BNFL)	43.7	0.268	0.105	0.0082
	MCNP	Italy	53.1 (1.6%)	0.260	0.126	0.0092
Axially averaged values over the cavity area						
2D	DOT 3.5	Japan	42.3	0.210	0.116	0.0090
	DORT	USA	45.8			
Monte Carlo (Gp)	SAS4	USA	38.5 (3%)	0.194	0.103	
Monte Carlo (Pt)	MCBEND	UK(AEA)	46.6 (6%)	0.232	0.114	0.0086
	MCNP	Italy	48.8 (1%)	0.239	0.119	0.0098

*surface value not directly calculated, inferred from SAS4(ave.) x DORT(midpoint)/DORT(ave.)

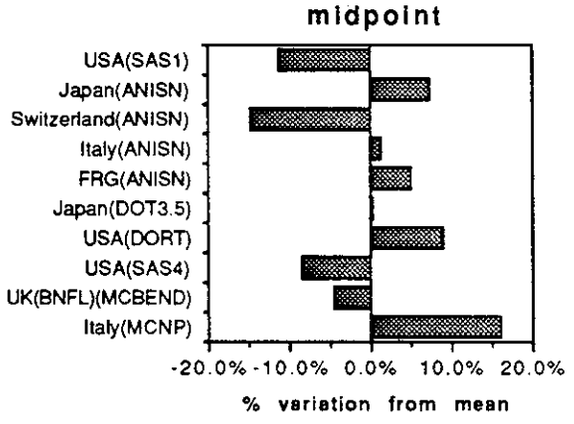

mean = 45.8 μSv/h

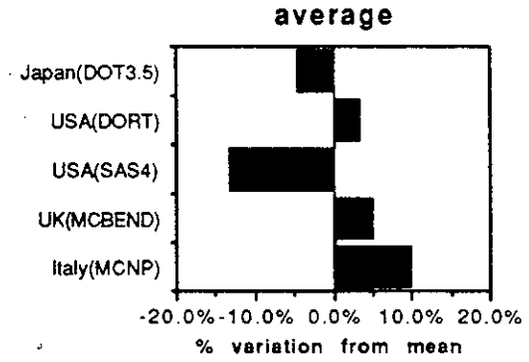

mean = 44.4 μSv/h

Problem 1c Radial-Neutrons

Cylindrical Source, Wet, Cast Iron Wall, No Neutron Shielding

The results averaged over the height of the cavity give a mean value of 52.0 μSv/hr with a standard deviation of 5.4 μSv/hr (10%) on the distribution. The agreement between results is thus close to the 8% standard deviation found for Problem 1(a) rather than the 16% observed in problem 1b. The modification of the spectrum in the source region by the flooded cavity is treated more consistently by the codes than was the addition of neutron shielding to the radial wall.

The ratio between the mid-height dose-rate and the cavity averaged value adopted in Section 6.1 is 1.07 which is larger that the values of 1.03 found here. The mid-height dose-rate is 55.6 μSv/hr if the factor of 1.07 is used. The one-dimensional results show a spread from underestimating by 29% to overestimating by 4%.

The geometric attenuations are very similar to those for problem 1a.

Table 19. 1 c radial neutron

METHOD	CODE	CONTRIBUTOR	DOSE RATE AT SURFACE (microSv/h)	DOSE ATTENUATION 1 m	2 m	10 m
Values at the axial mid-point						
1D Sn	SAS1	USA	47.1	0.312	0.174	0.0155
	ANISN	Belgium	40.0	0.350	0.190	0.0145
	ANISN	Japan	55.4			
	ANISN	Finland	39.0**	0.308	0.159	0.0128
	ANISN	Italy	53.4	0.304	0.163	0.0131
	ANISN	FRG	58.0	0.310	0.172	0.0172
2D	DORT	USA	47.2	0.305	0.161	0.0136
	DOT 3.5	Japan	55.4	0.283	0.164	0.0140
Monte Carlo (Gp)	SAS4	USA	49.5*	0.305	0.163	0.0135
Monte Carlo (Pt)	MCBEND	UK	55.6	0.324	0.173	0.0130
Axially averaged values over the cavity area						
2D	DOT 3.5	Japan	53.7	0.263	0.149	0.0138
	DORT	USA	45.8			
Monte Carlo (Gp)	SAS4	USA	48.0 (4%)	0.223	0.125	
Monte Carlo (Pt)	MCNP	Italy	49.4 (5%)	0.277	0.148	0.0148
	TRIPOLI	France	60.4 (5%)	0.280	0.147	0.0138
	MCBEND	UK	54.7 (4%)	0.287	0.152	0.0130

*surface value not directly calculated, inferred from SAS4(ave.) x DORT(midpoint)/DORT(ave.)
**not included in mean

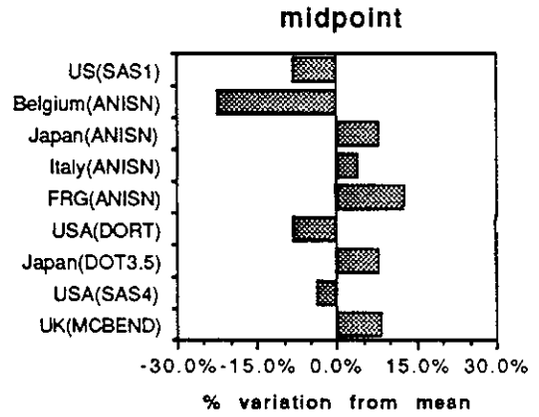

mean = 51.3 μSv/h

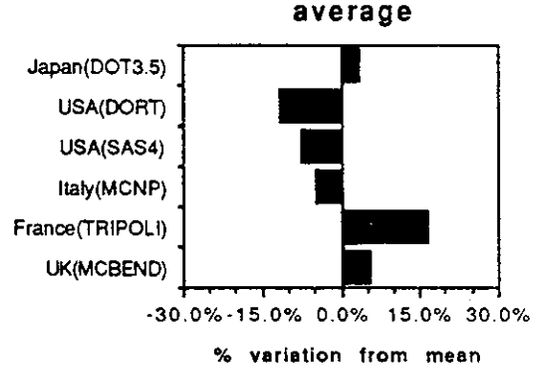

mean = 52.0 μSv/h

Problem 1c Radial Fission Product Gamma-rays

Cylindrical Source, Wet, Cast Iron Wall, No Neutron Shielding

The mean of the cavity averaged values is 195 μSv/hr, with a standard deviation on the distribution of 28 μSv/hr (14%). This agreement is significantly worse than that for problem 1a where the standard deviation was 6% and it is difficult to understand why flooding the cavity should produce such a change in the performance of the codes.

The adopted ratio of mid-height value to that averaged over the cavity is 1.03 giving a scaled mid-height dose-rate of 201 μSv/hr.

Three of the kernel methods give results which are in good agreement with this as does SAS4, DORT and SAS1. The four ANISN results range from underestimating by 14% to overestimating by 42%.

The geometric factors are similar to that for Problem 1a.

Table 20. 1 c radial FP gamma

METHOD	CODE	CONTRIBUTOR	DOSE RATE AT SURFACE (microSv/h)	DOSE ATTENUATION 1m	2m	10m
Values at the axial mid-point						
Kernel	QAD	US	203	0.432	0.275	0.0397
	QAD-CGGP	Japan(a)	251	0.434	0.228	
		Japan(b)	201	0.433	0.276	
	QAD-CG	Belgium	193	0.425	0.269	0.0363
1D Sn	SAS1	USA	185	0.381	0.231	0.0278
	ANISN	Belgium	255	0.408	0.259	0.0313
	ANISN	Japan	280			
	ANISN	FRG (c)	174	0.351	0.213	0.0230
	ANISN	FRG (d)	293	0.355	0.212	0.0240
2D	DOT 3.5	Japan	258	0.381	0.221	0.0191
	DORT	USA	186	0.392	0.232	0.0251
Monte Carlo (Gp)	SAS4	USA	196*	0.346	0.210	0.0246
Monte Carlo (Pt)						
Axially averaged values over the cavity area						
2D	DOT 3.5	Japan	251	0.354	0.197	0.0188
	DORT	USA	162			
Monte Carlo (Gp)	SAS4	USA	193 (3%)	0.270	0.162	
Monte Carlo (Pt)	MCNP	Italy	168 (5%)	0.351	0.202	0.0256
	TRIPOLI	France	195	0.351	0.202	0.0025
	MCBEND	UK	198 (6%)	0.356	0.203	0.0250

(a) Monoenergetic sources
(b) Group sources
(c) GAM50 library
(d) EURLIB library

*surface value not directly calculated, inferred from SAS4(ave.) x DORT(midpoint)/DORT(ave.)

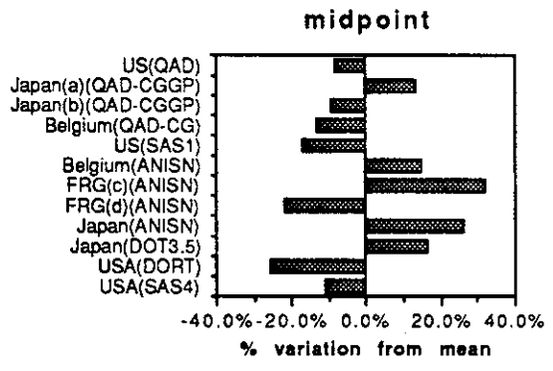

mean = 221.4 μSv/h

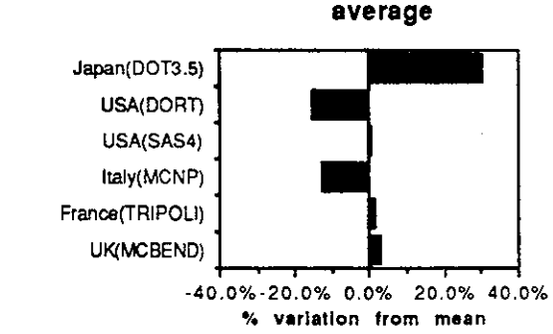

mean = 194.5 μSv/h

Problem 1c Radial Secondary Gamma-rays

Cylindrical Source, Wet, Cast Iron Wall, No Neutron Shielding

The results for this problem are in agreement.

Table 21. 1 c radial secondary gamma

METHOD	CODE	CONTRIBUTOR	DOSE RATE AT SURFACE (microSv/h)	DOSE ATTENUATION 1 m	2 m	10 m
Values at the axial mid-point						
1D Sn	SAS1	US	0.30	0.333	0.167	0.0167
	ANISN	Italy	0.28	0.325	0.175	0.0143
2D	DORT	USA	0.30	0.333	0.167	0.0133
Monte Carlo (Gp)	SAS4	USA	0.31*	0.290	0.162	0.0129
Monte Carlo (Pt)						
Axially averaged values over the cavity area						
2D	DORT	USA	0.29			
Monte Carlo (Gp)	SAS4	USA	0.30 (5%)	0.233	0.133	
Monte Carlo (Pt)						

*surface value not directly calculated, inferred from SAS4(ave.) x DORT(midpoint)/DORT(ave.)

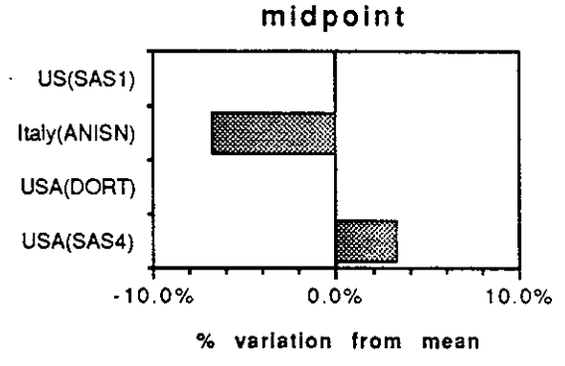

mean = 0.30 μSv/h

Problem 1c Lid -Neutrons

Cylindrical Source, Wet, Steel Lid

The two point-energy calculations give a mean value of 61.2 μSv/hr for the cavity-averaged value and this is in agreement with the DOT result. The DORT and SAS4 results agree with each other but give a mean value of 36.6 μSv/hr which is significantly lower. This is similar to the behaviour observed for the lid in problems 1a and 1b, but contrasts with the better agreement between DORT and SAS4 and the point-energy codes for the cast iron flask walls or base. It suggests that there is a difference between the multigroup and point-energy treatment of the cross-sections for stainless steel.

The mean value of 1.31 for the ratio of the mid-point to cavity averaged values from DOT and DORT is close to the 1.33 found for problems 1a and 1b.

The geometric attenuation factors are similar to those calculated for problems 1a and 1b.

Table 22. 1 c lid neutron

METHOD	CODE	CONTRIBUTOR	DOSE RATE AT SURFACE (microSv/h)	DOSE ATTENUATION 1 m	2 m	10 m
Values at the mid-point						
1D Sn	ANISN	Belgium (a)	20.5	0.132	0.046	0.00195
	ANISN	Belgium (b)	32.0			
	ANISN	FRG	34.0	0.294	0.103	0.00588
2D	DOT 3.5	Japan	79.2**	0.164	0.076	0.00309
	DORT	USA	47.0	0.117	0.036	0.00164
Monte Carlo (Gp)	SAS4	USA	48.2*	0.133	0.042	0.00195
Monte Carlo (Pt)						
Radially averaged values over the cavity area						
2D	DOT 3.5	Japan	59.9	0.174	0.079	0.00379
	DORT	USA	36.1			
Monte Carlo (Gp)	SAS4	USA	37.0 (10%)	0.086	0.040	
Monte Carlo (Pt)	MCNP	Italy	64.4 (8%)	0.149	0.051	0.00248
	MCBEND	UK	57.9 (6%)	0.161	0.042	0.00300

(a) Using geometric factor to adjust 1-D results
(b) Using buckling in ANISN

*surface value not directly calculated, inferred from SAS4(ave.) x DORT(midpoint)/DORT(ave.)
**not included in mean

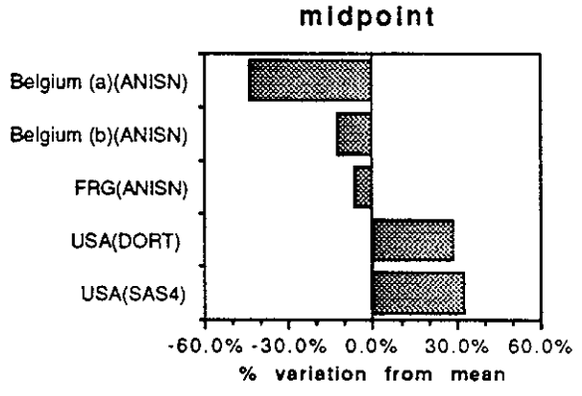

mean = 36.3 μSv/h

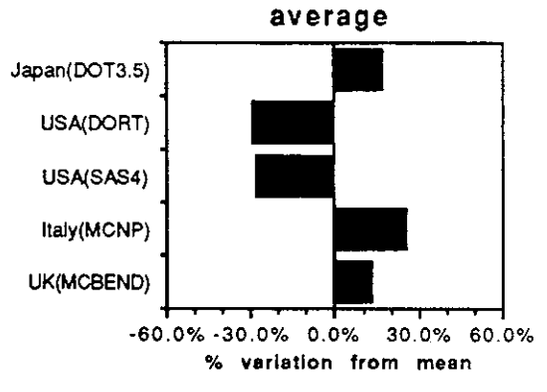

mean = 51.1 μSv/h

Problem 1c Lid Fission Product Gamma-rays

Cylindrical Source, Wet, Steel Lid

The mean value of the cavity averaged dose-rates is 18.9 μSv/hr with a standard deviation on the distribution of 1.9 μSv/hr (10%).

The DOT 3.5 results again show an anomalous value for the ratio between the mid-point and the cavity-averaged dose-rate, the ratio of 0.86 suggesting the presence of ray-effects. Scaling the cavity-averaged dose-rate of 18.9 μSv/hr by the factor of 1.37 as adopted in Section 6.1 gives a mid-point equivalent of 25.9 μSv/hr. The kernel results underestimate this by about 11%.

The geometric attenuation factors are similar to those for problems 1a and 1b.

Table 23. 1 c lid FP gamma

METHOD	CODE	CONTRIBUTOR	DOSE RATE AT SURFACE (microSv/h)	DOSE ATTENUATION 1 m	2 m	10 m
Values at the mid-point						
Kernel	QAD	US	22.8	0.405	0.173	0.0110
	QAD-CG	Belgium	24.0	0.404	0.167	0.0100
	ANISN	Belgium	18.5	0.389	0.141	0.0081
1D Sn	ANISN	FRG	23.0	0.304	0.091	0.0044
2D	DOT 3.5	Japan	19.6	0.435	0.248	0.0074
	DORT	USA	27.5	0.193	0.068	0.0035
Monte Carlo (Gp)	SAS4	USA	25.1*	0.232	0.087	0.0032
Monte Carlo (Pt)	MCBEND	UK	25.8			
Radially averaged values over the cavity area						
2D	DOT 3.5	Japan	22.7	0.301	0.151	0.0057
	DORT	USA	16.4			
Monte Carlo (Gp)	SAS4	USA	17.7 (7%)	0.112	0.076	
Monte Carlo (Pt)	MCNP	Italy	18.5 (11%)	0.294	0.115	0.0064
	MCBEND	UK	19.1 (5%)	0.272	0.110	0.0063

*surface value not directly calculated, inferred from SAS4(ave.) x DORT(midpoint)/DORT(ave.)

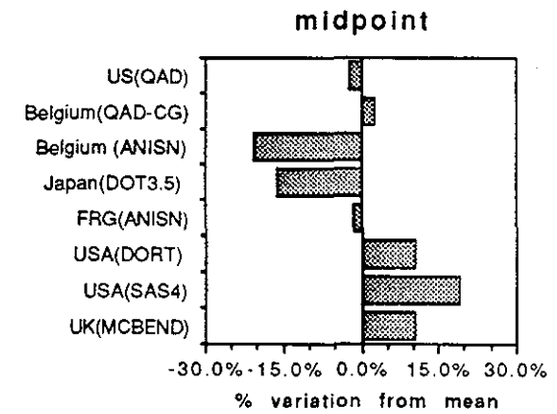

mean = 23.4 μSv/h

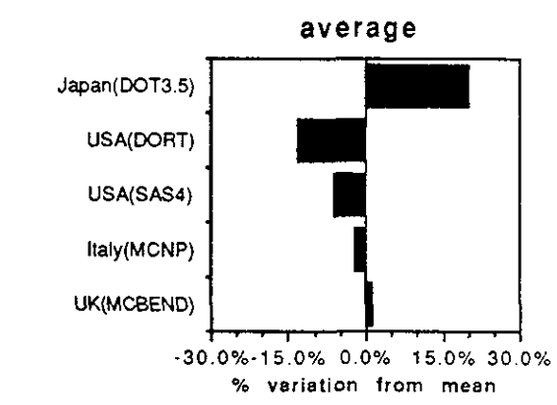

mean = 18.9 μSv/h

Problem 1c Lid - Secondary Gamma-rays

Cylindrical Source, Wet, Steel Lid

The results from DORT and SAS4 are in good agreement.

Table 24. 1 c lid secondary gamma

METHOD	CODE	CONTRIBUTOR	DOSE RATE AT SURFACE (microSv/h)	DOSE ATTENUATION 1 m	2 m	10 m
Values at the mid-point						
1D Sn						
2D	DORT	USA	0.26	0.135	0.042	0.0385
Monte Carlo (Gp)	SAS4	USA	0.25*	0.136	0.044	0.0400
Monte Carlo (Pt)						
Radially averaged values over the cavity area						
2D	DORT	USA	0.20			
Monte Carlo (Gp)	SAS4	USA	0.19 (13%)	0.105	0.042	
Monte Carlo (Pt)						

*surface value not directly calculated, inferred from SAS4(ave.) x DORT(midpoint)/DORT(ave.)

Problem 1c Bottom - Neutrons

Cylindrical Source, Wet, Cast Iron Base

The mean cavity-averaged value is 52.2 μSv/hr with a standard deviation on the distribution of 9.4 μSv/hr (18%). Again there is a tendency for DORT and SAS4 to give lower results, their mean value being 26% below that of DOT and MCNP. (For the steel lid the mean given by DORT and SAS4 was 40% lower than that given by the remaining codes).

The ratios between the peak and the cavity averaged dose-rates are 1.33 for DOT and 1.30 for DORT which are consistent with the value of 1.33 adopted for the lid and the base in the previous problems.

If the MCNP point-energy value is adopted for the cavity-averaged dose-rates then the scaled result for the mid-point is 81.5μSv/hr. The three results derived with one-dimensional treatments are very much lower than this, which illustrates the difficulty of allowing for the geometry with such a simple approach.

Table 25. 1 c bottom neutron

METHOD	CODE	CONTRIBUTOR	DOSE RATE AT SURFACE (microSv/h)	DOSE ATTENUATION 1 m	2 m	10 m
Values at the mid-point						
1D Sn	ANISN	Belgium (a)	24.0	0.120	0.042	0.00167
	ANISN	Belgium (b)	36.0			
	ANISN	FRG	33.0	0.303	0.106	0.00606
2D	DOT 3.5	Japan	78.1	0.168	0.079	0.00366
	DORT	USA	61.5	0.116	0.036	0.00163
Monte Carlo (Gp)	SAS4	USA	53.6*	0.126	0.039	0.00187
Monte Carlo (Pt)						
Radially averaged values over the cavity area						
2D	DOT 3.5	Japan	58.8	0.179	0.082	0.00456
	DORT	USA	47.4			
Monte Carlo (Gp)	SAS4	USA	41.3 (8%)	0.078	0.036	
Monte Carlo (Pt)	MCNP	Italy	61.3 (8%)	0.148	0.049	0.00245

(a) Using geometric factor to adjust 1-D results
(b) Using buckling in ANISN

*surface value not directly calculated, inferred from SAS4(ave.) x DORT(midpoint)/DORT(ave.)

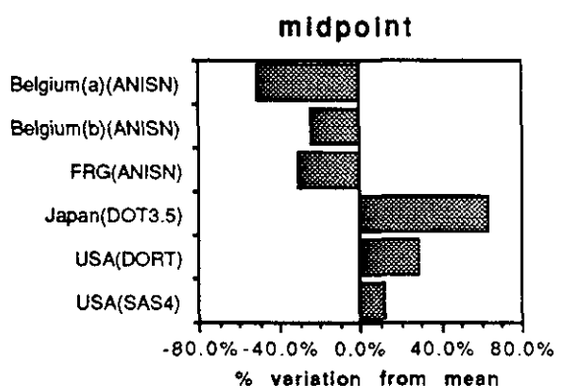

mean = 47.7 μSv/h

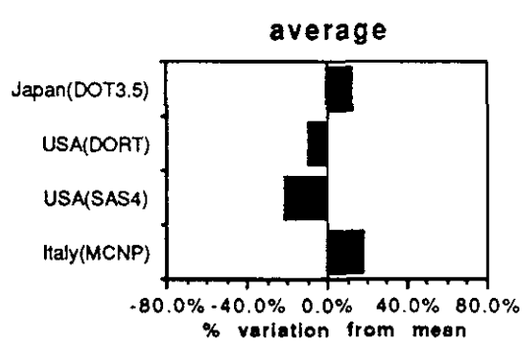

mean = 52.2 μSv/h

Problem 1c Bottom - Fission Product Gamma-rays

Cylindrical Source, Wet, Cast Iron Base

The mean cavity averaged dose-rate is 214 μSv/hr with a standard deviation on the distribution of 29 μSv/hr (13%). Again the mean of the DORT and SAS4 dose-rates would be lower than the mean of the DOT and MCNP results by 23%.

The DOT value for the ratio of mid-point to cavity averaged dose-rates is 1.02, while that from DORT 1.51. Using the value of 1.37 adopted previously would give an equivalent mid-point dose-rate of 293 μSv/hr, with the two QAD results giving underestimates by 16% and 11%.

The geometric attenuation factors from DOT 3.5 appear anomalous which is consistent with there being ray-effects which influence the predictions of the radial shape at the surface (the ratio peak: average is only 1.02) and the attenuation with distance.

Table 26. 1 c bottom FP gamma

METHOD	CODE	CONTRIBUTOR	DOSE RATE AT SURFACE (microSv/h)	DOSE ATTENUATION 1 m	2 m	10 m
Values at the mid-point						
Kernel	QAD	US	245	0.373	0.154	0.0094
	QAD-CG	Belgium	261	0.363	0.149	0.0086
	ANISN	Belgium (a)	449	0.388	0.140	0.0080
	ANISN	Belgium (b)	381			
1D Sn	DOT 3.5	Japan	256	0.354	0.181	0.0024
	DORT	USA	298	0.192	0.067	0.0035
	ANISN	FRG	250	0.300	0.088	0.0040
2D	SAS4	USA	245*	0.203	0.076	0.0040
Monte Carlo (Gp)						
Monte Carlo (Pt)						
Radially averaged values over the cavity area						
2D	DOT 3.5	Japan	250	0.271	0.128	0.0023
	DORT	USA	223			
Monte Carlo (Gp)	SAS4	USA	183 (9%)	0.083	0.057	
Monte Carlo (Pt)	MCNP	Italy	234 (2.4%)	0.274	0.101	0.0052

(a) Using geometric factor to adjust 1-D results
(b) Using buckling in ANISN

*surface value not directly calculated, inferred from SAS4(ave.) x DORT(midpoint)/DORT(ave.)

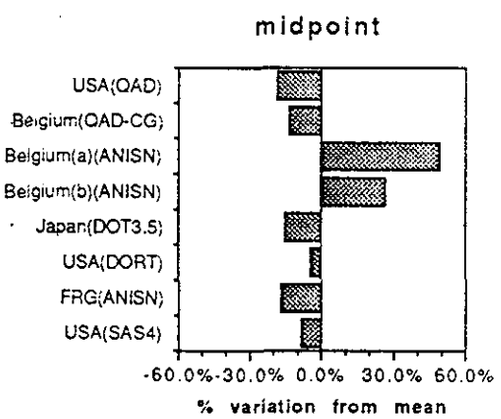

mean = 300.6 μSv/h

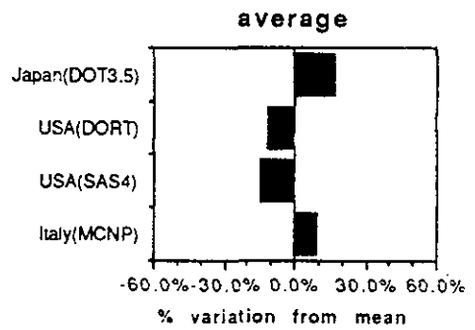

mean = 214.3 μSv/h

94270079

Problem 1c Bottom - Secondary Gamma-rays

Cylindrical Source, Wet, Cast Iron Base.

The DORT and SAS4 results are again consistent.

Table 27. 1c bottom secondary gamma

METHOD	CODE	CONTRIBUTOR	DOSE RATE AT SURFACE (microSv/h)	DOSE ATTENUATION 1 m	2 m	10 m
Values at the mid-point						
1D Sn						
2D	DORT	USA	0.38	0.137	0.045	0.0026
Monte Carlo (Gp)	SAS4	USA	0.35*	0.128	0.037	0.0028
Monte Carlo (Pt)						
Radially averaged values over the cavity area						
2D	DORT	USA	0.30			
Monte Carlo (Gp)	SAS4	USA	0.28 (15%)	0.089	0.054	
Monte Carlo (Pt)						

*surface value not directly calculated, inferred from SAS4(ave.) x DORT(midpoint)/DORT(ave.)

Problem 2a Radial Neutron

Cylindrical Source, Dry, Steel Wall containing two rings of Polyethylene Rods

There are five results for the azimuthally averaged dose-rate at the cavity mid-height obtained with the polyethylene rods being represented discretely. These have a mean value of 65.1 μSv/hr with a standard deviation on the distribution of 17.5 μSv/hr (27%). DORT and SAS4 results again appear to be lower than the remainder and give a mean of 46.7 μSv/hr leaving the other three to give a mean of 77.3 μSv/hr. This behaviour is similar to that for the steel lid in problems 1a, 1b, and 1c where DORT and SAS4 gave dose-rates below those of the point-energy codes. It is not possible to determine the "true" answer, but the problems encountered with multigroup data suggest that greater weight should be given to the point-energy results.

The TWODANT results with the EURLIB library agree with the point-energy results so that this implies that the spread is due to nuclear data rather than method.

The results also give the maximum and minimum values of the dose-rate at the mid-height of the cavity as the dose-point is moved azimuthally around the surface of the flask, The discrete-ordinates codes with their azimuthal mesh enable the fine structure to be predicted; the Monte Carlo codes using volume-averaged scoring cannot give such detail. There is again a spread in the absolute results but the ratios of maximum to mean are 1.1 for all three codes, with 0.92, 0.92, and 0.90 for the minimum to mean ratio from DORT, TWODANT and MCNP respectively.

The azimuthal variation is shown in Figure 8 with the minimum occurring opposite the outer polyethylene rod.

The feature of this problem is the need for a three dimensional modelling capability in order to represent the polyethylene rods explicitly. The one dimensional and some two-dimensional calculations have smeared the polyethylene into annular rings. In some cases the polyethylene has been kept as a single material having the same area as the rods in either one or two rings. In other cases the polyethylene and steel have been smeared azimuthally, again in either one or two rings. The MCBEND results show that the dose-rate is decreased by a factor of 0.62 when the model is changed from discrete rods to two smeared rings. The MORSE results show that the use of a single annular ring of polythene gives a corresponding reduction by 0.75.

This underestimation arising from the use of smeared models is confirmed by the one-dimensional results, particularly if the value of 77.3 μSv/hr is adopted as the reference dose-rate. The ratios for the ANISN result to the discrete model results in this case range from 0.2 to 0.61.

Table 28. 2 a radial neutron

METHOD	CODE	CONTRIBUTOR	DOSE RATE AT SURFACE (microSv/h)	DOSE ATTENUATION 1 m	2 m	10 m
Values at the axial mid-point (averaged over θ)						
1D Sn	ANISN	Belgium (c)	15.8	0.348	0.190	0.0144
	ANISN	Belgium (b)	21.0	0.333	0.190	0.0140
	ANISN	Japan (a)	47.4	0.344	0.238	0.0388
	ANISN	FRG (a)	37.0	0.297	0.162	0.0135
	ANISN	Switzerland (d)	40.0	0.200	0.143	
	ONEDANT	Switzerland (d)	41.0	0.293	0.161	
	SAS 1	USA (b)	34.3	0.315	0.175	0.0163
2D	DOT 3.5	Japan(a)	46.4	0.308	0.185	0.0146
	DORT	USA(e)	50.1			
	TWODANT	Switzerland (e)	73.6			
Monte Carlo (Gp)	SAS 4	USA (e)	43.3	0.343	0.184	0.0166
Monte Carlo (Pt)	MCBEND	UK(e)	74.2	0.311	0.164	0.0140
	MCNP	Italy (f)	85.7 (1.7%)			
	MCNP	Italy (e)	84.2 (3%)	0.311	0.176	0.0150
Values at the axial mid-point (max. values)			max.	θ		
2D	DORT	USA(e)	55.0	0 deg		
	TWODANT	Switzerland (e)	81.0	0.9 deg		
Monte Carlo (Pt)	MCNP	Italy (e)	94.0 (2.4%)	0-2 deg		
Values at the axial mid-point (min. values)			min.	θ		
2D	DORT	USA(e)	46.0	6 deg.		
	TWODANT	Switzerland (e)	67.7	5.2 deg		
Monte Carlo (Pt)	MCNP	Italy (e)	77.3 (2.6%)	4-6 deg		
Axially averaged values over the cavity area (averaged over θ)						
2D	DOT 3.5	Japan (a)	45.6	0.305	0.180	0.0132
Monte Carlo (Gp)	SAS 4	USA (e)	47.0 (3%)	0.262	0.143	0.0156
	MORSE	Japan(a)	52.0 (7%)	0.311	0.177	0.0160
	MORSE	Japan(e)	69.7 (7%)	0.330	0.199	0.0178
Monte Carlo (Pt)	MCBEND	UK (d)	41.6	0.283	0.154	0.0149
	MCBEND	UK (e)	66.9 (4%)	0.296	0.157	0.0157

(a) Polythene smeared into an annular shell (1 ring)
(b) Polythene smeared into an annular shell (2 rings)
(c) Polythene/steel smeared into an annular shell (1 ring)
(d) Polythene/steel smeared into an annular shell (2 rings)
(e) Polythene represented by discrete rods
(f) Infinite model in z

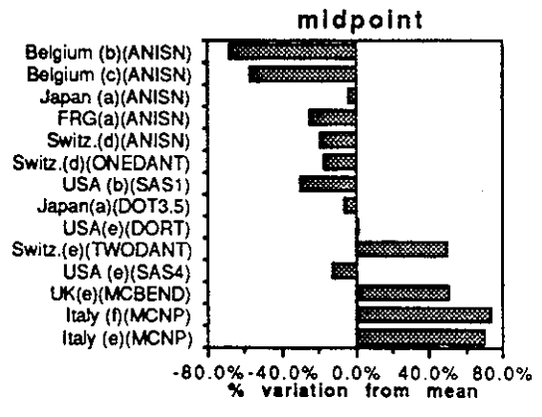

mean = 49.6 μSv/h

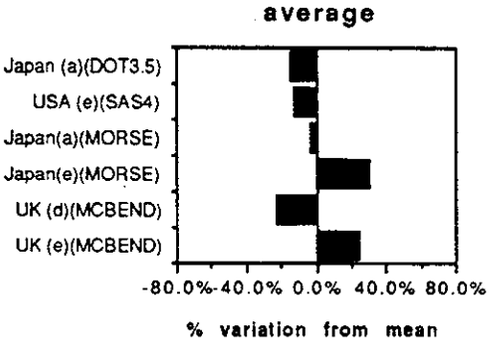

mean = 53.8 μSv/h

Problem 2a Radial Fission Product Gamma-rays

Cylindrical Source, Dry, Steel Wall containing two rings of Polyethylene Rods

There are again 5 calculations in which the rods are modelled discretely. Using the MCBEND result to scale the SAS4 cavity averaged value to the mid-height dose-rates gives a dose-rate of 532 x 1.07 = 568 μSv/hr. The mean of the five mid-height values averaged azimuthally is then 635 μSv/hr with a standard deviation on the distribution of 100 μSv/hr (16%). The two point energy calculations are in agreement, with DORT and SAS4 giving lower results and TWODANT predicting a much higher dose-rate.

The effect of modelling the rods as two smeared rings of steel and polyethylene is shown by the MCBEND results to reduce the dose-rate by a factor of 0.7. The various models used in the one-dimensional calculations all give results which are below the mean of the 5 discrete models, the ratios varying from 0.6 to 0.97.

The DOT results show only a 4.4% increase in the dose-rate when the angular quadrature is increased from 8 to 16 and the Legendre expansion of the cross-section is increased from 3 to 5.

The MCNP results for the mid-height value calculated with finite and infinite models show a ratio of 1.17 although the statistical uncertainties are small. This ratio appears to be unreasonable with a source which is 4.5m high, and indicate perhaps that the statistical standard deviations in Monte Carlo cannot be used to set confidence limits as one would with a normal distribution.

The MCNP, DORT and TWODANT results again show considerable azimuthal variation as can be seen in Fig 9. The ratios of the maximum to mean dose-rate for azimuthal locations at the mid-height of the cavity are 1.87, 1.44, and 1.16 respectively for DORT, TWODANT, and MCNP, with corresponding values of 0.56, 0.74, and 0.60 for the minimum-to-mean ratios. There is thus significant fine structure in the azimuthal variation of the dose-rate which would be important in determining the maximum surface value. The three sets of results are however inconsistent in their predictions of the amount of variation. The occurrence of the peak in the TWODANT results, at a position displaced from the reflecting boundary passing through the centre of polyethylene rod in the outer ring, suggests that the numerical solution is introducing distortions. The Monte Carlo results given in three azimuthal intervals over the 6° sector cannot show the same resolution as the discrete ordinates codes, and thus give a smaller variations. The calculated dose-rates are azimuthally uniform at 1 metre from the flask.

Table 29. 2 a radial FP gamma.

METHOD	CODE	CONTRIBUTOR	DOSE RATE AT SURFACE (microSv/h)	DOSE ATTENUATION 1 m	2 m	10 m
Values at the axial mid-point (averaged over θ)						
1D Sn	ANISN	Belgium (c)	583	0.405	0.261	0.0409
	ANISN	Belgium (b)	616	0.409	0.261	0.0400
	ANISN	Japan (a)	585	0.426	0.262	0.0385
	ANISN	FRG (g)	351	0.353	0.211	0.0228
	ANISN	FRG (h)	565	0.354	0.212	0.0230
	SAS 1	USA (b)	385	0.382	0.231	0.0278
	ONEDANT	Switzerland (d)	585	0.393	0.239	
2D	DOT 3.5 (P3S8)	Japan (a)	540	0.383	0.230	0.0161
	DOT 3.5 (P5S16)	Japan (a)	564	0.371	0.227	0.0204
	DORT	USA (e)	533			
	TWODANT	Switzerland (e)	792			
Monte Carlo (Pt)	MCBEND	UK (e)	623 (9%)	0.370	0.220	0.0236
	MCNP	Italy (f)	566 (2.2%)	0.346	0.205	0.0233
	MCNP	Italy (e)	660 (8%)	0.370	0.220	0.0236
Values at the axial mid-point (max. values)			max.	θ		
2D	DORT	USA(e)	999	6 deg		
	TWODANT	Switzerland(e)	1143	5.2 deg		
Monte Carlo (Pt)	MCNP	Italy(e)	763.5 (3.1%)	4-6 deg.		
Values at the axial mid-point (min. values)			min.	θ		
2D	DORT	USA(e)	300	0 deg.		
	TWODANT	Switzerland(e)	585	1.3 deg		
Monte Carlo (Pt)	MCNP	Italy(e)	398.2 (2.4%)	0-2 deg		
Axially averaged values over the cavity area (averaged over θ)						
2D	DOT 3.5 (P3S8)	Japan (a)	524	0.355	0.204	0.0153
	DOT 3.5 (P5S16)	Japan (a)	547	0.343	0.203	0.0180
Monte Carlo (Gp)	SAS 4	USA(e)	532 (2%)	0.265	0.159	0.0088
Monte Carlo (Pt)	MCBEND	UK (d)	406	0.352	0.202	0.0244
	MCBEND	UK (e)	584 (5%)	0.352	0.199	0.0233

(a) Polythene smeared into an annular shell (1 ring)
(b) Polythene smeared into an annular shell (2 rings)
(c) Polythene/steel smeared into an annular shell (1 ring)
(d) Polythene/steel smeared into an annular shell (2 rings)
(e) Polythene represented by discrete rods
(f) Infinite model in z
(g) GAM50 library
(h) EURLIB library

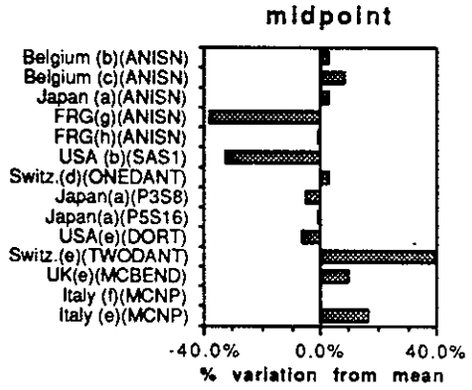

mean = 567.7 μSv/h

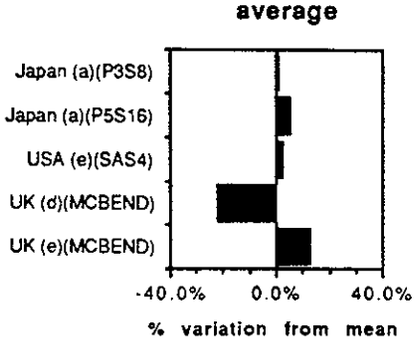

mean = 518.6 μSv/h

Problem 2a Radial Secondary Gamma-rays

Cylindrical Source, Dry, Steel Wall Containing two rings of Polyethylene Rods

There are three calculations in which explicit modelling of the rods was used to predict the azimuthally averaged dose-rates at the mid-height of the cavity. A fourth code, MCBEND gives the axially-averaged dose-rate, and this can be scaled to a mid-height value of 3.44 μSv/hr by using the ratio of 1.09. The mean of the four results is then 4.31 μSv/hr with a standard deviation of 1.0 μSv/hr (23%) so that the agreement is not good.

The MCBEND results suggest that approximation of the model in the case of secondary gamma-rays leads to an overestimate of the dose-rates, which contrasts with the underestimation found for the primary source. Moreover this conclusion is not supported by the one-dimensional results which are mostly below the mean of 4.31 μSv/hr.

The azimuthal variation at the mid-height gives values of 1.15, 1.14, and 1.06 for the ratio of the maximum-to-mean dose-rates from DORT, TWODANT, and MCNP respectively, with corresponding value of 0.88, 0.93, and 0.86 for the minima. The ratios are thus closer to the fine structure observed for neutrons than for the fission product sources, but the locations of the maxima and minima are reversed ie, the secondary gamma-ray dose-rate is highest where the neutron dose-rate is lowest. The variations are shown graphically in Figure 10.

Table 30. 2 a radial secondary gamma

METHOD	CODE	CONTRIBUTOR	DOSE RATE AT SURFACE (microSv/h)	DOSE ATTENUATION 1 m	2 m	10 m
Values at the axial mid-point (averaged over θ)						
1D Sn	ANISN	Belgium (b)	3.80			
	ANISN	Japan (a)	4.08	0.380	0.255	0.0368
	ANISN	FRG (a)	8.80	0.352	0.205	0.0230
	SAS 1	USA (b)	3.90	0.359	0.215	0.0205
	ONEDANT	Switzerland (d)	4.70	0.383	0.234	
2D	DOT 3.5	Japan (a)	4.02	0.353	0.207	0.0130
	DORT	USA (e)	3.40			
	TWODANT	Switzerland(e)	5.20			
Monte Carlo (Gp)						
Monte Carlo (Pt)	MCNP	Italy	5.10 (1.3%)	0.333	0.182	0.0166
Values at the axial mid-point (max. values)			max.	θ		
2D	DORT	USA (e)	3.90	6 deg.		
	TWODANT	Switzerland(e)	5.91	5.83deg		
Monte Carlo (Pt)	MCNP	Italy(e)	5.40 (2.0%)	4-6 deg		
Values at the axial mid-point (min. values)			min.	θ		
2D	DORT	USA (e)	3.00	0 deg.		
	TWODANT	Switzerland(e)	4.83	0.54 deg		
Monte Carlo (Pt)	MCNP	Italy(e)	4.40 (2.0%)	0-2 deg		
Axially averaged values over the cavity area (averaged over θ)						
2D	DOT 3.5	Japan (a)	3.79	0.333	0.190	0.0132
Monte Carlo (Gp)						
Monte Carlo (Pt)	MCBEND	UK (d)	5.86	0.337	0.183	0.0188
	MCBEND	UK (e)	3.25 (5%)	0.335	0.178	0.0185

(a) Polythene smeared into an annular shell (1 ring)
(b) Polythene smeared into an annular shell (2 rings)
(c) Polythene/steel smeared into an annular shell (1 ring)
(d) Polythene/steel smeared into an annular shell (2 rings)
(e) Polythene represented by discrete rods
(f) Infinite model in z

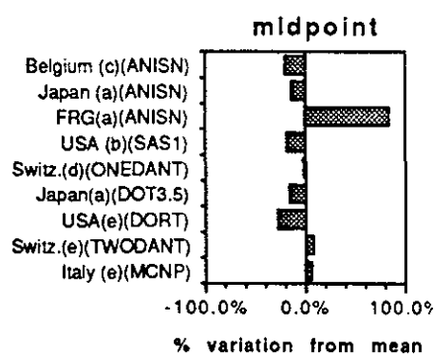

mean = 4.78 μSv/h

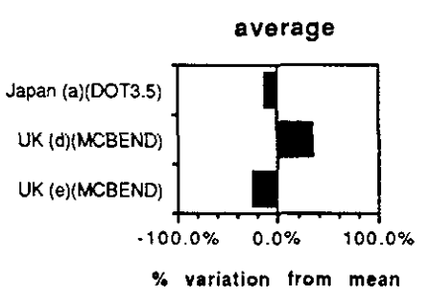

mean = 4.30 μSv/h

Problem 2b Radial-Neutron

Cylindrical Source, Dry, Cast Iron Wall with bands of Epoxy Resin

The mean value of the dose-rate averaged over the height of the cavity for the calculations with a discrete representation of the epoxy bands is 189 μSv/hr with a standard deviation on the distribution of 3.1 μSv/hr (1.6%) so that the agreement is good. The DOT and MORSE calculations with the resin and steel smeared in the outer region both give a reduction in the dose-rate by a factor of 0.75 when compared with the results with an explicit model. When scaled by the factor of 1.07 the averaged dose-rate of 189 μSv/hr is equivalent to an axial mid-point value of 202 μSv/hr. The two one-dimensional calculations with their smeared models show differences from this dose rate of +10% and -25%.

The DORT and SAS4 values at the mid-point are much lower than this but this is attributed to the axial fine structure which depresses the neutron dose-rate opposite an epoxy band.

Table 31. 2 b radial neutron

METHOD	CODE	CONTRIBUTOR	DOSE RATE AT SURFACE (microSv/h)	DOSE ATTENUATION 1 m	2 m	10 m
Values at the axial mid-point						
1D Sn	ANISN	Japan (a)	152	0.368	0.252	0.0442
	ANISN	FRG (a)	220	0.332	0.177	0.0159
2D	DOT 3.5	Japan(a)	149	0.321	0.188	0.0124
	DORT	USA (b)	167	0.379	0.208	0.0188
Monte Carlo (Gp)	SAS 4	USA (b)	169	0.405	0.219	0.0190
Monte Carlo (Pt)						
Axially averaged values over the cavity area						
2D	DOT 3.5	Japan(a)	141	0.308	0.177	0.0120
	DORT	USA (b)	186			
Monte Carlo (Gp)	MORSE (a)	Japan(a)	142 (3%)	0.354	0.197	0.0197
	MORSE (b)	Japan (b)	192	0.344	0.192	0.0174
	SAS 4	USA (b)	188 (2%)	0.245	0.138	0.0192
Monte Carlo (Pt)						

(a) Iron and resin homogenised
(b) Iron and resin represented separately

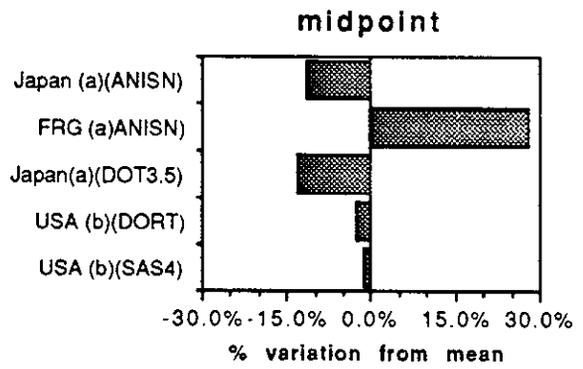

mean = 171.4 μSv/h

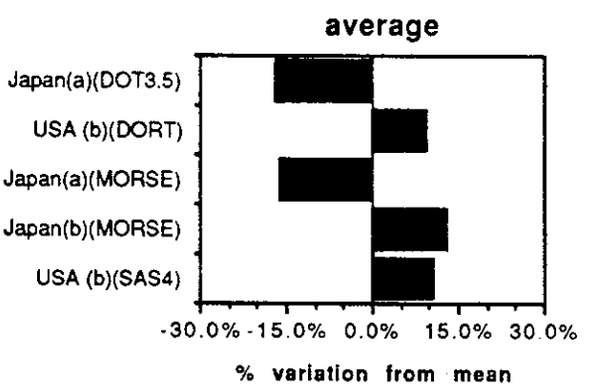

mean = 169.8 μSv/h

Problem 2b Radial Fission Product Gamma-rays

Cylindrical Source, Dry, Cast Iron Wall with bands of Epoxy Resin

The DORT and SAS4 results for the dose-rate averaged over the height of the cavity agree with a mean value of 593 μSv/hr. The results obtained with the smeared models are mostly higher than this which suggests that in this case the simplified model overestimates the dose-rate. There are however, no direct comparisons where the same code and data have been used for both discrete and smeared representation of the epoxy resin bands.

The change in the order of the angular quadrature in DOT from 8 to 16 together with P5 expansions of the cross-sections in place of P3 gave an increase in the dose-rate of only 4%.

The DORT and SAS4 results show values of the peak to mean ratio of 1.12 which is much higher than the value of 1.03 adopted in Section 6.1. This is again attributed to the fine structure in the dose-rate, the value being high opposite the epoxy band in the case of gamma-rays.

Table 32. 2 b radial FP gamma

METHOD	CODE	CONTRIBUTOR	DOSE RATE AT SURFACE (microSv/h)	DOSE ATTENUATION 1m	2m	10m
Values at the axial mid-point						
1D Sn	ANISN	Japan (a)	824	0.242	0.152	0.0226
	ANISN	FRG (c)	525	0.360	0.219	0.0280
	ANISN	FRG (d)	835	0.354	0.211	0.0231
2D	DORT	USA (b)	652	0.353	0.213	0.0236
	DOT 3.5 (P3S8)	Japan (a)	764	0.382	0.229	0.0161
	DOT 3.5 (P5S16)	Japan (a)	796	0.371	0.226	0.0202
Monte Carlo (Gp)	SAS 4	USA (b)	671	0.322	0.206	0.0235
Monte Carlo (Pt)						
Axially averaged values over the cavity area						
2D	DOT 3.5 (P3S8)	Japan (a)	741	0.355	0.205	0.0152
	DOT 3.5 (P5S16)	Japan (a)	772	0.345	0.203	0.0180
	DORT	USA (b)	584			
Monte Carlo (Gp)	SAS 4	USA (b)	601 (2%)	0.270	0.163	0.0242
Monte Carlo (Pt)						

(a) Iron and resin homogenised
(b) Iron and resin represented separately
(c) GAM50 library
(d) EURLIB library

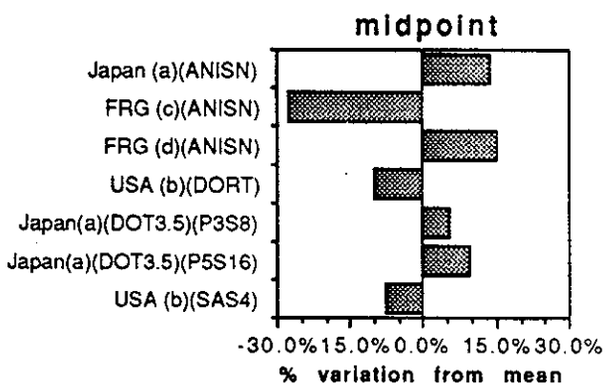

mean 723.9 μSv/h

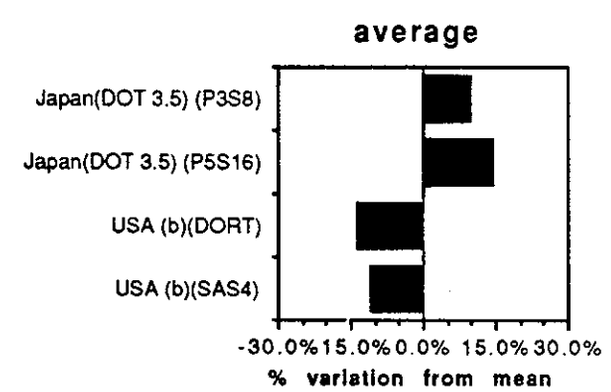

mean 674.5 μSv/h

Problem 2b Radial - Secondary Gamma-rays

Cylindrical Source, Dry, Cast Iron Wall with bands of Epoxy Resin

The DORT and ANISN calculations with the RADHEAT library give values which exceed those given by DORT, whereas the ANISN calculation with the EURLIB library is in agreement. Only the DORT calculation represented the epoxy resin bands explicitly so that it is not possible to draw clear conclusions on the effect of homogenisation of the resin and iron.

Table 33. 2 b radial secondary gamma

METHOD	CODE	CONTRIBUTOR	DOSE RATE AT SURFACE (microSv/h)	DOSE ATTENUATION 1 m	2 m	10 m
Values at the axial mid-point						
1D Sn	ANISN	Japan (a)	36.2	0.301	0.208	0.0303
	ANISN	FRG (a)	22.0	0.277	0.145	0.0136
2D	DOT 3.5	Japan (a)	37.0	0.236	0.129	0.0068
	DORT	USA (b)	22.1	0.252	0.126	0.0100
Monte Carlo (Gp)						
Monte Carlo (Pt)						
Axially averaged values over the cavity area						
2D	DOT 3.5	Japan (a)	34.4	0.221	0.121	0.0072
	DORT	USA (b)	19.6			
Monte Carlo (Gp)						
Monte Carlo (Pt)						

(a) Iron and resin homogenised
(b) Iron and resin represented separately

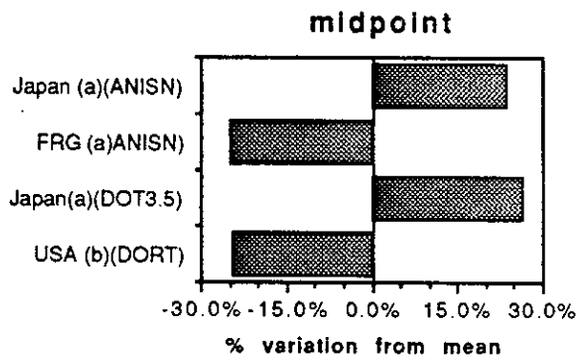

mean 29.3 μSv/h

Problem 3a Radial Neutron

Cylindrical Source, Dry, Steel Wall with Fins

Only one result was submitted.

Table 34. 3 a radial neutron

METHOD	CODE	CONTRIBUTOR	DOSE RATE AT SURFACE (microSv/h)	DOSE ATTENUATION 1 m	2 m	10 m
Values at the axial mid-point						
1D Sn	ANISN	FRG	36	0.333	0.194	0.0166
2D						
Monte Carlo (Gp)						
Monte Carlo (Pt)						

Problem 3a Radial Fission Product Gamma-rays

Cylindrical Source, Dry, Steel wall with Fins

The two results again illustrate the effect of using different data libraries with the same code, the ratio between the two dose-rates being 1.7.

Table 35. 3 a radial FP gamma

METHOD	CODE	CONTRIBUTOR	DOSE RATE AT SURFACE (microSv/h)	DOSE ATTENUATION 1 m	2 m	10 m
Values at the axial mid-point						
1D Sn	ANISN	FRG (a)	111	0.387	0.234	0.0270
	ANISN	FRG (b)	188	0.388	0.234	0.0270
2D						
Monte Carlo (Gp)						
Monte Carlo (Pt)						

Problem 3a Radial Secondary Gamma-rays

Cylindrical Source, Dry, Steel Walls with Fins

Only one result was submitted for this problem.

Table 36. 3 a radial secondary gamma

METHOD	CODE	CONTRIBUTOR	DOSE RATE AT SURFACE (microSv/h)	DOSE ATTENUATION 1 m	2 m	10 m
Values at the axial mid-point						
1D Sn	ANISN	FRG	3.7	0.405	0.243	0.0270
2D						
Monte Carlo (Gp)						
Monte Carlo (Pt)						

Problem 3b Radial Neutrons

Cylindrical Source, Dry, Cast Iron Wall With Fins and bands of Epoxy Resin

The results with the discrete model of the fins and the epoxy resin as obtained with the point energy codes give a mean dose-rate of 152 μSv/hr averaged over the combined height of a fin and a band at the cavity mid-height. This dose is at the radius of the fin tips. At the surface of the epoxy resin between the fins the dose-rate is higher by a factor of 1.78.

The DORT calculation also used a discrete model and its mean value is in good agreement being lower than that of the Monte Carlo codes by 12%. The axial variation as calculated by DORT, MCNP and MCBEND at a radius corresponding to the fin tips is shown in Figure 11. The Monte Carlo codes again show less resolution than the discrete-ordinates methods, but the latter seems to have an anomalous shape with its peak at 10mm from the centre of the epoxy. The ratio between the maximum and minimum values given by DORT is 1.5.

The MCBEND results show that the model with a smear of the resin and steel surrounded by a smear of the fins and void gives a dose-rate which is lower by a factor of 0.8. The approach of calculating for two separate models and weighting the results in combination gives a better agreement than those from the single smeared model.

Table 37. 3 b radial neutron

METHOD	CODE	CONTRIBUTOR	DOSE RATE AT SURFACE (microSv/h)	DOSE ATTENUATION 1m	2m	10m
Values at the axial mid-point (averaged over fin and epoxy)						
1D Sn	ANISN	Belgium (c)	138	0.391	0.217	0.0170
	ANISN	Belgium (b)	100	0.380	0.210	0.0170
	ANISN	FRG	128	0.344	0.203	0.1950
2D Sn						
Monte Carlo (Gp)						
Monte Carlo (Pt)	MCBEND	UK (b)	117.4	0.331	0.183	0.0177
Axially averaged values over the surface near the midplane						
2D Sn	DORT	USA(d)	133			
Monte Carlo (Gp)						
Monte Carlo (Pt)	MCNP	Italy (a)	161 (4.0%)	0.347	0.189	0.0166
	MCNP	Italy (d)	150.7 (1.2%)			
	MCBEND	UK (a)	149.5(2.5%)	0.367	0.208	0.0168
	MCBEND	UK (d)	145.8(3.7%)			
Dose rates on epoxy surface (averaged over surface near axial midplane)						
Monte Carlo (Pt)	MCNP	Italy (a)	262.8 (1.3%)			
	MCBEND	UK (a)	284.5 (4.2%)			
	MCBEND	UK (d)	266.6(4.7%)			

(a) Discrete model of each fin and epoxy band
(b) 2 smeared bands of finbase/epoxy and fin/void
(c) Combination of model with fin & model with epoxy coating
(d) Model of half fin & half absorber with reflection

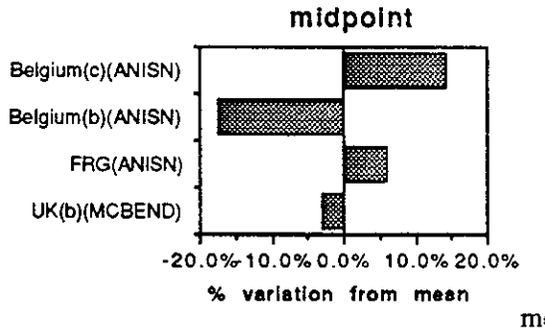

mean 120.9 μSv/h

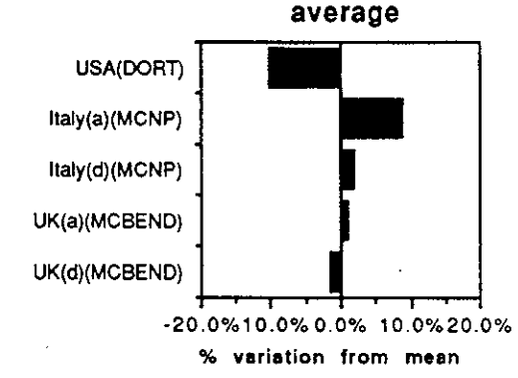

mean 148.0 μSv/h

Problem 3b Radial Fission Product Gamma-rays

Cylindrical Source, Dry, Cast Iron Wall with Fins and bands of Epoxy Resin

The three calculations which use point-energy data give a mean dose-rate averaged over the height of a fin and an epoxy band of 367 μSv/hr at the mid-height of the cavity. This is at the radius corresponding to the fin tips.

The DORT calculations also modelled the fins and epoxy separately and its result is in good agreement with the Monte Carlo results being 11% lower. The axial variation at the radius of the fin tips is shown in Figure 11, the results from DORT giving the most detailed resolution. In that case the variation from the minimum opposite the fin to the maximum at the centre of the resin is a factor of 4.4.

The MCBEND calculation with the smeared model gives a dose-rate which is lower than those of the discrete model by a factor of 0.59, and the one-dimensional calculations with such models underestimate the dose-rate.

At the surface of the resin between the fins the dose-rate is found to be 868 μSv/hr from the two point-energy calculations, and this would be an important consideration when ensuring that a flask met the transport requirements for the surface dose-rate.

Table 38. 3 b radial FP gamma

METHOD	CODE	CONTRIBUTOR	DOSE RATE AT SURFACE (microSv/h)	DOSE ATTENUATION 1 m	2 m	10 m
Values at the axial mid-point (averaged over fin and epoxy)						
1D Sn	ANISN	Belgium (b)	256	0.484	0.316	0.0500
	ANISN	FRG (e)	173	0.393	0.243	0.0324
	ANISN	FRG (f)	300	0.387	0.237	0.0270
2D Sn						
Monte Carlo (Gp)						
Monte Carlo (Pt)	MCBEND	UK (b)	200.8	0.398	0.234	0.0250
Axially averaged values over the surface near the midplane						
2D Sn	DORT	USA(d)	325			
Monte Carlo (Gp)						
Monte Carlo (Pt)	MCNP	Italy (a)	390 (3.5%)	0.418	0.259	0.0379
	MCNP	Italy (d)	366.6 (3.4%)			
	MCBEND	UK (a)	343.1	0.440	0.283	0.0420
Dose rates on epoxy surface (averaged over surface near axial midplane)						
Monte Carlo (Pt)	MCNP	Italy	895.4 (2.9%)			
	MCBEND	UK	840.6(2.5%)			

(a) Discrete model of each fin and epoxy band
(b) 2 smeared bands of finbase/epoxy and fin/void
(c) Combination of model with fin & model with epoxy coating
(d) Model of half fin & half absorber with reflection
(e) GAM50 library
(f) EURLIB library

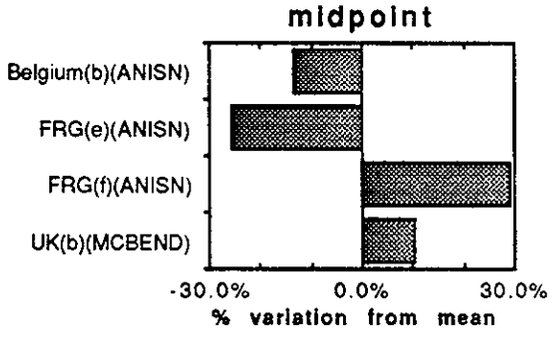

mean 232.5 µSv/h

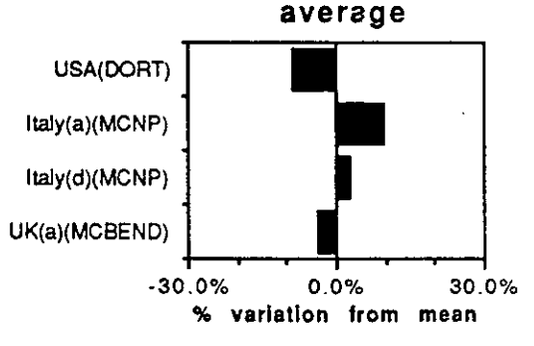

mean 356.2 µSv/h

Problem 3b Radial - Secondary Gamma-rays

Cylindrical Source, Dry, Cast Iron Wall with Fins and bands of Epoxy Resin

The four point-energy calculations give a mean value of 13.6 μSv/hr for the dose-rate averaged over the height of a fin and an epoxy band at the mid-point of the cavity. This is 10% higher than the result of the DORT calculations which also modelled the fins and epoxy resin as discrete regions.

Figure 11 shows the axial variation of the dose-rate at the radius of the fin tips. It is almost uniform opposite the region of epoxy but drops by 20% opposite the fin.

The MCBEND results suggest that the dose-rate from secondary gamma-rays is increased by a factor of about 1.2 when a smeared model is used. This tendency is confirmed by the one-dimensional results which are both much higher than those from the discrete model.

The dose-rate on the surface of the epoxy resin bands is predicted to be higher than that averaged over the height of a fin and a band at the radial position of the fin tips by factors of 2.7, 2.5, and 2.6 by the three calculations.

Table 39. 3 b radial secondary gamma

METHOD	CODE	CONTRIBUTOR	DOSE RATE AT SURFACE (microSv/h)	DOSE ATTENUATION 1 m	2 m	10 m
Values at the axial mid-point (averaged over fin and epoxy)						
1D Sn	ANISN	Belgium (b)	26.0			
	ANISN	FRG	25.0	0.332	0.188	0.0160
2D Sn						
Monte Carlo (Gp)						
Monte Carlo (Pt)	MCBEND	UK (b)	15.8	0.337	0.177	0.0120
Axially averaged values over the surface near the midplane						
2D Sn	DORT	USA(d)	12.3			
Monte Carlo (Gp)						
Monte Carlo (Pt)	MCNP	Italy (a)	14.3 (4.0%)	0.329	0.175	0.0164
	MCNP	Italy (d)	14.8 (1.4%)			
	MCBEND	UK (a)	11.0	0.326	0.184	0.0140
	MCBEND	UK (d)	14.3 (2.3%)			
Dose rates on epoxy surface (averaged over surface near axial midplane)						
Monte Carlo (Pt)	MCNP	Italy (a)	38.0 (1.6%)			
	MCBEND	UK (a)	27.9 (7.8%)			
	MCBEND	UK (d)	37.4 (3.5%)			

(a) Discrete model of each fin and epoxy band
(b) 2 smeared bands of finbase/epoxy and fin/void
(c) Combination of model with fin & model with epoxy coating
(d) Model of half fin & half absorber with reflection

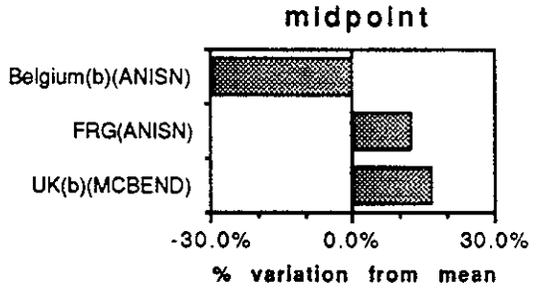

mean 22.3 μSv/h

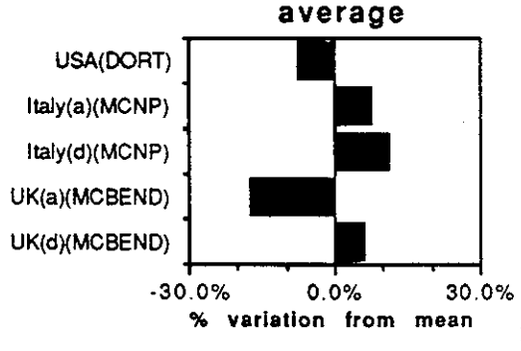

mean 13.3 μSv/h

Problem 4a Radial-Neutrons (Steel Flask)

Fuel Element Source, Dry, Steel Wall*, No Neutron Shielding

The fuel elements in their basket are explicitly modelled in the MCNP calculation which gives the dose-rate of 836 μSv/hr. Smearing the fuel pins within a basket compartment is shown to reduce the dose-rate by 0.95, although this is not really significant in view of the statistical uncertainty of 6% on the factor. The MORSE result with the pins smeared within the compartments predicts a dose-rate which is higher by 17% than the MCNP result.

The other calculations use smeared annular representations of the basket and fuel. For DOT and ANISN (Japan) the model represented the centre element as a cylinder of diameter 269.7mm surrounded by a 10mm steel basket wall. The other four elements were smeared into an annular ring of diameter 613mm outside this wall; with a further 10mm wall of outer diameter 633mm to represent the basket. The 83.5mm annular gap between this wall and the surface of the cavity was treated as void. For SAS1 the model was similar to that for DOT except that the outer 10mm basket wall was touching the flask wall so that the outer ring of four elements were combined with the void. The results obtained with DOT and ANISN (Japan) are higher than those from MCNP by about 15%, but for the SAS1 model with its source nearer to the flask wall the difference is 45%. Details are not available for the model used in the ANISN (FRG) calculations.

* The problem specification was changed to a cast iron wall, but some calculations were also performed for a steel wall.

Table 40(i) 4 a radial neutron (steel flask)

METHOD	CODE	CONTRIBUTOR	DOSE RATE AT SURFACE (microSv/h)	DOSE ATTENUATION 1m	2m	10m
Values at the axial mid-point						
1D Sn	SAS1	USA (b)	1183	0.311	0.172	0.0155
	ANISN	Japan (c)	945	0.341	0.237	0.0390
	ANISN	FRG	630	0.289	0.144	0.0103
2D	DOT 3.5	Japan (c)	925	0.269	0.148	0.0070
Monte Carlo (Gp)						
Monte Carlo (Pt)	MCNP	Italy (a)	836 (4%)	0.276	0.135	0.0104
	MCNP	Italy (b)	796 (4%)	0.288	0.144	0.0110
Axially averaged values over the cavity area						
2D	DOT 3.5	Japan (c)	716	0.271	0.154	0.0097
Monte Carlo (Gp)	MORSE	Japan (b)	930 (4%)	0.298	0.149	0.0106
Monte Carlo (Pt)						

(a) Fuel pins represented separately
(b) Fuel assemblies smeared within basket compartments
(c) Annular epresentation of the basket

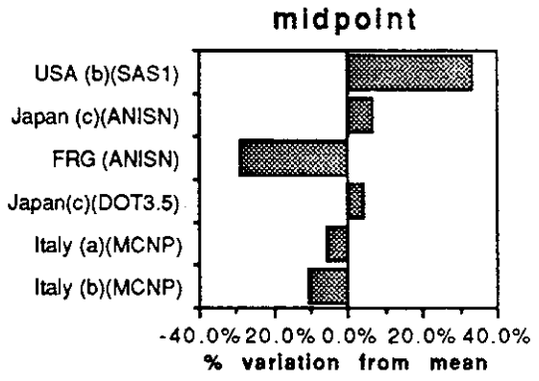

mean = 885.8 μSv/h

Problem 4a Radial Neutrons

Fuel Element Source, Dry, Cast Iron Wall, No Neutron Shielding

The SAS4 results confirm that smearing the fuel pins changes the dose-rate by a statistically insignificant amount.

From the DOT results for Problem 4a with a steel flask the ratio of the mid-height dose-rate to that averaged over the cavity is 1.29 (In this problem the source is restricted to the length of the active fuel). If the SAS4 result with fuel pins represented is scaled by this factor the dose-rate becomes 624 μSv/hr, which is only 6% lower than the value of 665 μSv/hr given by MCNP.

It is of interest to note that the dose-rate is lower by a factor of 0.82 than that obtained for a steel flask of the same thickness.

Table 40(ii) 4 a radial neutron (cast iron flask)

METHOD	CODE	CONTRIBUTOR	DOSE RATE AT SURFACE (microSv/h)	DOSE ATTENUATION 1 m	2 m	10 m
Values at the axial mid-point						
1D Sn						
2D						
Monte Carlo (Gp)						
Monte Carlo (Pt)	MCNP	Italy (a)	665(1.7%)	0.293	0.144	0.0110
Axially averaged values over the cavity area						
2D						
Monte Carlo (Gp)	SAS 4	USA (b)	507 (2%)	0.215	0.117	
	SAS 4	USA (a)	484 (3%)	0.216	0.117	
Monte Carlo (Pt)						

(a) Fuel pins represented separately
(b) Fuel assemblies smeared within basket compartments

Problem 4a Radial-Fission Product Gamma-Rays (Steel Flask)

Fuel Element Source, Dry, Steel Wall*, No Neutron Shielding

The MCNP calculation models the basket and fuel explicitly resulting in a dose-rate of 68.1 μSv/hr at the cavity mid-height. The other result with explicit modelling, only the pins being smeared, is the SAS4 dose-rate of 64.5 μSv/hr averaged over the cavity height. The DOT 3.5 results give a ratio of mid-point to axially averaged values of 1.26 compared with 1.29 found for neutrons. Scaling the MCNP results by this factor would give 54.0 μSv/hr which is lower than the SAS4 value of 64.5 μSv/hr. The results with the smeared models are all much higher than these, mostly by more than a factor of 2, which suggests that the self-shielding effects of the source are greater in the explicit model.

The effect of moving from P_3S_8 to P_5S_{16} in the angular quadrature and representation of the angular distribution of scatter is again to increase the dose-rate by a small amount (9%) (For problem 2a the corresponding increase was 4%).

* The problem specification was changed to a cast iron wall, but some calculations were also performed for a steel wall.

Table 41(i) 4 a radial FP gamma (steel flask)

METHOD	CODE	CONTRIBUTOR	DOSE RATE AT SURFACE (microSv/h)	DOSE ATTENUATION 1 m	2 m	10 m
Values at the axial mid-point						
Kernel						
1D Sn	SAS1	USA (c)	136	0.379	0.230	0.0282
	ANISN	Japan (c)	174	0.428	0.261	0.0385
	ANISN	FRG (d)	140	0.350	0.200	0.0185
	ANISN	FRG (e)	331*	0.350	0.202	0.0180
2D	DOT 3.5 (P3S8)	Japan (c)	151	0.368	0.218	0.0111
	DOT 3.5 (P5S16)	Japan (c)	165	0.363	0.216	0.0161
Monte Carlo (Gp)						
Monte Carlo (Pt)	MCNP	Italy (a)	68.1 (7%)	0.369	0.198	0.0172
Axially averaged values over the cavity area						
2D	DOT 3.5 (P3S8)	Japan (c)	121	0.357	0.212	0.0152
	DOT 3.5 (P5S16)	Japan (c)	131	0.353	0.211	0.0185
Monte Carlo (Gp)	SAS 4	USA (b)	64.5 (6%)	0.251	0.150	
Monte Carlo (Pt)						

(a) Fuel pins represented separately
(b) Fuel assemblies smeared within basket compartments
(c) Annular representation of the basket
(d) GAM50 library
(e) EURLIB library
*not included in mean

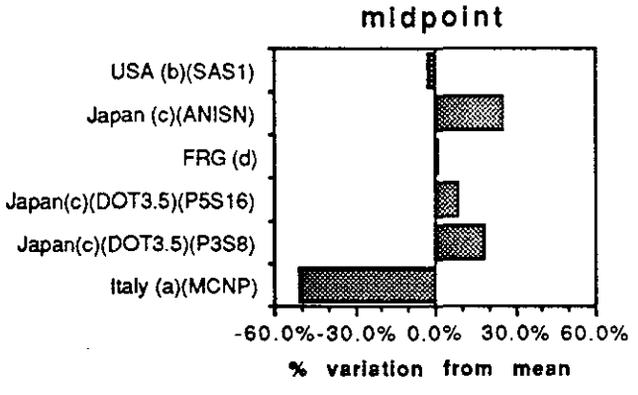

mean = 139.0 μSv/h

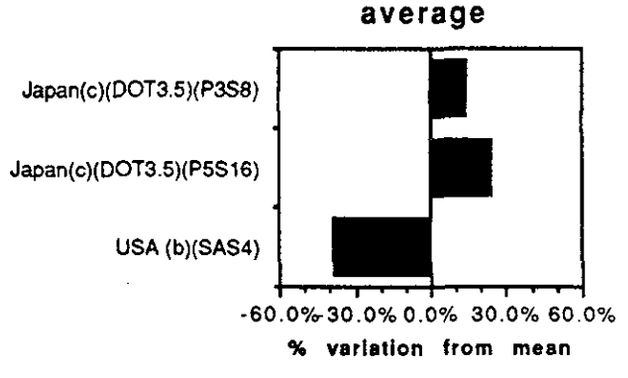

mean = 105.5 μSv/h

Problem 4a Radial Fission Product Gamma-rays

Fuel Element Source, Dry, Cast Iron Wall, No Neutron Shielding

The SAS4 results in this case show no statistically significant difference between representing the fuel pins explicitly or smearing them within the compartments. If the mean of the two results is scaled by the factor of 1.26 postulated for the ratio between maximum and mean values for Problem 4 the equivalent mid-height dose-rate from SAS4 is 248 μSv/hr. This is higher than the MCNP value by only 5% so that the two are in close agreement.

The QAD result is also in agreement which suggests that the simple kernel approach in which the basket can be modelled is preferable to a transport calculation in which a smeared model has to be used.

The dose-rate is higher by a factor of 3.5 than that for the steel-walled flask which is to be expected as the iron has a lower density.

Table 41(ii) 4 a radial FP gamma (cast iron flask)

METHOD	CODE	CONTRIBUTOR	DOSE RATE AT SURFACE (microSv/h)	DOSE ATTENUATION 1 m	2 m	10 m
Values at the axial mid-point						
Kernel	QAD	Belgium	241	0.432	0.271	0.0297
1D Sn						
2D						
Monte Carlo (Gp)						
Monte Carlo (Pt)	MCNP	Italy (a)	235.5 (2.5%)	0.381	0.216	0.0200
Axially averaged values over the cavity area						
2D						
Monte Carlo (Gp)	SAS 4	USA (b)	205 (5%)	0.255	0.152	
Monte Carlo (Pt)	SAS 4	USA (a)	189(10%)	0.255	0.152	

(a) Fuel pins represented separately
(b) Fuel assemblies smeared within basket compartments
(c) GAM50 library
(d) EURLIB library

Problem 4a Radial - Secondary Gamma-rays

Fuel Element Source, Dry, Steel Wall* No Neutron Shielding

The results for the secondary gamma-rays are similar to those for the primary sources with the SAS1 model in which the centre fuel element is a cylinder surrounded by an annular ring representing the other four, leading to a significant overestimate of the dose-rate.

* The problem specification was changed to a cast iron wall, but some calculations were also performed fore a steel wall.

Table 42(i) 4 a radial secondary gamma (steel flask)

METHOD	CODE	CONTRIBUTOR	DOSE RATE AT SURFACE (microSv/h)	DOSE ATTENUATION 1m	2m	10m
Values at the axial mid-point						
1D Sn	SAS1	USA (b)	10.8	0.327	0.184	0.0167
2D						
Monte Carlo (Gp)						
Monte Carlo (Pt)	MCNP	Italy (a)	4.6 (9.0%)	0.260	0.130	0.0100
	MCNP	Italy (b)	4.2 (7.0%)	0.286	0.143	0.0010
Axially averaged values over the cavity area						
1D Sn						
2D						
Monte Carlo (Gp)						
Monte Carlo (Pt)						

(a) Fuel pins represented separately
(b) Fuel assemblies smeared within basket compartments

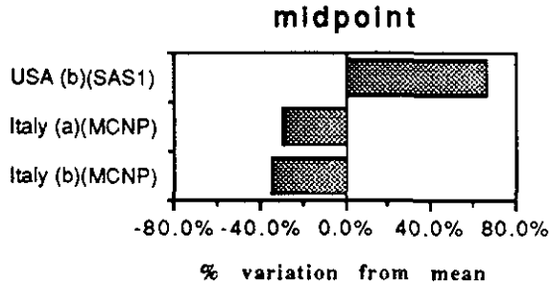

mean = 6.5 μSv/h

Problem 4a Radial-Secondary Gamma-rays

Fuel Element Source, Dry, Cast Iron Wall, No Neutron Shielding

The dose-rate is higher than that for the steel flask by 15% so that the effect of the density of the wall is much less marked than it was for the fission-product sources.

Table 42(ii) 4 a radial secondary gamma (cast iron flask)

METHOD	CODE	CONTRIBUTOR	DOSE RATE AT SURFACE (microSv/h)	DOSE ATTENUATION 1 m	2 m	10 m
Values at the axial mid-point						
1D Sn						
2D						
Monte Carlo (Gp)						
Monte Carlo (Pt)	MCNP	Italy (a)	5.3 (3.3%)	0.283	0.142	0.0110
Axially averaged values over the cavity area						
2D						
Monte Carlo (Gp)						
Monte Carlo (Pt)						

(a) Fuel pins represented separately
(b) Fuel assemblies smeared within basket compartments

Problem 4b Radial - Neutrons (Steel Flask)

Fuel Element Source, Wet, Steel Wall*, No Neutron Shielding

The MCNP and SAS1 results are in excellent agreement so that the flooding of the cavity removes the error from the one-dimensional model which was found in Problem 4a. (The SAS1 model was identical with water being added to the smeared fuel). The ANISN (Japan) model is also similar to that for Problem 4a, but in this case the outer annulus of thickness 83.5mm surrounding the fuel is filled with water which gives additional attenuation leading to an underestimate.

The MCNP results again show no significant difference between discrete and smeared representations of the fuel pins.

The ANISN calculations carried out in Finland employed several models of the cavity. These were based on smearing the basket, fuel, and water in a number of annular rings ranging from 1 to 5. The spread in the result shows the significance of modelling, but it is not possible to draw conclusions about the accuracy because the BUGLE library used in the calculations was found to seriously underestimate the dose-rates in problem 1a.

* The problem specification was changed to a cast iron wall, but some calculations were also performed for a steel wall.

Table 43(i) 4 b radial neutron (steel flask)

METHOD	CODE	CONTRIBUTOR	DOSE RATE AT SURFACE (microSv/h)	DOSE ATTENUATION 1 m	2 m	10 m
Values at the axial mid-point						
1D Sn	ANISN	Japan (c)	17.5*	0.340	0.237	0.0387
	SAS1	USA (b)	61.7	0.311	0.173	0.0154
	ANISN	Finland(d)	31.6*			
	ANISN	Finland(e)	33.4*			
	ANISN	Finland(f)	59.8*			
	ANISN	Finland(g)	45.2*			
	ANISN	Finland(h)	59.5*			
	ANISN	FRG	66.0	0.303	0.167	0.0136
2D						
Monte Carlo (Gp)						
Monte Carlo (Pt)	MCNP	Italy (a)	58.8 (3%)	0.272	0.134	0.0119
	MCNP	Italy (b)	59.2 (7%)	0.269	0.132	0.0118
Axially averaged values over the cavity area						
2D						
Monte Carlo (Gp)						
Monte Carlo (Pt)						

(a) Fuel pins represented separately
(b) Fuel assemblies smeared within basket compartments
(c) Annular representation of the basket
(d) to (h) are variations in the homogenised model of the basket. (See paper by Wasastjerna.)
* not included in the mean

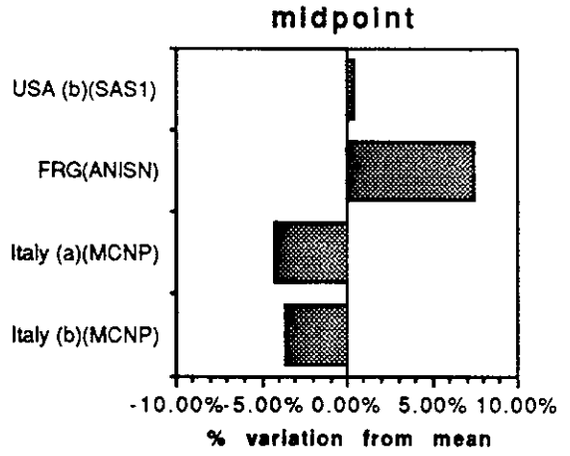

mean = 61.4 μSv/h

Problem 4b Radial-Neutron

Fuel Element Source, Wet, Cast Iron Wall, No Neutron Shielding

The MCBEND and MCNP results are in agreement with a mean value of 48.2 μSv/hr.

If the scaling factor of 1.29 from problem 4a is assumed to apply here also, then the SAS4 result is equivalent to 46.2 μSv/hr which is also in agreement.

Table 43(ii) 4 b radial neutron (cast iron flask)

METHOD	CODE	CONTRIBUTOR	DOSE RATE AT SURFACE (microSv/h)	DOSE ATTENUATION 1 m	2 m	10 m
Values at the axial mid-point						
1D Sn						
2D						
Monte Carlo (Gp)						
Monte Carlo (Pt)	MCNP	Italy (a)	50.4 (2.5%)	0.295	0.146	0.0106
	MCBEND	UK (b)	45.9 (4.7%)	0.300	0.146	0.0113
Axially averaged values over the cavity area						
2D						
Monte Carlo (Gp)	SAS 4	USA (b)	35.8 (3%)	0.200	0.109	0.0154
Monte Carlo (Pt)						

(a) Fuel pins represented separately
(b) Fuel assemblies smeared within basket compartments

Problem 4b Radial Fission Product Gamma-rays (Steel Flask)

Fuel Element Source, Wet, Steel Wall*, No Neutron Shielding

The calculations with the one-dimensional models again overestimate the dose-rate, although by slightly smaller amounts than for the dry flask. The effect of the water on gamma-rays is thus much less than it was for neutrons, as might be expected.

* The problem specification was changed to a cast iron wall, but some calculations were also performed for a steel wall.

Table 44(i) 4 b radial FP gamma (steel flask)

METHOD	CODE	CONTRIBUTOR	DOSE RATE AT SURFACE (microSv/h)	DOSE ATTENUATION 1m	2m	10m
Values at the axial mid-point						
1D Sn	ANISN	Japan (c)	83.9	0.429	0.262	0.0387
	SAS1	USA (b)	79.6	0.379	0.230	0.0281
2D						
Monte Carlo (Gp)						
Monte Carlo (Pt)	MCNP	Italy (a)	41.8 (6%)	0.356	0.197	0.0199
Axially averaged values over the cavity area						
2D						
Monte Carlo (Gp)						
Monte Carlo (Pt)						

(a) Fuel pins represented separately
(b) Fuel assemblies smeared within basket compartments
(c) Annular representation of the flask

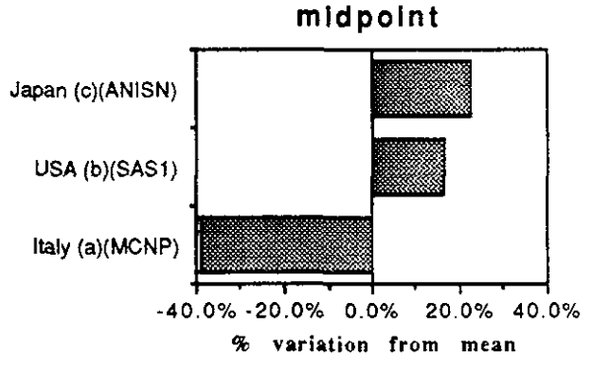

mean = 68.4 μSv/h

Problem 4b Radial Fission Product Gamma-rays

Fuel Element Source, Wet, Cast Iron Wall, No Neutron Shielding

MCBEND and MCNP give a mean value of 158 μSv/hr for the dose-rate at the flask mid-height.

The cavity-averaged dose-rate of 118 μSv/hr predicted by SAS4 can be scaled to 149 μSv/hr at the mid-height by using the factor of 1.26 for problem 4. This overestimates the MCNP result by 2.8%.

The one-dimensional models again give dose-rates which are higher than those obtained with explicit representations of the fuel elements and their basket.

Table 44(ii) 4 b radial FP gamma (cast iron flask)

METHOD	CODE	CONTRIBUTOR	DOSE RATE AT SURFACE (microSv/h)	DOSE ATTENUATION 1 m	2 m	10 m
Values at the axial mid-point						
1D Sn	ANISN	FRG (d)	181	0.359	0.210	0.0230
	ANISN	FRG (e)	305*	0.354	0.213	0.0240
2D						
Monte Carlo (Gp)						
Monte Carlo (Pt)	MCNP	Italy (a)	145 (3%)	0.374	0.214	0.0200
	MCBEND	UK (b)	171.3 (6.5%)	0.360	0.195	0.0180
Axially averaged values over the cavity area						
2D						
Monte Carlo (Gp)	SAS 4	USA (b)	118 (4%)	0.248	0.148	0.0281
Monte Carlo (Pt)						

(a) Fuel pins represented separately
(b) Fuel assemblies smeared within basket compartments
(c) Annular representation of the basket
(d) GAM50 library
(e) EURLIB library
*not included in mean

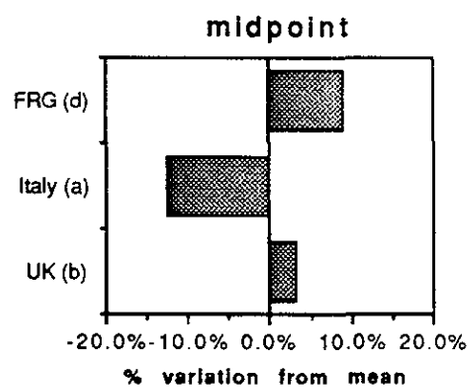

mean = 165.8 μSv/h

Problem 4b Radial-Secondary Gamma-rays (Steel Flask)

Fuel Element Source, Wet, Steel Wall*, No Neutron Shielding

The MCNP results again show no significant effect due to smearing of the pins within the basket compartments.

The SAS1 results are higher than MCNP by a factor of 2.3 which is almost identical to that in problem 4a so that the presence of the water does not improve the accuracy of the model for secondary gamma-rays in the way that it did for the neutron dose-rate. The actual dose-rate is however, reduced by a factor of 20 by flooding the cavity in both models.

* The problem specification was changed to a cast iron wall, but some calculations were also performed for a steel wall.

Table 45(i) 4 b radial secondary gamma (steel flask)

METHOD	CODE	CONTRIBUTOR	DOSE RATE AT SURFACE (microSv/h)	DOSE ATTENUATION 1 m	2 m	10 m
Values at the axial mid-point						
1D Sn	SAS1	USA (b)	0.44	0.318	0.182	0.0159
2D						
Monte Carlo (Gp)						
Monte Carlo (Pt)	MCNP	Italy (a)	0.193	0.278	0.138	0.0110
	MCNP	Italy (b)	0.187	0.303	0.144	0.0090
Axially averaged values over the cavity area						
2D						
Monte Carlo (Gp)						
Monte Carlo (Pt)						

(a) Fuel pins represented separately
(b) Fuel assemblies smeared within basket compartments

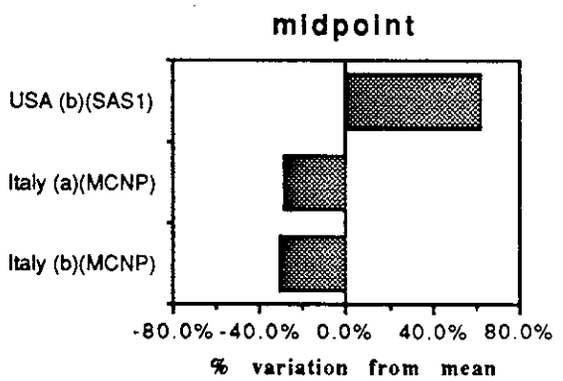

mean = 0.273 μSv/h

Problem 4b Radial-Secondary Gamma-rays

Fuel Element Source, Wet, Cast Iron Wall, No Neutron Shielding

The MCNP result gives a dose-rate which is lower than that for the dry flask by a factor of 24.

Table 45(ii) 4 b radial secondary gamma (cast iron flask)

METHOD	CODE	CONTRIBUTOR	DOSE RATE AT SURFACE (microSv/h)	DOSE ATTENUATION 1 m	2 m	10 m
Values at the axial mid-point						
1D Sn						
2D						
Monte Carlo (Gp)						
Monte Carlo (Pt)	MCNP	Italy (a)	0.223	0.322	0.156	0.0120
Axially averaged values over the cavity area						
2D						
Monte Carlo (Gp)						
Monte Carlo (Pt)						

(a) Fuel pins represented separately
(b) Fuel assemblies smeared within basket compartments

Problem 4b Lid-Neutrons

Fuel Element Source, Wet, Steel Lid

The representation of the end fittings for the fuel elements has reduced the dose-rate from the value of 80 μSv/hr found in Problem 1c when the source, fuel, basket, and water were smeared over the volume of the cavity.

Table 46. 4 b lid neutron

METHOD	CODE	CONTRIBUTOR	DOSE RATE AT SURFACE (microSv/h)	DOSE ATTENUATION 1 m	2 m	10 m
Values at the axial mid-point						
1D Sn						
2D						
Monte Carlo (Gp)						
Monte Carlo (Pt)	MCBEND	UK(b)	0.93 (13%)	0.194	0.086	

Problem 4b Lid-Fission Product Gamma-rays

Fuel Element Source, Wet, Steel Lid

The predicted dose-rate is much lower than the value of 27.6 μSv/hr found for problem 1c where the source, fuel, basket and water were smeared over the volume of the cavity.

Table 47. 4 b lid FP gamma

METHOD	CODE	CONTRIBUTOR	DOSE RATE AT SURFACE (microSv/h)	DOSE ATTENUATION 1 m	2 m	10 m
Values at the axial mid-point						
1D Sn						
2D						
Monte Carlo (Gp)						
Monte Carlo (Pt)	MCBEND	UK(b)	0.95 (11%)	0.526	0.211	0.0840

TABLE 48

MEAN TOTAL CROSS-SECTIONS
FOR IRON (DFN 906)

Group No	Group Upper Energy (ev)	Cross-Section (barns)							
		Min in Group	Max in Group	Weighting		MCBEND Weighting Distance from flask axis			
				$\frac{1}{E}$	$\frac{1}{E\Sigma_T}$	r=40 cm	r=52 cm	r=65 cm	r=78 cm
28	1.00,6	0.99	3.49	2.29	1.91	2.01	1.87	1.73	2.01
29	9.07,5	1.97	3.37	2.63	2.33	2.31	2.26	2.27	2.57
30	8.21,5	2.41	4.98	3.74	3.42	3.49	3.33	3.47	2.94
31	7.43,5	0.83	4.49	2.91	2.13	2.49	2.16	2.05	1.84
32	6.72,5	0.81	2.71	1.81	1.36	1.48	1.41	1.46	1.47
33	6.08,5	1.07	3.68	2.35	1.97	2.14	2.01	1.89	1.99
34	5.50,5	2.09	4.09	2.99	2.66	2.70	2.70	2.67	2.68
35	4.98,5	1.32	4.18	3.01	2.48	2.51	2.63	2.55	2.69
36	4.51,5	2.08	6.63	4.55	4.13	4.36	4.18	3.98	3.91
37	4.08,5	0.94	6.88	4.10	2.71	3.20	2.93	3.30	2.04
38	3.69,5	0.56	6.54	2.08	1.11	1.48	1.29	1.21	1.08
39	3.34,5	0.71	6.31	2.93	1.77	2.56	1.80	1.91	1.68
40	3.02,5	1.18	7.23	2.92	2.19	2.55	2.34	2.63	2.25
41	2.73,5	0.60	3.29	2.24	1.65	1.86	1.75	1.78	1.59
42	2.47,5	1.64	4.63	3.18	2.69	3.01	2.76	2.78	2.83
43	2.24,5	0.64	8.06	3.34	2.10	2.72	2.28	2.60	2.26
44	2.02,5	0.85	13.05	6.07	3.49	4.70	4.50	4.36	3.37
45	1.83,5	0.93	7.78	3.17	1.90	2.03	2.07	2.23	1.71
46	1.66,5	1.66	3.53	2.63	2.45	2.44	2.45	2.47	2.36
47	1.50,5	0.27	15.41	5.95	1.21	3.05	2.51	2.10	1.28
48	1.36,5	0.93	6.29	2.62	1.51	1.87	1.60	1.67	1.49
49	1.23,5	1.66	2.69	2.08	2.04	2.07	2.05	2.04	2.03
50	1.11,5	2.57	6.45	3.66	3.44	3.51	3.47	3.45	3.36
51	8.66,4	0.58	22.73	5.70	2.40	3.25	2.78	2.78	2.10
52	6.74,4	2.29	6.44	3.78	3.50	3.65	3.64	3.62	3.39
53	5.25,4	3.81	6.07	4.39	4.32	4.31	4.30	4.31	4.30

The MCBEND weighting applies for four distances through the cast iron wall of the flask in problem 1a.

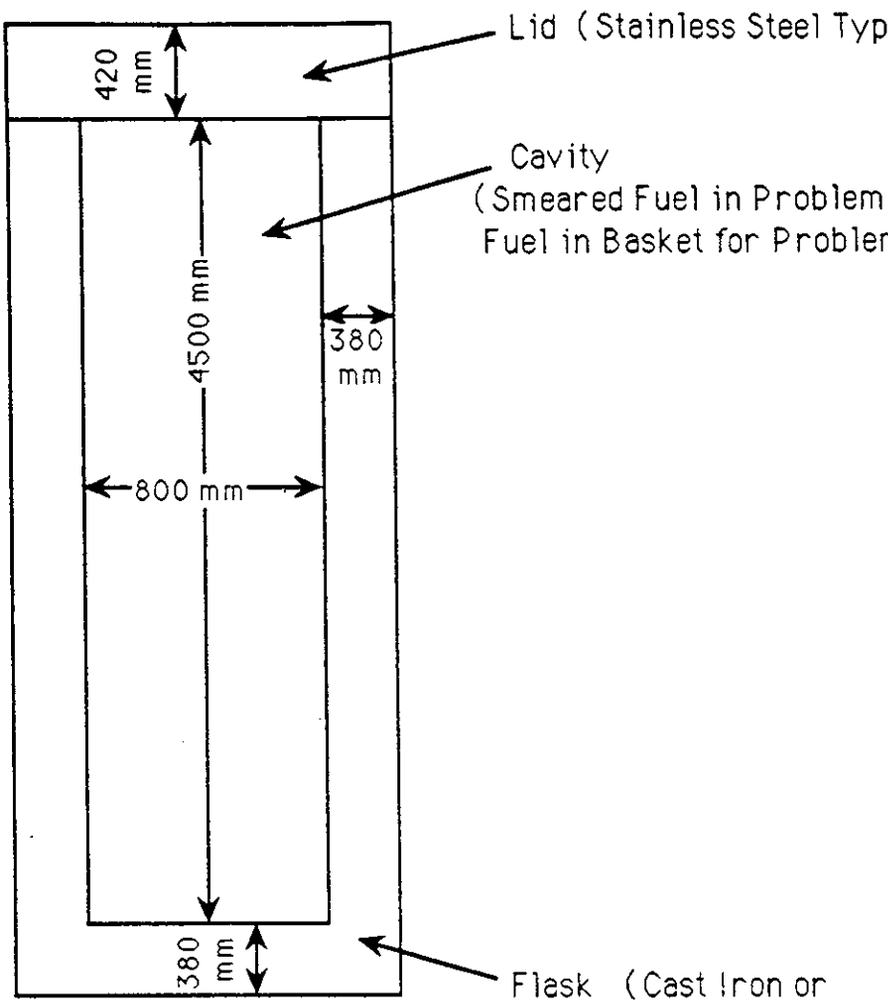

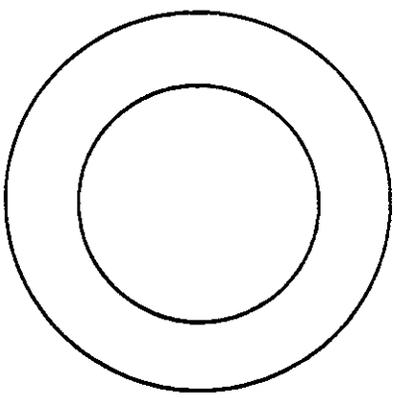

Neutron shielding is introduced into the radial walls in Problems 1b, 2a, 2b, 3a, and 3b and external fins are added in Problems 3a and 3b.

Figure 1 Dimensions of the Basic Flask

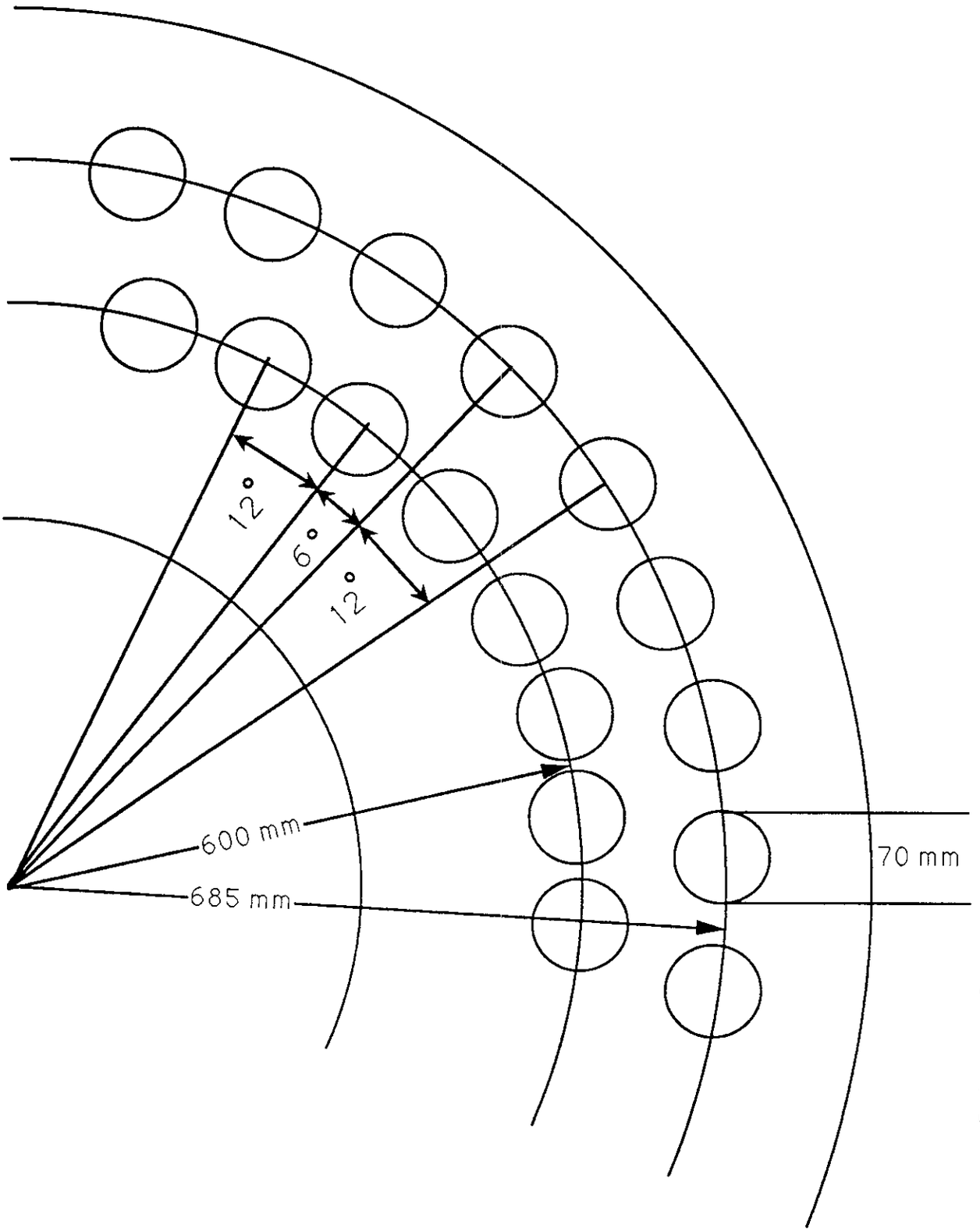

Figure 2 Polyethylene Rods in the Flask Wall for Problem 2a

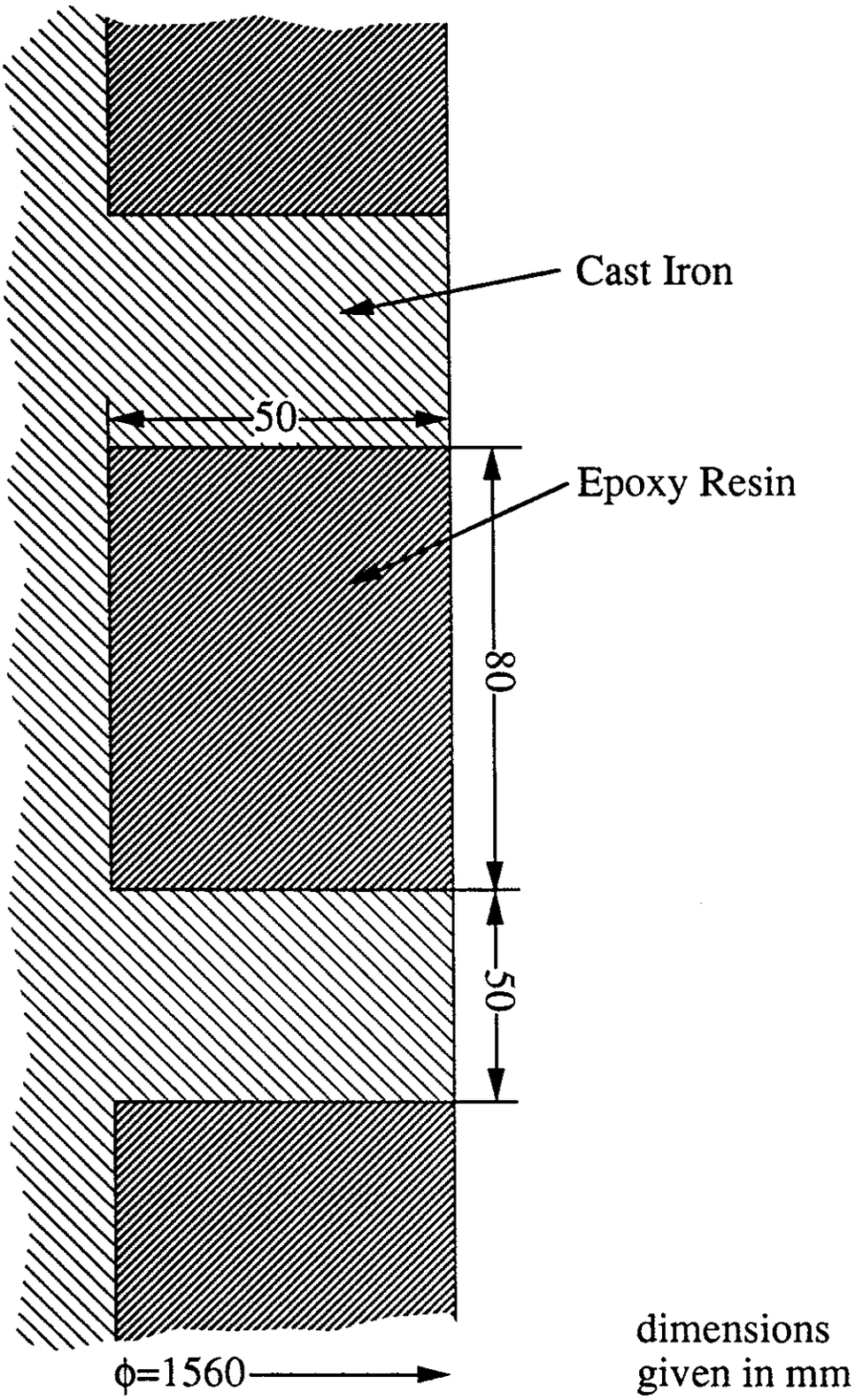

Fig 3 Bands of Epoxy Resin for Problem 2b

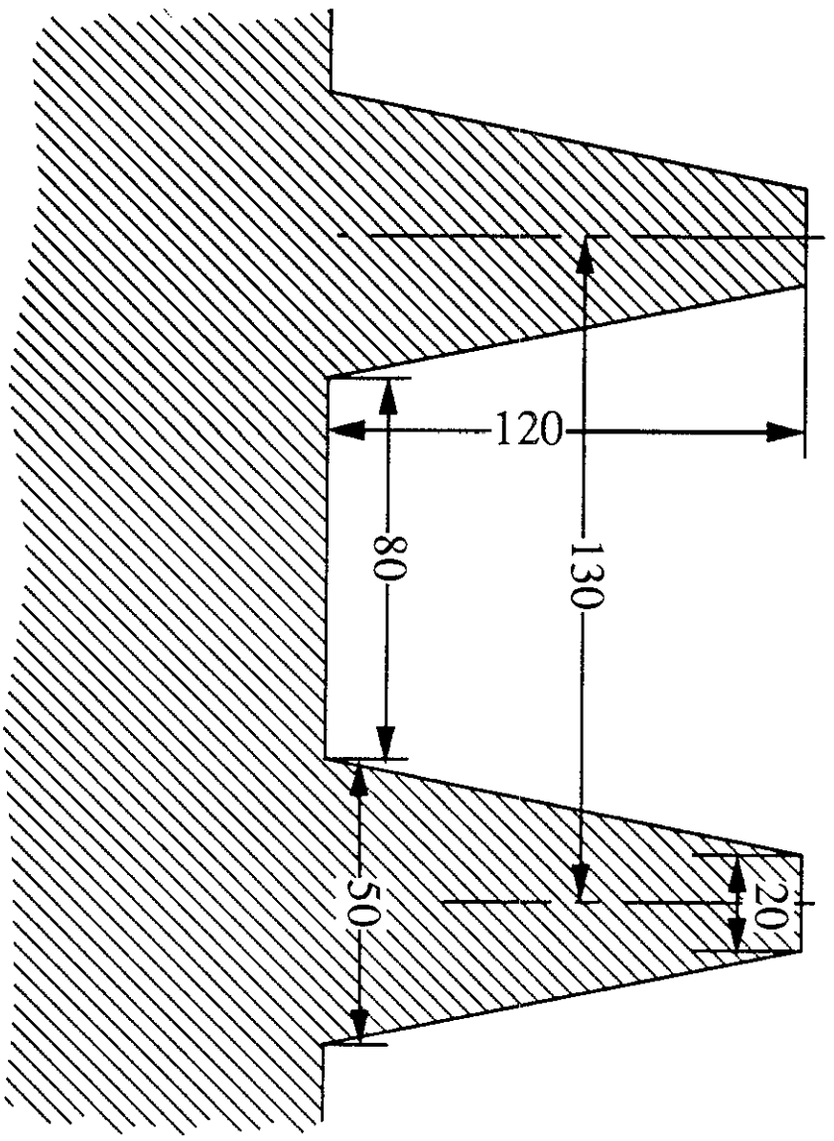

Fig 4 Cooling Fins for Problem 3a

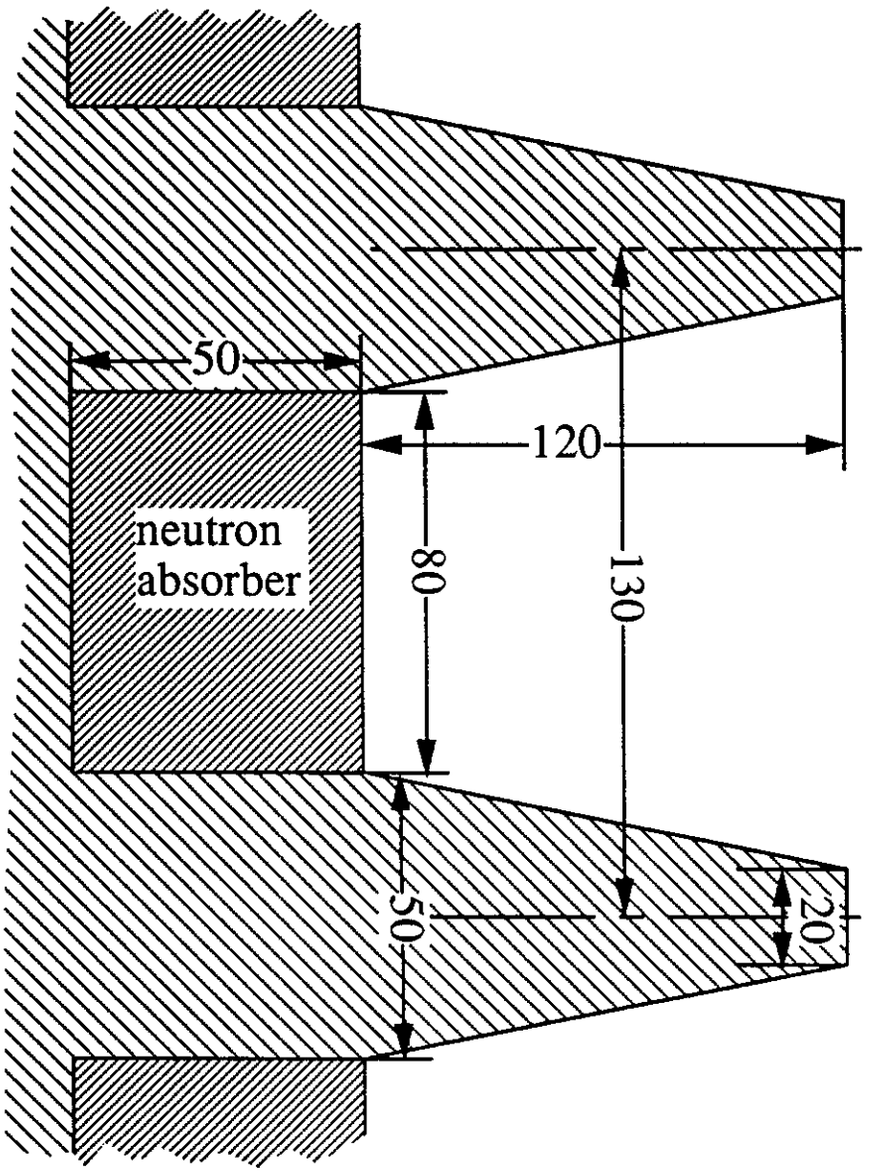

Fig 5 Cooling Fins and Epoxy Resin Bands for Problem 3b

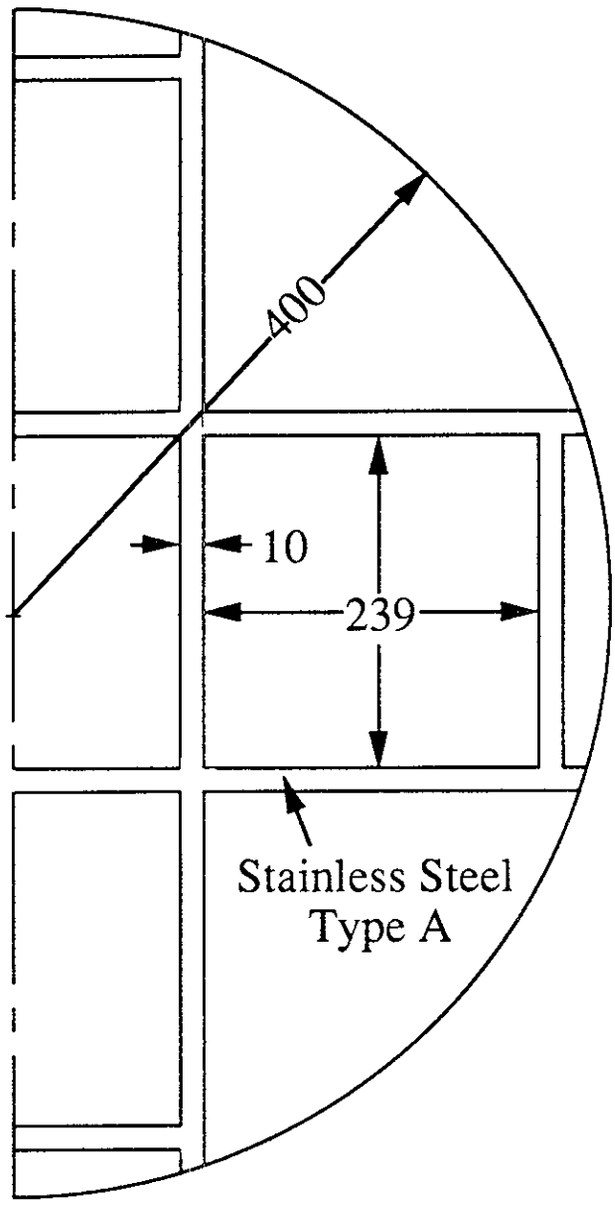

Figure 6 Fuel Basket

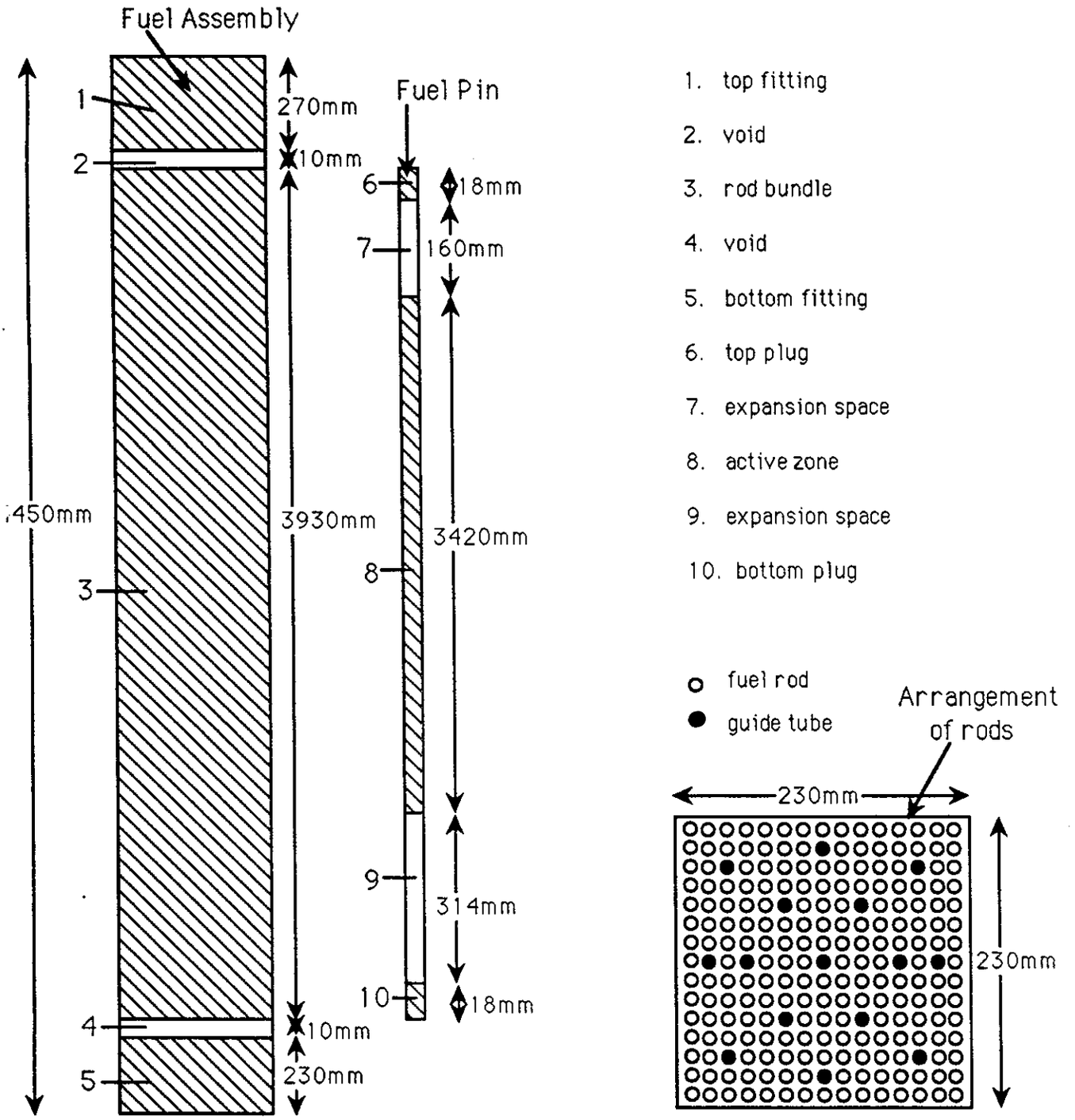

Figure 7 Fuel Assembly for Problem 4

Figure 8. Problem 2a. Azimuthal variation of neutron dose-rate at the surface.

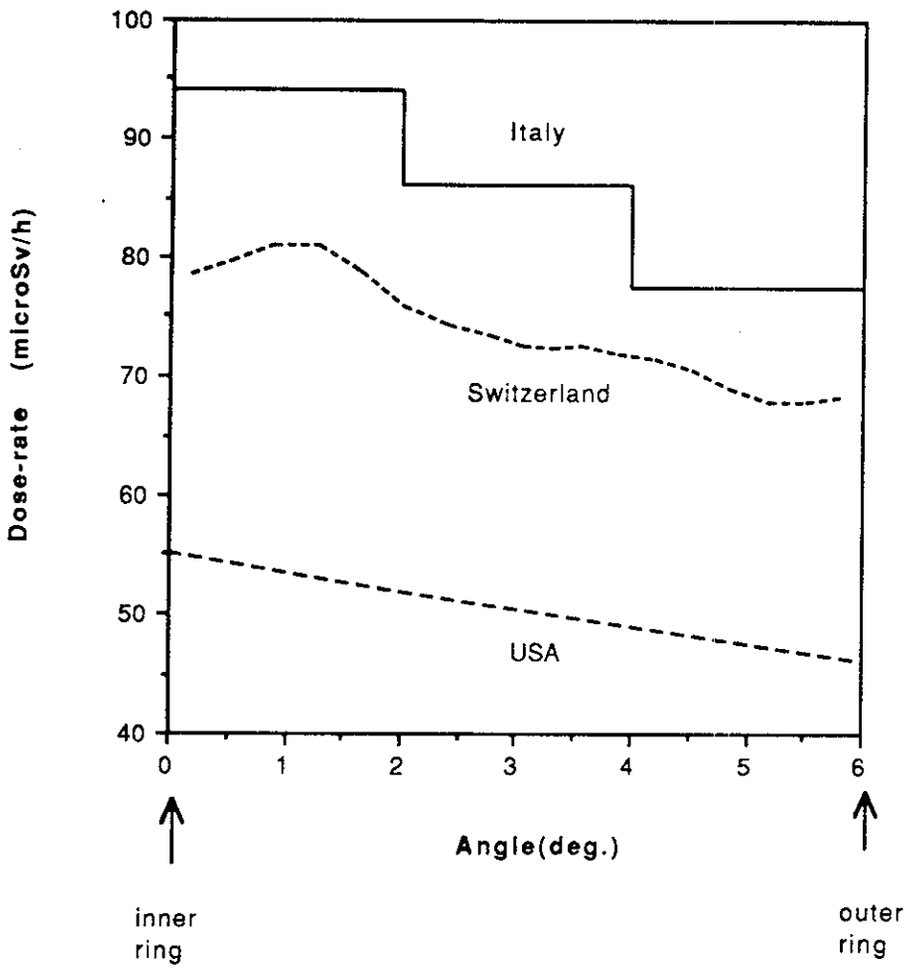

Figure 9. Problem 2a. Azimuthal variation of the F.P. gamma dose-rate at the surface.

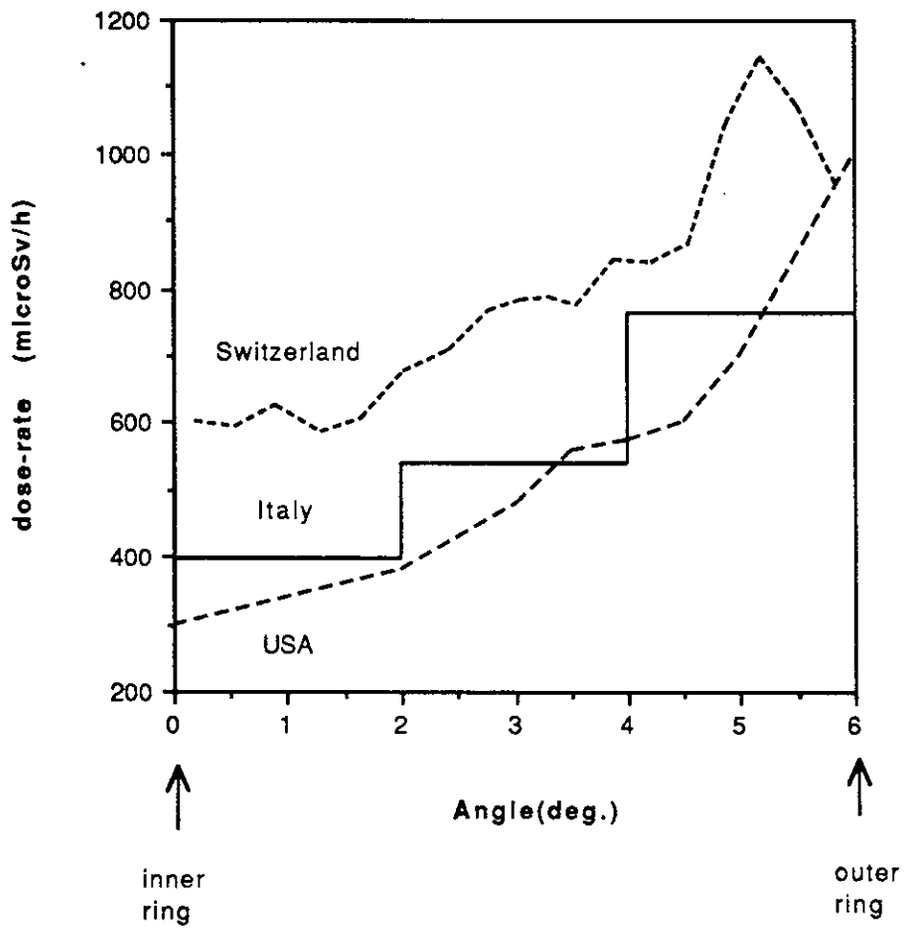

Figure 10. Problem 2a. Azimuthal variation of the secondary gamma dose-rate at the surface.

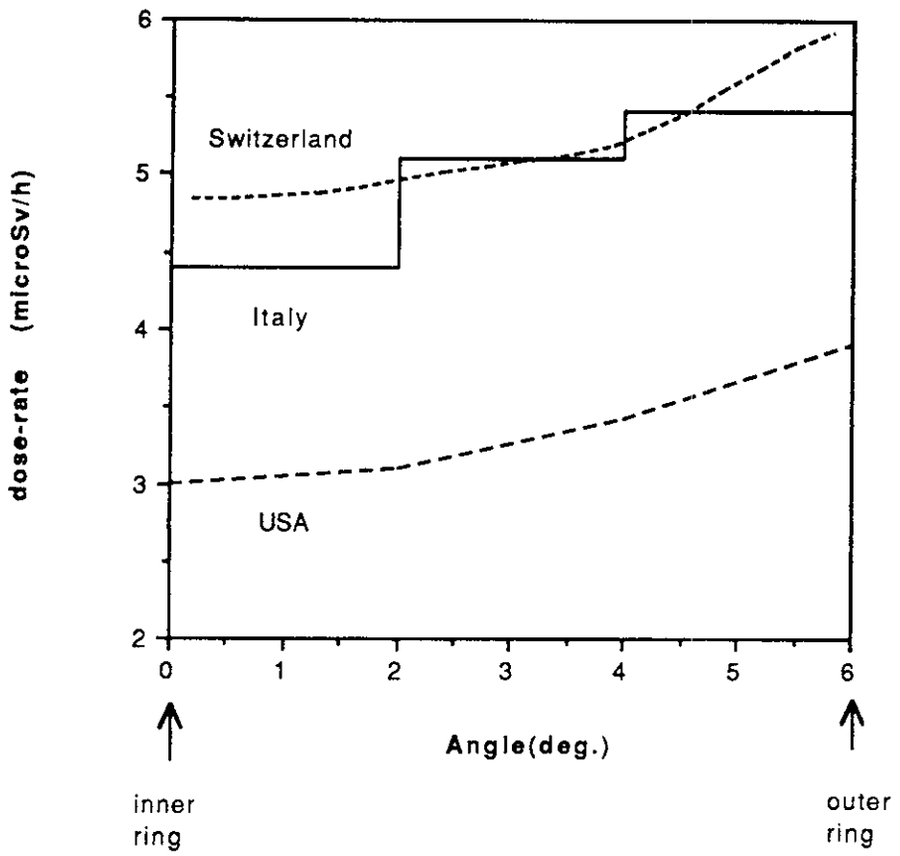

Figure 11. Problem 3b. Surface dose-rate profiles.

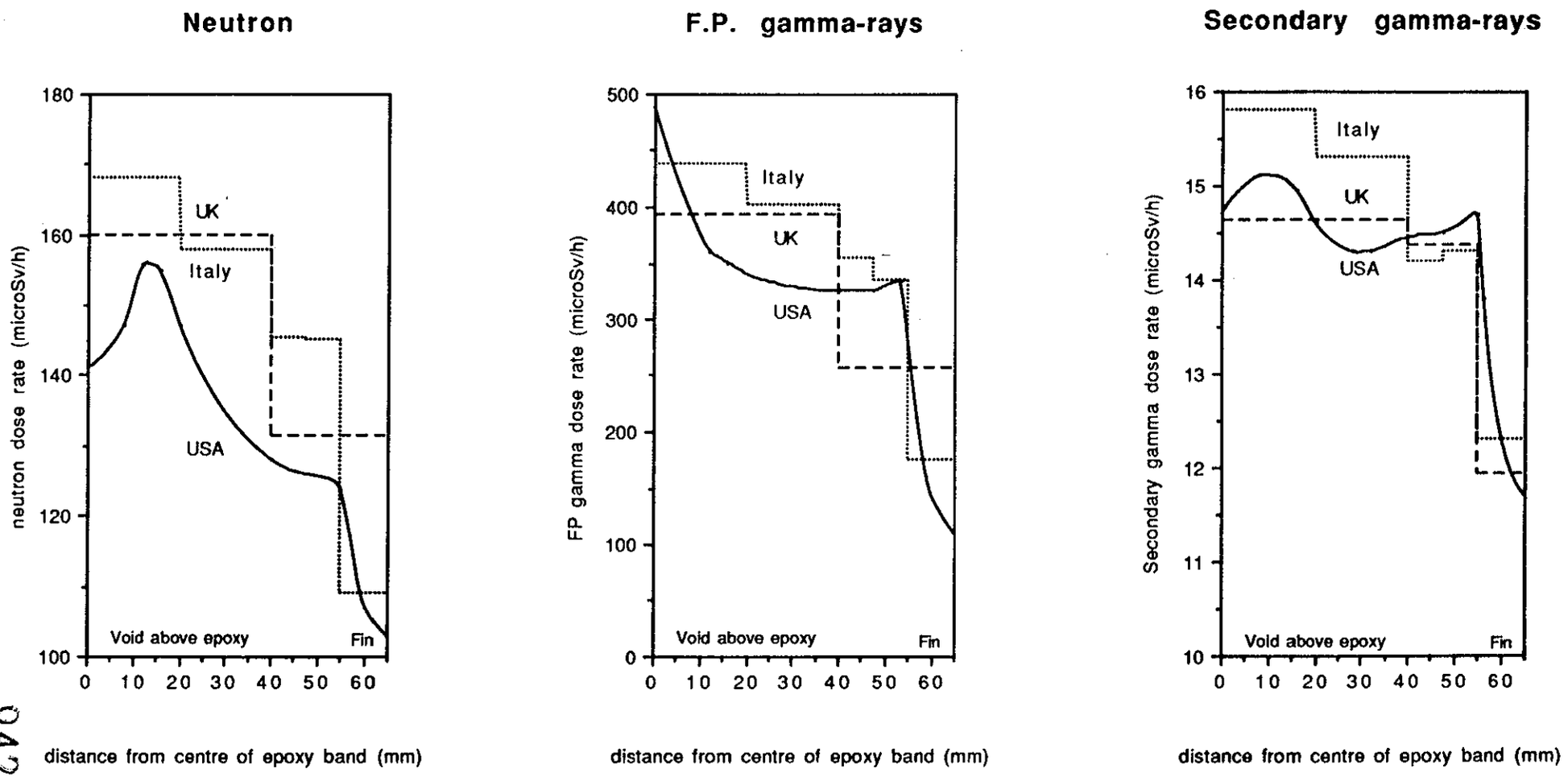

Jean-François.

Pourrais-tu me faire 1 ex de ces
3 rapports. Merci d'avance

Solange